FLORIDA INTERNATIONAL UNIVERSITY

Miami, Florida

INVESTIGATION OF MEMORY RELATED CORTICAL THALAMIC CIRCUITRY IN THE HUMAN BRAIN

A dissertation submitted in partial fulfillment of

the requirements for the degree of

DOCTOR OF PHILOSOPHY

in

COGNITIVE NEUROSCIENCE

by

Puck Charlotte Reeders

2021

To: Dean Michael R. Heithaus
College of Arts, Sciences and Education

This dissertation, written by Puck Charlotte Reeders, and entitled Investigation of Memory Related Cortical Thalamic Circuitry in the Human Brain, having been approved in respect to style and intellectual content, is referred to you for judgment.

We have read this dissertation and recommend that it be approved.

Aaron Mattfeld

Angela Laird

Anthony Dick

Timothy Allen, Major Professor

Date of Defense: October 29, 2021

The dissertation of Puck Charlotte Reeders is approved.

Dean Michael R. Heithaus
College of Arts, Sciences and Education

Andrés G. Gil
Vice President for Research and Economic Development
and Dean of the University Graduate School

Florida International University, 2021

DEDICATION

I dedicate this dissertation to my best friend and mom Nienke Antonides, and my dad Jacques Reeders. They taught me to always follow my dreams, set an example on how to work hard and reach for your goals, and have always supported me on all of my out of the ordinary endeavors. I am lucky to have such inspiring, positive, and supportive parents.

ACKNOWLEDGMENTS

I would first like to express my deepest appreciation for my mentor and major professor Dr. Timothy Allen. His mentorship, guidance, training, support, incredible teachings, and patience not only helped drive this dissertation project, but he also taught me how to think critically as a scientist in every aspect of life. Dr. Allen has been an amazing inspiration making me strive to always learn and grow, both professionally but also personally. I would also like to express my deepest appreciation for my second mentor, Dr. Aaron Mattfeld. Without his enormous support, this work would not have been possible. He has welcomed me with open arms into his lab as well, to help me develop human neuroimaging research skills. I am beyond grateful for his brilliant teachings, his unlimited patience, and all the work he has contributed to this dissertation. I want to extend a big thank you to all the members of the Allen Lab and the Mattfeld lab: I have learned so much from all of you and value your support and input. I wanted to give a big thanks to Maria Andere, for helping me so much. I also want to give a big thank you to the rest of my committee members Dr. Angela Laird, and Dr. Anthony Dick. I have learned a lot from you, and I appreciate everything you have done for this program. I would also like to extend a thank you to my friends Alexis, Jessica, and Katie, for all your love – you have kept me sane throughout grad school. Finally, I am beyond grateful for the support, love, and encouragement I have received from my parents, Nienke and Jacques, my sister, Loes, and my boyfriend, Ben. Without your love and never-ending support, this PhD would not have been possible. This dissertation was partially funded by the FIU University Graduate School Dissertation Year Fellowship and the Feinberg Foundation.

ABSTRACT OF THE DISSERTATION

INVESTIGATION OF MEMORY RELATED CORTICAL THALAMIC CIRCUITRY IN THE HUMAN BRAIN

by

Puck Charlotte Reeders

Florida International University, 2021

Miami, Florida

Professor Timothy A. Allen, Major Professor

This dissertation examined the role of medial prefrontal cortex (mPFC) and the hippocampus (HC) in episodic memory, and provides a novel approach to identify the midline thalamus mediating mPFC-HC interactions in humans. The mPFC and HC are critical to the temporal organization of episodic memory, and these interactions are disrupted in several mental health and neurological disorders. In the first study, I provide evidence that the mPFC is involved in ordinal retrieval, and the HC is active in temporal context retrieval in remembering the order of when events happen. In the second study, I focus on the anatomical basis of the mPFC-HC interactions which is reliant on the midline thalamus. I review in detail the anatomy of the midline thalamus both in location, and connectivity profile with the rest of the brain comparing the extensive anatomical evidence in rodents with the available evidence in monkeys and humans. This section also elaborates on the role of the midline thalamus in memory, stress regulation, wakefulness, and feeding behavior, and how pathological markers along the midline thalamus are a vanguard of several neurological disorders including Alzheimer's Disease, schizophrenia, depression, and drug addiction. Lastly, I devised a new approach to

identify the midline thalamus in humans *in vivo* using diffusion weighted imaging, capitalizing on known fiber connections gleaned from non-human animals, focusing on connections between the midline thalamus and the mPFC, medial temporal lobe and the nucleus accumbens. The success of this approach is promising for translational imaging. Overall, this dissertation provides new evidence on 1) complementary functional roles of the mPFC and HC in sequence memory, 2) a cross-species anatomical framework for understanding the midline thalamus in humans and neurological disorders, and 3) a new method for non-invasive identification of the midline thalamus in humans in vivo. Thus, this dissertation provides a new fundamental understanding of mPFC-midline thalamic-HC circuit in humans and tools for its non-invasive study in human disease.

TABLE OF CONTENTS

LIST OF FIGURES

FIGURE PAGE

ABBREVIATIONS AND ACRONYMS

3V	Third ventricle
ACC	Anterior cingulate cortex
AD	Alzheimer's Disease
AI	Agranular insular cortex
Amy	Amygdala
AM	Anteromedial nucleus of thalamus
AV	Anteroventral nucleus of the thalamus
BLA	Basolateral nucleus of the amygdala
BNST	Bed nucleus of the stria terminalis
BOLD	Blood oxygen level dependent
CA1-4	Cornu ammonis 1-4
CD	Central dorsal nucleus of thalamus
CeA:	Central nucleus of amygdala
CeM	Medial sector of central amygdala
CRH	Cortico-releasing hormone
Caud	Caudate
DWI	Diffusion weighted imaging
EEG	Electroencephalogram
EC	Entorhinal cortex
FA	Fasciculus nucleus of thalamus
Front Pol	Frontal pole

fMRI	Functional magnetic resonance imaging
GP	Globus Pallidus
HC, dHC, vHC	Hippocampus, dorsal, ventral
Hb	Habenula
HPA	Hypothalamic pituitary adrenal axis
HPT	Hypothalamus
IL	Infralimbic cortex (area 25)
IMD	Intermediodorsal nucleus of thalamus
Ins	Insular cortex
InSeq	In sequence
ithp	Inferior thalamic peduncle
lai	Lateral agranular insular cortex
LC	Locus Ceruleus
LH	Lateral hypothalamus
LSD	Least Square Difference
M1	Primary motor cortex
MD	Mediodorsal nucleus of thalamus
MRI	Magnetic resonance imaging
MTL	Medial temporal lobe
mtt	Mammillothalamic tract
mPFC	Medial prefrontal cortex
nACC	Nucleus accumbens
NMDA	N-methyl-D-aspartate

NREM	Non rapid eye movement
OFC	Orbitofrontal cortex
OlfTub	Olfactory Tubule
ORX	Orexin
OutSeq	Out of sequence
PAG	periaqueductal gray matter
PC	Paracentral nucleus of thalamus
PER	Perirhinal cortex
PET	Positron Emission Tomography
PFC	Prefrontal cortex
PIR	Piriform cortex
PL	Prelimbic cortex (area 32)
PBN	Parabrachial Nucleus
PrSub	Presubiculum
Put	Putamen
PT	Parataenial nucleus
PV	Paraventricular nucleus
R	Reticular nucleus of thalamus
RE	Nucleus Reuniens
REM	Rapid eye movement
RH	Rhomboid nucleus
RN	Raphe nuclei
RSME	Root mean square error

RSC	Retrospenial cortex
S1	Primary motor cortex
S2	Secondary motor cortex
Sept	Septum
Smt	Stria medullaris of thalamus
SMI	Sequence Memory Index
SN	Nucleus of the solitary tract
SPECT	Single-photon emission computed tomography
SSRI	Serotonin reuptake inhibitor
Stria	Striatum
Sub	Subiculum
TCM	Temporal Context Memory
VAmc	Magnocellular division of VA
VApr	Parvocellular division of ventral anterior
vSub	Ventral Subiculum
VLM	Ventrolateral medulla
VM	Ventral medial nucleus of thalamus
VTA	Ventral tegmental area
ZI	Zona incerta
WM	Working memory

CHAPTER 1

INTRODUCTION

The overarching goal of this dissertation was to investigate functional and anatomical aspects of the memory circuit in the human brain. Specifically, this dissertation examined the role of medial prefrontal cortex (mPFC) and the hippocampus (HC) in episodic memory, provided a cross species framework of the midline thalamus, and developed a novel approach to identify the midline thalamus mediating mPFC-HC interactions in humans. Interactions in the mPFC – midline thalamus – HC circuit are disrupted in several mental health and neurological disorders. Understanding the roles of these brain regions, and having the tools to investigate them, is of general importance for the understanding and investigation of mental health and neurological disorders.

1.1 Sequence memory is a fundamental component of episodic memory

Episodic memory allows us to remember past experiences (Tulving, 2002). How we remember sequences of events is a fundamental component of episodic memory. Remembering the order of sequences of events allows us to disambiguate episodes with similar content and make detailed predictions supporting decision making. Event sequences can be retrieved multiple different ways. Sequence memory retrieval can be driven both by ordinal associations, and temporal contexts. In an ordinal retrieval mode, items are remembered by their position within an event sequence (Dubrow and Davachi 2013; Allen et al. 2014; Long and Kahana 2019), providing sequential memory through well-established semantic or abstracted relationships (1^{st}, 2^{nd}, 3^{rd}, etc.). While for a temporal context retrieval mode, events are remembered through a gradually changing temporal context within which specific items have been associated (Howard and Kahana, 2002). The mPFC and HC are critical to memory processes including sequence memory. In chapter 2, I investigated the functional contributions of the mPFC and HC during a

sequence memory task that provides behavioral evidence of both ordinal and temporal context retrieval modes. To test ordinal modes, items were transferred between sequences but retained their position (e.g., AB3). Ordinal modes activated mPFC, but not HC. To test temporal contexts, I examined items that skipped ahead across lag distances (e.g., ABD). HC, but not mPFC, tracked temporal contexts. These current results suggest that the mPFC and HC are concurrently engaged in different retrieval modes in support of remembering *when* an event occurred. This evidence provides an important baseline for further investigation in impairment of sequence memory in aging and diseases such as Alzheimer's Disease, especially since studies have shown that individuals become more reliant on ordinal retrieval modes, and less dependent on temporal context memory (TCM) retrieval mode as they age (Bastin and Van der Linden 2010; Allen et al. 2015).

1.2 The medial prefrontal cortex and hippocampus do not work in isolation

Although the communication between the mPFC and HC are critical to memory, they do not have strong bidirectional structural connectivity with one another. More specifically, the HC has strong direct structural projections to the mPFC (Hoover and Vertes, 2007), but there are very few direct return projections from the mPFC to the HC in the rodent (Malik et al., 2021). In fact, return projections from mPFC to HC have only been described by one recent study (Malik et al., 2021), and these projections were observed only the to the dorsal HC.

Therefore, for strong bidirectional communication, another brain structure comes to play. Studies have shown that the midline thalamus serves as a hub integrating the communication between the hippocampus and the mPFC, which is critical for memory processing in rodents (Thielen et al., 2015, Hallock et al., 2016). The midline thalamus

acts as an important structure closing the communication loop between HC and mPFC. Based on specific patterns of anatomical connectivity in rodents and macaques, four midline thalamic nuclei have been identified: the paratenial nucleus (PT), paraventricular nucleus (PV), rhomboid nucleus (RH), and the nucleus reuniens (RE), and are critical to memory processes that the mPFC and HC are involved in (Hallock et al., 2016). The midline thalamus has strong bidirectional projections to regions of the mPFC, including the orbitofrontal cortex, infralimbic cortex, prelimbic cortex, and the rostral anterior cingulate (Hsu and Price, 2007; Vertes et al., 2007; Hoover and Vertes, 2012; Dolleman-van der Weel et al., 2019). Accordingly, the midline thalamus also has strong bidirectional projections to regions of the medial temporal lobe important for memory, including the HC, parahippocampus, entorhinal cortex and amygdala (Hsu and Price, 2007; Vertes et al., 2007; Hsu and Price, 2009; Hoover and Vertes, 2012; Dolleman-van der Weel et al., 2019). This dense bidirectionally connectivity suggests that these brain regions work together as a circuit. In chapter 3, I elaborate on the detailed connectivity profile of each midline thalamic nuclei.

1.3 The midline thalamus is critical for memory

The midline thalamus is critical to memory due to the connections it has with the HC and mPFC. The midline thalamus has bidirectional connections to both the HC and mPFC in rodents and monkeys (Hsu and Price, 2007; Vertes et al., 2007; Hsu and Price, 2009; Hoover and Vertes, 2012; Dolleman-van der Weel et al., 2019). Midline thalamic nuclei are involved in controlling and managing the level of activity of cortical structures that are associated to memory processing (Xu and Südhof, 2013, Hallock et al., 2016). For example, the mPFC controls hippocampal activation levels during memory encoding

via the RE in mice (Xu and Südhof, 2013) and can determine how specific or generalized a memory trace becomes (Xu and Südhof, 2013). Additionally, inactivation of RE impairs spatial working memory in rodents (Hallock et al., 2016; Viena et al., 2018). And inactivating mPFC projections to the RE heavily impairs sequence memory in rodents but does not impair other behaviors such as running speed (Jayachandran et al., 2019). These studies show the importance of the midline thalamus in memory processes.

1.4 The midline thalamus is involved in everyday functions

Moreover, the midline thalamic nuclei are also involved in other every day functions including stress regulation, wakefulness, and feeding behavior (Bubser and Deutch, 1991; Otake et al. 2002; Ren et al., 2018; Beas et al., 2020). For example, the PV is consistently activated following a wide variety of stressors including conditioned fear, sleep deprivation, foot shock, forced swimming, and handling (Otake et al., 2002; Spencer et al., 2004; Hsu et al., 2014;). Rodent and macaque studies show that projections from PV to brain regions involved in stress regulation representing pathways by which the PV can influence structures that regulate stress (Otake et al., 2002; Hsu et al., 2014). The midline thalamus is also involved in arousal and wakefulness (Ren et al., 2018). When the PV of the dorsal midline thalamus is suppressed, there is a reduction in wakefulness, and when activated, there is an induced transition from sleep to wakefulness (Ren et al., 2018). Additionally, activation of the pathway from dorsal midline thalamus to the nucleus accumbens (nACC) is linked to food-seeking behavior (Beas et al., 2020), suggesting that the midline thalamus is involved in behavior in responses to appetite. In chapter 3, I elaborate on the role of the midline thalamus in these functions in detail.

1.5 Impairment of the midline thalamus in neurological disorders

Impairments in the midline thalamus has been associated to multiple neurological disorders including Alzheimer's Disease, schizophrenia, depression, and drug addiction (Braak and Braak, 1991b; Pizagelli et al., 2003; Byne et al., 2009; Hamlin et al., 2009; Lisman et al., 2010). In Alzheimer's disease, while amyloid deposition was shown to be spread out through the thalamus, neurofibrillary tangles provided a more specific pattern of deposit in different nuclei of the thalamus, including the midline nuclei when symptoms are most severe (Braak & Braak, 1991b). In schizophrenia, the midline thalamus provides a nodal link for multiple functional circuits that are impaired (Byne et al., 2009), and may be involved in sending other brain regions in hyperdrive (Lisman et al., 2010). The role of PV in regulating chronic stress combined with its connectivity pattern and neurochemical input suggests it may play a role in clinical disorders and stress related psychopathology such as depression (Hsu and Price, 2009). Additionally, the PV of the midline thalamus is activated by exposure to drugs and to drug associated contexts and cues in drug addiction (Hamlin et al., 2009; Hsu and Price, 2009; Li and Kirouac, 2012). In chapter 3, I elaborate further on how pathology of the midline thalamus is involved in these neurological disorders in detail.

1.6 Finding the midline thalamus in humans

Given the importance of the midline thalamic nuclei, they have become popular brain regions in animal research studies, however, it is surprising that very little is known about the midline thalamic nuclei in humans. This, in part, is due to the difficulty in identifying the midline thalamus with current imaging technologies. First, the midline thalamic nuclei are relatively small compared to the rest of the brain, and second, there is

inter-individual variability in nuclear size, location, and their proximal location to the cerebrospinal fluid filled third ventricle. In chapter 4, I used a novel approach to identify and extract the midline thalamus in humans *in vivo* based on their known connectivity profile gleaned from non-human animal studies, by using probabilistic tractography and *k*-means clustering on diffusion weighted imaging (DWI) data. Thalamic nuclei were first clustered based on cortical and subcortical connectivity profiles, and clusters with high connectivity to regions with known connectivity to the midline thalamus found in rodent and macaque tracer studies were extracted. This approach revealed a midline thalamic cluster that is well connected to the agranular medial prefrontal cortex, nucleus accumbens, and medial temporal lobe and located directly adjacent the third ventricle. We created two masks for human midline thalamus dividing a dorsal midline thalamic mask, which includes the PV and PT, from a ventral midline thalamic mask, which includes the RH and RE. These are important divisions due to their different contributions to cognitive functions in rodents. Ultimately, this connectivity-based identification and segmentation method is important as it can be used to help characterize the involvement of the midline thalamus in functional and connectivity differences in neurological brain pathologies such as Alzheimer's Disease.

Overall, this dissertation provides evidence on the complimentary roles of the mPFC and HC in sequence memory, a cross-species anatomical framework for understanding the midline thalamus is humans and neurological disorders, and a novel approach for the identification of the midline thalamus in humans *in vivo*.

CHAPTER 2

Sequence memory retrieval modes in the human brain

Reeders, Hamm, Allen and Mattfeld (2021)

https://www.learnmem.cshlp.org/content/28/4/134.full

2.1 Summary

Remembering sequences of events defines episodic memory, but retrieval can be driven by both ordinality and temporal contexts. Whether these modes of retrieval operate at the same time or not remains unclear. Theoretically, medial prefrontal cortex (mPFC) confers ordinality, while the hippocampus (HC) associates events in gradually changing temporal contexts. Here, we looked for evidence of each with blood oxygenated level dependent (BOLD) fMRI in a sequence task that taxes both retrieval modes. To test ordinal modes, items were transferred between sequences but retained their position (e.g., AB3). Ordinal modes activated mPFC, but not HC. To test temporal contexts, we examined items that skipped ahead across lag distances (e.g., ABD). HC, but not mPFC, tracked temporal contexts. There was a mPFC and HC by retrieval mode interaction. These current results suggest that the mPFC and HC are concurrently engaged in different retrieval modes in support of remembering *when* an event occurred.

2.2 Introduction

Memory for sequences of events is a fundamental component of episodic memory (Tulving 1984; 2002; Allen and Fortin 2013; Howard and Eichenbaum 2013; Eichenbaum 2017). While different experiences share overlapping elements, the sequence of events is unique. Remembering the order of events allows us to disambiguate episodes with similar content and make detailed predictions supporting decision making.

At least two complementary memory processes contribute to the retrieval of events in the correct sequence: ordinal (Orlov et al. 2002) and temporal context (Howard and Kahana 2002) retrieval modes. Whether these disparate retrieval modes operate

coincidently or not remains an open question with consequences for understanding basic mechanisms of how we remember the events that unfold throughout our day. According to an ordinal retrieval mode, items are remembered by their position within an event sequence (Dubrow and Davachi 2013; Allen et al. 2014; Long and Kahana 2019) providing sequential memory through well-established semantic or abstracted relationships (1st, 2nd, 3rd, etc.). While for a temporal context retrieval mode, events are remembered through a gradually changing temporal context within which specific items have been associated. According to temporal contexts, when an element of a sequence is presented or retrieved (e.g., 'C' in AB**C**DEF), items that are more proximal in the sequence (e.g., the 'D' in the sequence) have a higher retrieval rate compared to items that are further away (e.g., the 'F' in the sequence). These temporal contexts result from item associations that are dependent on time varying neural activity (e.g., Eichenbaum 2014), and contribute to sequence memory through the reactivation of neighboring items during retrieval (Dubrow and Davachi 2013; Long and Kahana 2019).

The mPFC and HC are thought to contribute to sequence memory through ordinal representations and temporal contexts, respectively (Agster et al. 2002; Fortin et al. 2002; Kesner et al. 2002; DeVito and Eichenbaum 2011; Allen et al. 2016; Jenkins and Ranganath 2016). In rodents, mPFC disruptions impair sequence memory (DeVito et al. 2011; Jayachandran et al 2019), mPFC 'time cells' are evident (Tiganj et al. 2017), and positions within a sequence can be the main determinant of differential activity in mPFC neurons during spatial sequences (Euston and McNaughton 2006). In humans, mPFC activation is sensitive to temporal order memory (Preston and Eichenbaum 2013), and codes for information about temporal positions within image sequences regardless of the

image itself (Hsieh and Ranganath 2015). HC activations are also generally associated with temporal order memory (Kumaran and Maguire 2006; Ekstrom and Bookheimer 2007; Lehn et al. 2009; Ross et al. 2009; Jenkins and Ranganath 2010; Tubridy and Davachi 2011; Kalm et al. 2013; Hsieh et al. 2014; Goyal et al. 2018). Prior evidence further shows that the medial temporal lobe, specifically the HC formation, plays a critical role in the use of a TCM retrieval mode in the brain (Manns et al. 2007; Hsieh et al. 2014; Bladon et al. 2019). The HC binds events within temporal contexts (Eichenbaum et al. 2007; Dubrow and Davachi 2013; Bladon et al. 2019) through a gradually changing neural context (Manns et al. 2007; Mankin et al. 2012). Similarly, medial temporal lobe neuronal and BOLD activations in humans have demonstrated evidence for gradually evolving temporal contexts (Howard et al. 2012; Kalm et al. 2013; Kragel et al. 2015).

Here we tested the contributions of the mPFC and HC during a visual sequence memory task that provides behavioral evidence of both ordinal and temporal context retrieval modes (see Fig. 1A; task modified from Allen et al. 2014). Briefly, participants first memorized six visual sequences (six images each) in a single passive viewing phase, and then were instructed to make judgments as to whether individual items were subsequently presented in sequence (InSeq) or out of sequence (OutSeq) over 240 self-paced presentations of each of the six items from each sequence. In the task, the two retrieval modes are parsed using probe trials that place conflicting demands on ordinal (Allen et al. 2014; 2015; Orlov et al. 2000) and temporal context modes (Jayachandran et al. 2019). We first evaluated ordinal retrieval modes using items that were transferred from one sequence to another while retaining their ordinal position (Ordinal Transfers;

Fig. 1B). Evidence for an ordinal-based retrieval mode occurs when these probes are identified as in sequence because they occur in the same ordinal position as their original sequence. mPFC activations (but not HC) was strongest for these ordinal retrievals. Second, we evaluated a temporal context retrieval mode using items that skipped ahead (Skips; Fig. 1B) with shorter lag distances (ABC**F**EF) compared to larger lag distances (A**F**CDEF). Skips should be most difficult to detect on the shortest lag distances because proximal items in a sequence are more likely to be retrieved (Howard and Kahana 2002; Kragel et al. 2015) and thus judged as InSeq. HC activations (but not mPFC) tracked with lag distance, providing evidence the HC is more reflective of a temporal context-based retrieval mode. Importantly, a significant interaction was observed such that mPFC and HC differentially activated for ordinal and temporal context retrievals. Altogether, our data shows that sequence memory involves both retrieval modes. In line with these results, we suggest that understanding episodic memory requires more insight into the neurobiology of ordinal processing, in addition to the more often studied temporal contexts, in the mPFC and HC system.

2.3 Methods

Participants

Thirty-nine right-handed volunteers were recruited from Florida International University (FIU) and University of Miami to perform a magnetic resonance imaging (MRI) study that included a sequence memory task designed to investigate the ability of humans to learn and remember arbitrary sequences of items, and a temporal reward discounting task. Task order was counterbalanced across all participants. Here we report

results from the sequence memory task. All participants provided written consent in compliance with the local Institutional Review Board. Five participants were excluded from the final analysis due to failure to complete the task (n = 1) or because of poor performance (n = 4; sequence memory index score ≤0; see Sequence Memory Analysis section below). Participants excluded for poor performance had d-prime scores 2 standard deviations below the mean (M = 2.030, SD = 0.807). The final sample consisted of 34 individuals (19 females; mean age = 21 years, SD = 2).

Task Apparatus

The sequence task was run on a Dell computer using Matlab (R2015b) with custom scripts that included functions from Psychtoolbox (Psychtoolbox-3 distribution; http://www.psychtoolbox.org). Images were back-projected and viewed by participants with an angled mirror mounted on the head coil. Responses were recorded using a Current Designs MR-compatible 4-button inline response device (https://www.curdes.com).

Experimental Design and Statistical Analysis

Prescan Training

All participants began with a practice session to become acquainted with the structure of the task and the method of responding. During the practice session, participants viewed four low-memory demand sequence sets, each comprising six unique images: (1) individual arrows at 0°, 60°, 120°, 180°, 240°, and 300°, presented in a clockwise fashion (Fig1A, Seq1); (2) a dot moving from the upper left to the lower right corner (Fig. 1A, Seq2); (3) bars of different colors moving from left to right (not shown);

and (4) letters A, B, C, D, E, and F positioned in the center of the screen (not shown). Participants were asked to memorize sequences after a single "study" presentation during which the items were passively viewed. Later the practice sequences were tested with 15 unique memory probes per sequence. Testing was self-paced; each sequence was preceded by a screen with the words "Press the button to begin". To initiate an image in the sequence, participants were required to press and hold a button. If the image was in sequence (InSeq), participants were instructed to hold down the button until the image disappeared on its own at 1 s (the decision threshold), after which they could release the button. If the item was out of sequence (OutSeq), participants were instructed to release the button prior to the decision threshold (<1 s), at which point the image would disappear upon button release. The self-pacing resulted in a mean interval between items in a sequence of 0.412 ± 0.532, and a mean interval between sequence sets of 0.760 ± 0.252. Prescan training was conducted on a Dell desktop computer.

Sequence Memory Task

During the Sequence Memory Task, participants were presented with two sequences from prescan training (*low-memory demand;* Fig. 1A, Seq 1-2), and four novel sequences consisting of six unique fractal images (*high-memory demand;* Fig. 1A, Seq 3-6). The exact composition of the novel fractal sequence sets was different for each participant. Sets were selected randomly, without replacement, from a bank of 240 unique fractal images. Similar to the prescan training, participants were asked to view and memorize the sequences after a single presentation in a passive viewing phase. Following the passive viewing phase, sequences were presented in a pseudorandom

order, participants made judgments as to whether each item in a sequence was presented InSeq or OutSeq. Testing was self-paced and followed the same structure as the prescan training. The words “Press the button to begin” preceded the beginning of each sequence. A button depression with the right index finger initiated the presentation of each image in a sequence. If the participants judged the current image to be InSeq, they would hold the button until the decision threshold (1 s, when the image disappeared), after which they could release the button. If the image was OutSeq, they were instructed to release the button before the 1 s decision threshold. Sequence order was determined by the following rules: (1) each sequence was presented first with all images in the correct order. (2) In the first half of testing (first 120 sequences), OutSeq items were either the same image appearing twice (Repeats) or an item appearing too early (Skips; see probe trial description below). In the second half of testing (second 120 sequences), OutSeq items could now include images appearing from a different sequence, but in the correct ordinal position (Ordinal Transfers). Ordinal Transfers were introduced later so participants would not adopt an explicit ordinality strategy at the outset of the study given the dominance of ordinal retrieval modes early in sequence memory (Orlov et al. 2000). The six sequences were presented 40 times each, for a total of 240 sequence presentations. Half of the total sequences contained one OutSeq and five InSeq images; the remaining consisted only of correctly sequenced items. InSeq and OutSeq sequence sets were randomly presented throughout testing. The Sequence Memory Task consisted of 15 min blocks of continuous performance separated by a brief break (<1 min) to provide participants a rest. The number of blocks was dependent on the pace of the participant.

Out of all the analyzed participants, most participants completed the task in four blocks (n = 29), while the remainder finished in either three (n=1) or five (n=4).

OutSeq Probe Trials

Three distinct types of OutSeq probe trials were used during the test phase: Ordinal Transfers, Repeats (reverse lags) and Skips (forward lags). OutSeq items were counterbalanced across sequence sets, never presented in first position (Pos1), and each OutSeq instance was unique. Due to the nature of the OutSeq trials, there could not be equal distribution of probe trials across all possible positions, and occurred as follows: Pos1, 0%; Pos2, 7.5%; Pos3, 17,5%; Pos4, 50%; Pos5, 17.5%; Pos6, 7.5%.

Ordinal Transfers. OutSeq trials where an item from one sequence was 'transferred' to a different sequence while retaining its correct ordinal position were considered Ordinal Transfers (Fig. 1B, *Ordinal Transfer*). For example, consider two sequences consisting of ABCDEF and UVWXYZ. An ordinal transfer into the first sequence might have Y at the 5th position ABCDYF. While Y occupies its original 5th position, it otherwise does not belong to the current sequence (Y does not normally follow D). Distribution of Ordinal Transfers across all possible positions: Pos1, 0%; Pos2, 7.5%; Pos3, 17,5%; Pos4, 50%; Pos5, 17.5%; Pos6, 7.5%.

Repeats (reverse lags). An OutSeq item was considered a Repeat if the image previously appeared in the current sequence and was repeated (Fig. 1B, *Repeat*). Repeats occurred at multiple lag distances, represented as negative values from repeat presentation to the original presentation, ranging from -2 (e.g., ABCBEF) to -5 (e.g., ABCDEA). A lag distance of -1 was not used due to the lack of an intervening item.

Distribution of Repeats across all possible positions: Pos1, 0%; Pos2, 0%; Pos3, 7.5%; Pos4, 50%; Pos5, 27.5%; Pos6, 15%.

Skips (forward lags). OutSeq images were considered Skips when presented too early in the sequence (e.g., AB<u>E</u>DEF; Fig. 1B, *Skip*). Skips occurred at all lag distances, represented as positive values from early presentation to original presentation, ranging from +1 (e.g., ABCD<u>F</u>F) to +4 (e.g., A<u>F</u>CDEF). Distribution of Skips across all possible positions: Pos1, 0%; Pos2, 15%; Pos3, 27.5%; Pos4, 50%; Pos5, 7.5%; Pos6, 0%.

Sequence Memory Analysis

To evaluate whether participants demonstrated sequence memory, we compared the observed and expected frequencies of InSeq and OutSeq responses using *G*-tests (Sokal and Rohlf 1995). Responses to each item were sorted into a 2 x 2 matrix based on accuracy (correct/incorrect) and sequence condition (InSeq/OutSeq), as done previously (Allen et al. 2014; Jayachandran et al. 2019). For the sequence memory analysis, only "high memory" sequence sets were included. Responses to the first item of each sequence were excluded from analysis. Ordinal Transfers were excluded from this analysis because they were used to parse retrieval modes rather than measure performance. For comparison we evaluated sequence memory using d-prime, a measure of memory specificity derived from signal detection theory. Hits were defined as InSeq trials that were correctly identified as InSeq, misses were InSeq trials that were incorrectly identified as OutSeq, correct rejections were OutSeq probe trials that were correctly

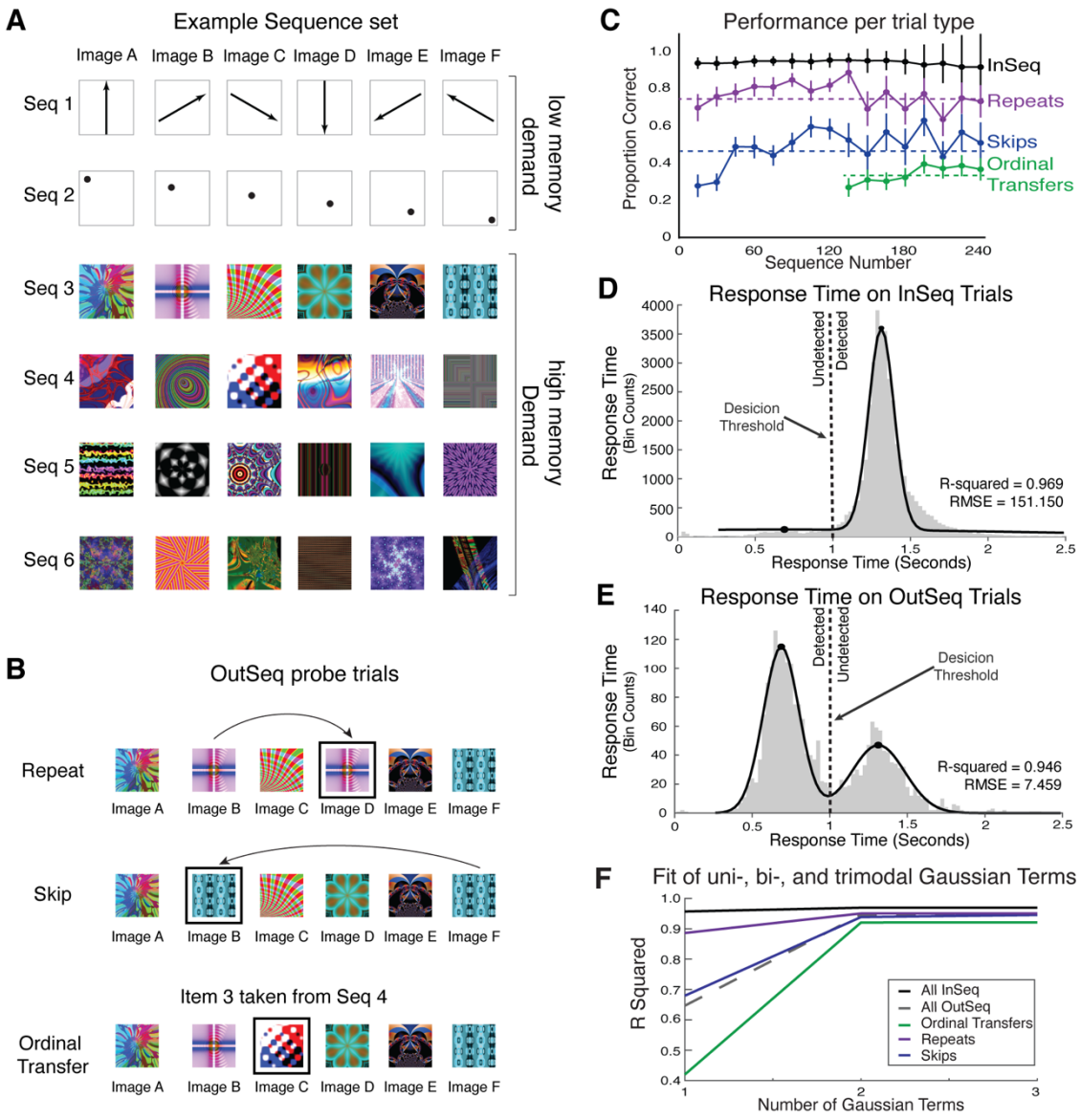

Figure 1. Sequence memory task and overall performance levels. Participants were tested on a sequence memory task that differentially burdens different retrieval modes using different out of sequence probe trial types. **A**, an example sequence set which included 6 sequences. Two sequences were *low memory demand* sequences and four were *high memory demand* sequences. **B**, there were three out of sequence probe trial types: Items that were repeated in the sequence (Repeats), items that were presented too early in the sequence (Skips), and items that transferred from one sequence to another, while remaining in their ordinal position (Ordinal Transfers). Repeats and Skips occurred throughout the whole task, whereas Ordinal Transfers occurred during the second half only. **C**, accuracy throughout the task (error bars = ± 1SD). Participants performed best on Repeats, then Skips, and poorest on Ordinal Transfers. **D**, distributions of response times for all InSeq trials (grey bars) and (**E**) for all OutSeq trials (grey bars) for all participants with a fitted 2-term Gaussian curve (black line). **F**, a bimodal Gaussian curve fit better than a unimodal curve for InSeq and OutSeq trials. A trimodal curve did not improve the fit and increased the root mean squared error (not shown), suggesting distinct decisions decision making between two decisions. It was very rare to observe responses outside of the two distributions.

identified as OutSeq, and false alarms were defined as OutSeq probe trials that were incorrectly judged to be InSeq. The same conclusions were drawn with both approaches, thus, here we only report the results from the G-tests given its robustness to response biases as the current task has an overall greater number of InSeq responses.

Additionally, we examined overall sequence memory performance, using a summary statistic called the Sequence Memory Index (SMI; Equation 1). SMI normalizes the proportion of InSeq and OutSeq items across different conditions and represents sequence memory performance as a single value ranging from -1 to 1. A SMI of "1" represents perfect sequence performance (response time > 1 s for all InSeq items and < 1 s for all OutSeq items), and 0 represents chance performance. Note that an SMI score of -1 would indicate an incorrect response to every single item (response times < 1 s for all InSeq items and > 1 s for all OutSeq items). Negative SMIs rarely occurred, poor performance was typically captured by SMI scores close to zero. SMI was calculated for both low and high memory demand sequences and has been used in previous human studies to facilitate comparisons (Allen et al. 2014; 2015).

Equation 1. $$SMI = \frac{(0.9\mathrm{Incor})(0.1\mathrm{Outcor}) - (0.9\mathrm{Ininc})(0.1\mathrm{Outinc})}{\sqrt{(0.9\mathrm{Incor}+0.9\mathrm{Ininc})(0.1\mathrm{Outcor}+0.1\mathrm{Outinc})(0.9\mathrm{Incor}+0.1\mathrm{Outinc})(0.9\mathrm{Ininc}+0.1\mathrm{Outcor})}}$$

Response Time Analysis

To evaluate whether participants made distinct InSeq and OutSeq decisions for the trial types, we analyzed the distribution of response times for all the participants for all InSeq trials, all OutSeq trials, and then the OutSeq trials divided up by Ordinal Transfers, Skips and Repeats. A distribution was created with response times bins of

0.025 seconds on the x-axis, and count on the y-axis for all the participant response times combined. If two distinct decisions were being made, we would expect to see a bimodal distribution: one peak occurring before 1 second (OutSeq decision) and the other peak occurring after 1 second (InSeq decision). To statistically evaluate whether the response time distribution fit better using a bimodal Gaussian distribution rather than a uni- or trimodal Gaussian distribution, we fitted a 1-term (unimodal), 2-term (bimodal) and 3-term (trimodal) Gaussian curve onto the data using cftoolbox in MATLAB. To compare which Gaussian model was the best fit for the response time distribution, we recorded the r-squared, root mean squared error and the x-values of the peaks of the models.

Detailed Position and Lag Analysis

To evaluate strategies or mechanisms of sequence memory performance, a detailed analysis based on ordinal position and lag distance was performed for each OutSeq probe type (Ordinal Transfers, Skips, and Repeats). For Ordinal Transfers, we evaluated performance across positions (Pos2 thru Pos6). For Skips, we evaluated performance across *n*-forward lag distances (*n*-forward lags: +1, +2, +3, and +4). Smaller *n*-forward lags occurred more often because more combinations were available. For Repeats, we evaluated performance across the *n*-reverse lags (Fig. 3A; *n*-reverse lags: -2, -3, -4, and -5). Smaller *n*-reverse lags occurred more often because more combinations were available. We compared each position or lag distance performance (accuracy and SMI) using repeated-measures ANOVAs followed by one-sample t-tests. To account for the potential of a response bias (the assumption by participants of each item being in sequence) in the accuracy measures, we calculated an adjusted response bias level as

follows: (1) we calculated the observed response bias for holding the button for >1 sec on Pos 2 through Pos 6, irrespective of the InSeq or OutSeq status, which was 90.466%, and (2) we calculated the complement of that response bias and set that as the response bias for probe trials, which was 9.534%. To assess differences in variability amongst probe trial types, trial specific performance was converted to a z-score across positions (Ordinal Transfers) and lags (Skips and Repeats) for each participant. Three mixed general linear models were performed with subject as a random effect and position or lag as a fixed effect. The resulting residuals were subsequently squared and averaged across positions or lags resulting in probe trial type specific residuals for each participant. We conducted a repeated measures ANOVA with Greenhouse-Geisser corrections and LSD posthoc testing to compare the averaged squared residuals across probe trial types (Ordinal Transfers, Skips and Repeats).

Neuroimaging Acquisition

Neuroimaging data were collected on a General Electric Discovery MR750 3.0T scanner using a 32-channel head coil at the University of Miami Neuroimaging Facility. Structural T1-weighted images were collected (186 slices, flip angle = 12°; TE = 3.68 ms, TR = 9.184 ms, TI = 650 ms, matrix = 256 x 256 mm; FOV = 256 mm, slice thickness = 1.0 mm). Whole-brain T2*-weighted, blood oxygen level dependent (BOLD) echo-planar imaging data (42 slices, interleaved, bottom-up; flip angle = 75°; TE = 25 ms; TR = 2000 ms; matrix = 96x96 mm; FOV = 240 mm, slice thickness = 3.0 mm, voxel size = 2.5 x 2.5 x 3.0 mm^3) were collected during the task.

Neuroimaging Preprocessing

Preprocessing was performed using a pipeline developed in Nipype v0.1 (Gorgolewski et al. 2011), wrapping tools from Analysis of Functional Neuroimages (AFNI v16.3.18; Cox 1996), FSL (v5.0.10), FreeSurfer (v5.1.0; Dale et al. 1999), Advanced Normalization Tools (v2.2.0; Avants et al. 2008), and Artifact Detection Tools (ART; www.nitrc.org). Following DICOM conversion, cortical surface reconstruction and cortical/subcortical segmentation was performed on all T1-weighted structural scans. Functional data were first 'despiked' to remove and replace intensity outliers in the functional time series. The data were simultaneously slice-time and motion corrected (Roche 2011). An affine transformation matrix was calculated during coregistration of the mean of each participant's functional scans to their structural scan using FreeSurfer's boundary-based registration algorithm (BBregister). Brain masks were created by binarizing the aparc+aseg (automatic cortical parcellation and automatic segmentation volume) file created using FreeSurfer, and dilating by one voxel. The resulting binary masks were subsequently coregistered to the functional data by applying the inverse of the affine coregistration matrix. Motion and intensity outliers were then identified using the rapid art artifact detection tool as implemented in nipype. Time-points at which intensity either exceeded three standard deviations or composite frame-wise displacement was greater than 1 mm were flagged as outliers to serve as subsequent regressors of no interest in the first-level general linear models. Finally, functional data were spatially filtered with a 5 mm FWHM maximum Gaussian kernel using the *SUSAN* algorithm (FSL).

Neuroimaging Normalization

A study-specific template was generated using Advanced Normalization Tools (ANTs). Each structural scan was skull-stripped by multiplying the T1-weighted structural scan by the binarized and dilated aparc+aseg file in structural space. Each skull-stripped brain was then rigid-body transformed (no scaling or shearing) to Montreal Neurological Institute space using FSL's *FLIRT* algorithm. This first pass was used to minimize large spatial shifts between participants and generate a template close to a commonly used reference. Following visual inspection, a study template was created using the buildtemplateparallel.sh script from ANTs. After template generation, each participant's skull-stripped brain was normalized using non-linear symmetric diffeomorphic mapping implemented by ANTs. The resulting warps were applied to contrast parameter estimates following fixed-effects modeling for subsequent group-level tests.

Neuroimaging Analysis

Functional data were analyzed according to a general linear model approach using FMRIB's Software Library (www.fmrib.ox.ac.uk/fsl). Two separate univariate general linear models were used for first-level analyses: (1) a performance (undetected/detected) model; and (2) a lag model.

All first-level models included event and nuisance regressors. The performance analysis contained eight event regressors of interest: detected and undetected InSeq, Repeats, Skips, and Ordinal Transfers. Event regressors were convolved with FSL's double gamma hemodynamic response function with an onset beginning at the first

stimulus item of a sequence and a duration equal to the length of time required to evaluate all the items in that sequence (mean = 9.917 s per subject). The lag analysis comprised six event regressors of interest: Repeats at different *n*-reverse lags (*n*-reverse lags: -2, -3, and -4), and Skips at different *n*-forward lags (*n*-forward lags: +1, +2, and +3). InSeq and Ordinal Transfers irrespective of behavioral performance were also included. We evaluated linear changes in activation across lags with the following contrast weights: -1, 0, 1 and 1, 0, -1 for Repeats (*n*-reverse lags: -2, -3, and -4) and Skips (*n*-forward lags: +1, +2, and +3). We did not include a lag of -5 or +4, as the numbers of trials with these lags per participant was not sufficient (1 trial). Regressors for baseline or low memory sequences were also included in both models. Nuisance regressors included motion parameters (x, y, z translations; pitch, roll, yaw rotations), first and second derivatives of the motion parameters, normalized motion, first, second, and third order Lagrange polynomials, as well as each outlier time-point that exceeded the artifact detection thresholds identified during preprocessing.

Following the first-level analysis, a fixed effects analysis across experimental runs was performed for each participant for the respective contrasts of interest (e.g., performance analysis: undetected versus detected probe trials; lag analysis: linear contrasts). The performance analysis contrasts were limited to sequences with undetected versus detected probe trials in an attempt to maintain parity in the number of events that were being compared. Contrast parameter estimates from the fixed effects analysis were normalized to the study-specific template and group-level analyses were performed using FSL's *randomise* threshold-free cluster enhancement (tfce) one sample t-test. To test *a priori* hypotheses with respect to the functional contributions of the mPFC and HC

during sequence memory retrieval, we constrained our voxel-wise analyses at the group level to the bilateral mPFC and medial temporal lobe using masks of these regions. Whole-brain exploratory analyses were used to follow up our anatomically directed tests. In the performance analysis, some participants were missing key events of interest (e.g., detected Ordinal Transfers or undetected Repeat probes). These participants were not included in the relevant analyses, reducing the sample size for the detected versus undetected Ordinal Transfer contrast to n = 26, and for the detected versus undetected Repeat probe trial contrast to n = 31.

To directly examine the relation between sequence memory retrieval mode and regional contribution, as a post hoc follow up to our voxel wise analyses, we used an anatomical region of interest analysis to perform a 2x2 repeated measures factorial ANOVA with brain region (right anterior HC vs. mPFC) and strategy (ordinal retrieval mode [Ordinal Transfer undetected > Ordinal Transfer detected] vs. temporal context retrieval mode [TCM; Positive Linear Skip contrast]) as the within subjects factors and participants as the repeated measure. Anterior HC region of interest was manually drawn in coronal slices. The anterior most boundary of the hippocampus was defined by the white matter separating the hippocampus from the amygdala, the lateral and medial boundaries were defined by the cerebral spinal fluid of the lateral ventricle, the inferior boundary was white matter of the parahippocampal gyrus, while the superior boundary was the wavelike contour of the pes digitations/alveus/horizontal line connecting the middle of the medial border of the lateral ventricle to the surface of the uncus. The anterior HC was delineated from the posterior HC by the presence of a small anatomical protrusion of medial HC into the lateral ventricle that was absent in the posterior HC –

uncal apex. The mPFC region of interest was created by binarizing the medial orbitofrontal, superior frontal, rostral anterior cingulate, and the caudal anterior cingulate FreeSurfer labels.

2.4 Results

Sequence Memory

First, we investigated behavioral sequence performance in two ways: (1) using a Sequence Memory Index (SMI), and (2) with accuracy measured as the simple percent correct. SMI is a summary statistic measuring the overall sequence memory performance and normalizes the proportion of in sequence (InSeq) items and out of sequence (Outseq) items across different conditions. SMI represents sequence memory performance as a single value ranging from -1 to 1 (Equation 1). An SMI of "1" represents perfect sequence performance (response times > 1 s for all InSeq items and < 1 s for all OutSeq items), and 0 represents chance performance (see Sequence Memory Analysis section in Methods). For accuracy, we evaluated the percentage of OutSeq items (Repeats, Skips and Ordinal Transfers) that were identified as out of sequence, and InSeq items that were identified as in sequence. We analyzed the low and high memory demand sequences separately (Fig. 1A). As expected, participants performed significantly better than chance (SMI = 0) on both low memory sequences (SMI_{low}: 0.751 ± 0.173; $SMI_{low\ vs.\ chance}$: $t_{(33)} = 37.065$, $p = 3.487 \times 10^{-23}$) and high memory sequences (SMI_{high}: 0.582 ± 0.170; $SMI_{low\ vs.\ chance}$: $t_{(33)} = 19.690$, $p = 5.391 \times 10^{-20}$), but performance was significantly better with low memory sequences ($SMI_{low\ vs.\ high}$: $t_{(33)} = -4.839$, $p = 2.958 \times 10^{-5}$). High memory sequences were used for all subsequent analyses because they optimally taxed the

different sequence retrieval modes. Importantly, there was no testing order effect (1st or 2nd experimental block) on sequence memory ($SMI_{1st\ block} = 0.571 \pm 0.190$, $SMI_{2nd\ block} = 0.594 \pm 0.152$; $SMI_{1st\ vs.\ 2nd}$: $t_{(32)} = -0.386$, $p = 0.702$), nor did we observe any sex differences ($SMI_{female} = 0.566 \pm 0.197$, $SMI_{male} = 0.602 \pm 0.133$; $SMI_{female\ vs.\ male} = t_{(32)} = -0.612$, $p = 0.545$). Thus, we pooled these groups.

Next, we evaluated overall performance across each of the three memory probes individually using percent correct for ease of interpretation. Overall, accuracy on InSeq items was 95.827 ± 4.396% (95.477 ± 4.393 % when excluding the first item of the sequence), and accuracy on OutSeq items was 52.726 ± 15.848%. As in previously published studies (Allen et al. 2014; 2015), we found that Ordinal Transfers (Fig. 1B-C; Accuracy = 34.927 ± 4.120%) were the most difficult, followed by Skips (Fig. 1B-C – Skips; Accuracy = 49.205 ± 2.686%), with Repeats being the easiest (Fig. 1B-C – Repeats; Accuracy = 78.584 ± 2.853%). There was a significant difference in performance across probe types ($F_{(2,66)} = 85.714$, $P = 3.433 \times 10^{-14}$) suggesting differences in the available retrieval modes driven by the different conditions. Post hoc pairwise comparisons showed that the performance on Repeats was significantly higher compared to Skips (mean difference = 0.294 ± 0.020, $p = 8.137 \times 10^{-16}$) and Ordinal Transfers (mean difference = 0.437 ± 0.039, $p = 1.078 \times 10^{-12}$) and performance on Skips was significantly higher compared to Ordinal Transfers (mean difference = 0.143 ± 0.039, $p = 0.001$). The same pattern of results was evident when using SMI which controls for idiosyncratic response patterns. Importantly, participants performed each of the three probe types significantly better than chance (Ordinal Transfers: $t_{(33)} = 6.164$, $p = 5.951 \times 10^{-7}$, Repeats: $t_{(33)} = 24.201$, $p = 1.403 \times 10^{-22}$; Skips: $t_{(33)} = 14.771$, $p = 4.203 \times 10^{-16}$).

For all probe types, learning was rapid (asymptotic within a few trials), and performance was steady throughout the duration of the experiment (Fig. 1C). Thus, performance on the task, and the accompanying differences in the brain imaging data, primarily reflect the distinct memory retrieval modes driven by the specific probe conditions.

Next, we looked whether participants made distinct responses on trials that were InSeq or OutSeq by examining the distribution of response times in detail (Wolpert and Land 2012; Maloney and Zhang 2010). Due to the nature of our task, we expected to observe a bimodal distribution of response times (by design in Allen et al. 2014). For all trial types we observed bimodal distributions suggesting two distinct decisions (InSeq vs. OutSeq) were being made under all conditions (Fig. 1D-E; grey bars). To explore the nature of these distributions statistically, we evaluated the InSeq and OutSeq response distributions by fitting Gaussian curves and comparing fits with unimodal (1-term Gaussian curve), bimodal (2-term Gaussian curve), and trimodal (3-term Gaussian curve) models (Fig. 1F). The outcomes indicated that 2-term Gaussian curves were a better fit for InSeq trials (Fig. 1D; Black line; R-squared = 0.969, root mean square error (RMSE) = 151.150, $x_{peak\ 1} = 0.688$, $x_{peak\ 2} = 1.313$) compared to a 1-term Gaussian curve (Fig. 1F; R-squared = 0.9568, RMSE = 176.950, $x_{peak\ 1} = 1.313$) or 3-term Gaussian curve (Fig. 1F; R-squared = 0.969, RMSE = 152.918, $x_{peak\ 1} = 0.688$, $x_{peak\ 2} = 1.313$, $x_{peak\ 3} = 1.313$). OutSeq trials were also better fit by 2-term Gaussian curve (Fig. 1E; Black line; R-squared = 0.946, RMSE = 7.4596, $x_{peak\ 1} = 0.688$, $x_{peak\ 2} = 1.3125$) compared to a 1-term Gaussian curve (Fig. 1F; R-quared = 0.6465, RMSE = 18.846, $x_{peak} = 0.713$) or 3-term Gaussian curve (Fig. 1F; R-squared = 0.946, RMSE = 7.546, $x_{peak\ 1} = 0.688$, $x_{peak\ 2} = 1.313$, $x_{peak\ 3} = 2.338$). The mean response time for detected InSeq items was 1.369 ±

0.089 seconds, and for undetected InSeq items 0.708 ± 0.111 seconds. For detected OutSeq items the mean response time was 0.717 ± 0.0539 seconds, and 1.353 ± 0.110 seconds for undetected OutSeq items. These results provide further evidence that two sequence decisions are being made, and that undetected or incorrect responses reflected a sequence memory error. Importantly, it was very rare to observe early or late responses outside of these bimodal response distributions. Such responses would be observed with accidental releases or inattentional effects that might confound subsequent behavioral and BOLD fMRI analyses.

Ordinal Memory Retrievals

An ordinal retrieval mode is known to contribute to memory for sequences of events which we tested for here using Ordinal Transfer probe trials (e.g., A**2**CDEF, Fig. 2A). If participants *exclusively* used an ordinal retrieval mode (e.g., A goes in the 1st position, B goes in the 2nd position, etc.), then these probes would always be remembered as being InSeq (since "2" is in the same position as B). An ordinal retrieval mode would drive performance on these trials to very low detection levels, possibly to chance, if no other retrieval mode was engaged because of this ordinal interference. Moreover, if an ordinal retrieval mode was used, we would not expect large differences in accuracy as a function of transfer position. Conversely, if participants relied exclusively on another process, such as a temporal context mode, then Ordinal Transfers would be very easily identified as OutSeq (since "2" does not follow A, and in fact it doesn't go with any of the items in that sequence). Non-ordinal retrieval modes would drive performance to very

high levels on Ordinal Transfer probe trials, probably to the same levels as at Repeats (as a good empirical benchmark for asymptotic performance) or higher.

We found Ordinal Transfers were performed significantly better than chance across all positions (Fig. 2B, red stars; Table 1A; Pos2: 0.314 ± 0.357; $Pos2_{vs.\ Response\ bias}$: $t_{(33)} = 3.566$, $p = 0.001$; Pos3: 0.338 ± 0.313; $Pos3_{vs.\ Response\ bias}$: $t_{(33)} = 4.512$, $p = 7.712 \times 10^{-5}$; Pos4: 0.347 ± 0.258; $Pos4_{vs.\ Response\ Bias}$: $t_{(33)} = 5.670$, $p = 2.549 \times 10^{-6}$; Pos5: 0.354 ± 0.283; $Pos5_{vs.\ Response\ bias}$: $t_{(33)} = 5.334$, $p = 6.892 \times 10^{-6}$; Pos6: 0.373 ± 0.336; $Pos6_{vs.\ Response\ bias}$: $t_{(33)} = 4.811$, $p = 3.212 \times 10^{-5}$) suggesting participants utilized non-ordinal retrieval modes for these trials. However, performance was much lower than Repeats (Fig. 2B, purple stars; Table 1C; $Pos2_{vs.\ Repeats}$: $t_{(33)} = -7.711$, $p = 7.019 \times 10^{-9}$; $Pos3_{vs.\ Repeats}$: $t_{(33)} = -8.338$, $p = 1.224 \times 10^{-9}$; $Pos4_{vs.\ Repeats}$: $t_{(33)} = -9.917$, $p = 1.996 \times 10^{-11}$; $Pos5_{vs.\ Repeats}$: $t_{(33)} = -8.919$, $p = 2.621 \times 10^{-10}$; $Pos6_{vs.\ Repeats}$: $t_{(33)} = -7.175$, $p = 3.185 \times 10^{-8}$) and Skips (Fig. 2B, blue stars; Table 1B; $Pos2_{vs.\ Skips}$: $t_{(33)} = -2.912$, $p = 6.390 \times 10^{-3}$; $Pos3_{vs.\ Skips}$: $t_{(33)} = -2.870$, $p = 7.104 \times 10^{-3}$; $Pos4_{vs.\ Skips}$: $t_{(33)} = -3.284$, $p = 2.426 \times 10^{-3}$; $Pos5_{vs.\ Skips}$: $t_{(33)} = -2.854$, $p = 7.400 \times 10^{-3}$; $Pos6_{vs.\ Skips}$: $t_{(33)} = -2.075$, $p = 4.589 \times 10^{-2}$) suggesting a heavy reliance on an ordinal retrieval mode.

We found no significant difference in performance across positions (Fig. 2B; $F_{(4, 132)} = 0.331$, $p = 0.786$). The observed behavioral performance suggests that participants were disproportionally using an ordinal retrieval mode (e.g., lower performance when compared to Repeats and Skips) in combination with other non-ordinal retrieval modes to a lesser extent (i.e., performance was still better than the response bias chance levels). A 2-term Gaussian curve (Fig. 2C, black line) best fit the Ordinal Transfer response time distribution (Fig. 2C, green bars; R-squared =0.938, RMSE = 4.956, $x_{peak\ 1} = 0.688$, $x_{peak\ 2}$

= 1.313) compared to a 1-term Gaussian curve (Fig. 1F; R-squared =0.679, RMSE = 11.182, $x_{peak\ 1}$ = 1.313) or 3-term Gaussian curve (Fig 1F; R-squared = 0.945, RMSE = 4.726, $x_{peak\ 1}$ = 0.713, $x_{peak\ 2}$ = 1.313, $x_{peak\ 3}$ = 2.3875). The mean response time for Ordinal Transfers undetected was 1.337 ± 0.097 seconds and for Ordinal Transfers detected 0.710 ± 0.119 seconds. Again, these data suggest that two distinct sequence decisions were being made.

Table 1A	**Ordinal Transfer vs Response Bias**		
	t-value	df	prob.
Position 2	3.566	33	0.001
Position 3	4.512	33	7.712 x 10-5
Position 4	5.670	33	2.549 x 10-6
Position 5	5.334	33	6.892 x 10-6
Position 6	4.811	33	3.212 x 10-5

Table 1B	**Ordinal Transfer vs Skips**		
	t-value	df	prob.
Position 2	7.711	33	7.019 x 10-9
Position 3	-8.338	33	1.224 x 10-9
Position 4	-9.917	33	1.996 x 10-11
Position 5	-8.919	33	2.621 x 10-10
Position 6	-7.175	33	3.185 x 10-8

Table 1C	**Ordinal Transfer vs Repeats**		
	t-value	df	prob.
Position 2	-2.912	33	6.390 x 10-3
Position 3	-2.870	33	7.104 x 10-3
Position 4	-3.284	33	2.426 x 10-3
Position 5	-2.854	33	7.400 x 10-3

Table 1. *Ordinal Transfer performance.* Performance compared to the calculated response bias, and performances on Skips and Repeats, sorted by position in the sequence.

A prediction from the these conflicting retrieval modes is that performance variability would be high between participants and across positions. In line with this hypothesis, we observed higher Ordinal Transfer variability when compared to Repeats, and much higher when compared to Skips (Fig. 2D-E; $M_{residual}$ = 0.795 ± 0.074). A repeated-measure ANOVA with Greenhouse-Geisser correction showed significant main effect among regression residuals of Ordinal Transfers, Skips and Repeats ($F_{(2, 54)}$ = 23.866, p = 1.843 x 10^{-8}). Regression residuals of Ordinal Transfers were significantly higher compared to Skips (mean difference = 0.530 ± 0.089, p = 2.523 x10^{-6}) and Repeats (mean difference = 0.158

$\pm$ 0.028, $p = 5.627x10^{-6}$). Regression residuals of Repeats were significantly higher compared to Skips (mean difference = 0.373 $\pm$ 0.099, p = 0.001).

mPFC Activations and Ordinal Retrievals

We hypothesized that using an ordinal retrieval mode would be related to activations in the mPFC (e.g., Hsieh and Ranganath, 2015). Algorithmically, this would be evident when contrasting undetected (i.e., using an ordinal retrieval mode) versus detected (i.e., using a non-ordinal retrieval mode) during Ordinal Transfer trials. We also reasoned that the use of an ordinal retrieval mode would facilitate the detection of Skips and Repeats (because of the ordinal position mismatch), thus, when assuming an ordinal retrieval mode for Skips and Repeats, we evaluated activations contrasting detected versus undetected trials. We used an anatomical region of interest (ROI) analysis to evaluate mPFC activity across the three probe trial types. In support of our hypothesis the mPFC was significantly more active on Ordinal Transfers relative to both Skips and Repeats for contrasts that assumed ordinal retrieval modes (Fig. 2F; $F_{(2, 56)} = 4.038$, p = 0.034). Post hoc tests (LSD) further supported the conclusion that the mPFC was most active in the comparison of undetected versus detected Ordinal Transfers (M = 0.708 $\pm$ 1.998) relative to detected versus undetected Skips (M = -0.649 $\pm$ 1.445, p = 0.051) and Repeats (M = -0.431 $\pm$ 1.728, p = 0.005). No significant difference was identified in mPFC activation between detected versus undetected Skips and Repeats (mean difference = 0.061 $\pm$ 0.437, p = 0.890). As a follow-up to explore contributions of distinct regions within our anatomical mPFC ROI we evaluated the same contrasts at the voxel-wise level. We observed activations throughout the mPFC bilaterally (prelimbic cortex,

anterior cingulate cortex, medial superior frontal gyrus), following the comparison of undetected versus detected Ordinal Transfers (Fig. 2G-H; FWE-tfce $p < 0.05$), while no mPFC clusters survived corrections for multiple comparisons when comparing detected versus undetected Skips (data not shown) and Repeats (data not shown; FWE-tfce $p > 0.05$).

One potential confound is that mPFC activations might reflect relative performance levels (incorrect/undetected > correct/detected trials) rather than the utilization of ordinal retrieval modes per se. If true, we would expect similar mPFC activation clusters when examining incorrect compared to correct Skips and Repeats if performance was the main contributor to activation. When evaluating performance related activations for Repeats and Skips, undetected (i.e., incorrect) compared to detected (i.e., correct) Skips exhibited activations predominantly in rostrolateral prefrontal cortex (Fig. 2I) while a cluster for detected greater than undetected Repeats was identified in the right fusiform gyrus (data not shown). We explored this with a repeated measures ANOVA where we compared the mPFC and rostrolateral PFC and the three trial types (Ordinal Transfers, Skips and Repeats incorrect – correct contrast). For this analysis we had to exclude 5 participants as these participants either did not detect any Ordinal Transfers or detected every single Repeat trial. There was no main effect for trial type $F_{(2, 56)} = 0.395$, $p = 0.678$, but there was a trend in main effect for brain region $F_{(2, 56)} = 3.819$, $p = 0.061$, and no significant interaction effect ($F_{(2, 56)} = 1.149$, $p = 0.324$). Although not significant, the trend in brain region suggests that unique processes within PFC subregions. These results further support the view that the mPFC contributes to ordinal retrieval modes. However, we were unable to isolate how much mPFC activity is

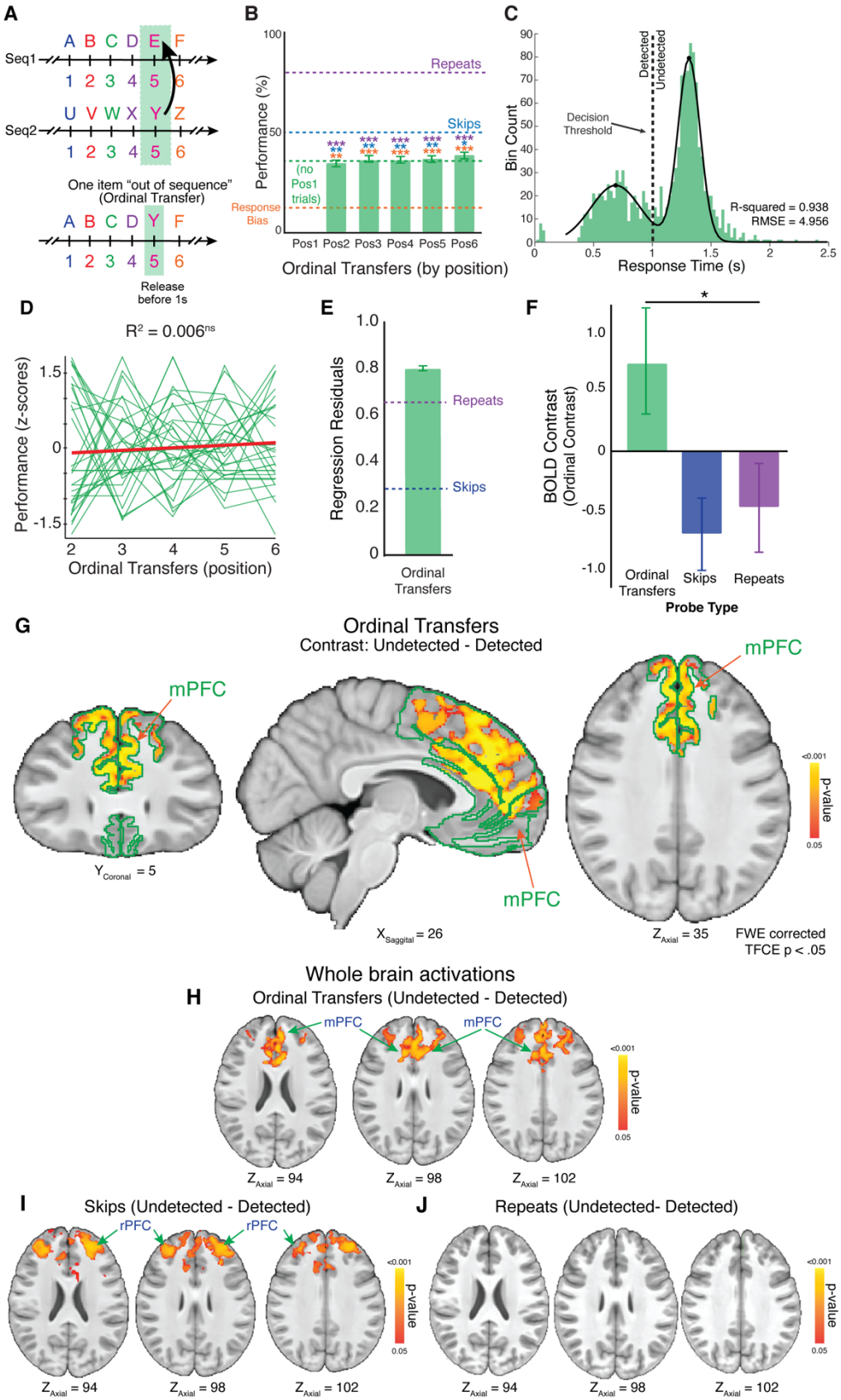
A
Seq1
A B C D E F
1 2 3 4 5 6
Seq2
U V W X Y Z
1 2 3 4 5 6
One item "out of sequence"
(Ordinal Transfer)
A B C D Y F
1 2 3 4 5 6
Release
before 1s
B
Performance (%)
Repeats
Skips
(no Pos1 trials)
Response Bias
Pos1 Pos2 Pos3 Pos4 Pos5 Pos6
Ordinal Transfers (by position)
C
Bin Count
Detected
Undetected
Decision Threshold
R-squared = 0.938
RMSE = 4.956
Response Time (s)
D
R² = 0.006ns
Performance (z-scores)
Ordinal Transfers (position)
E
Regression Residuals
Repeats
Skips
Ordinal Transfers
F
BOLD Contrast (Ordinal Contrast)
Ordinal Transfers
Skips
Repeats
Probe Type
G
Ordinal Transfers
Contrast: Undetected - Detected
mPFC
mPFC
mPFC
Y Coronal = 5
X Saggital = 26
Z Axial = 35
FWE corrected
TFCE p < .05
p-value
<0.001
0.05
Whole brain activations
H
Ordinal Transfers (Undetected - Detected)
mPFC
mPFC
Z Axial = 94
Z Axial = 98
Z Axial = 102
I
Skips (Undetected - Detected)
rPFC
rPFC
J
Repeats (Undetected- Detected)

Figure 2. mPFC activations and ordinal retrievals. **A**, Ordinal retrieval modes were probed using Ordinal Transfer trials. **B**, Ordinal Transfers occurred in every position in each sequence except the first. For each position, mean performance was significantly higher than the calculated response bias (red dashed line), and significantly lower than the mean performance on Repeats (purple dashed line) and Skips (blue dashed line). Performance did not significantly differ among positions. **C**, response times of all participants were bimodal (green bars) and best fit using a bimodal Gaussian curve (black line) indicating the two distinct decisions (InSeq vs. OutSeq). **D**, the normalized performance slope did not significantly differ across positions, and variability, measured by the averaged squared residuals per participant of the linear regression, was high overall. The high variability suggests conflicting cognitive strategies. **E**, the variability on Ordinal Transfers is higher for than for Repeats and Skips. For BOLD analysis, we focused on contrasts for the ordinal retrieval mode. When an ordinal retrieval mode is engaged, participants would identify Ordinal Transfers as InSeq, but would identify Repeats and Skips as OutSeq. **F**, a BOLD fMRI mPFC ROI analysis showed that on Ordinal Transfers the ordinal contrast (Undetected – Detected) activation was significantly higher compared with Repeats and Skips (Detected – Undetected contrasts). **G**, a voxel-wise BOLD fMRI analysis using mPFC as a mask (outlined in green) revealed significant activity in a large area of the mPFC on Ordinal Transfers. **H**, in whole brain analysis mPFC activation was also evident for Ordinal Transfers. **I**, we found activation on Skips was centered on the rostrolateral prefrontal cortex. **J**, wo significant activation was found on Repeats. Symbol(s): ns, not significant; *, $p < 0.05$, **, $p < 0.01$, *** $p < 0.001$.

attributable to performance accuracy when making ordinal decisions and/or how much is attributable other ordinal processes which can be explored in future experiments that explicitly manipulate difficulty levels with probe types. The observed activations in the rostrolateral prefrontal cortex during undetected Skips, and the fusiform gyrus for detected Repeats may reflect prospective memory (Umeda et al. 2011; Volle et al. 2011; Benoit et al. 2012) and object processing (Grill-Spector et al. 1998), respectively.

Sequence Memory as a Function of Lag Direction and Distance

Memory for sequences of events at different lags can be supported by a variety of cognitive processes including working memory (WM) and temporal context memory (TCM) retrieval modes. The use of WM and TCM retrieval modes predict different

patterns in behavioral performance across n-forward and n-reverse lags (see Fig. 3A & B; also see Jayachandran et al. 2019), which can be exploited here to test the use of different retrieval modes (e.g., WM versus TCM).

Skips (forward lags). OutSeq probe trials that skipped ahead in the sequence (n-forward, e.g., the "D" in AB<u>D</u>DEF) afford the opportunity to evaluate predictions of the use of a TCM retrieval mode during rapid sequence memory decisions. Specifically, successful performance on Skips relies on a TCM retrieval mode as it requires participants to have precise expectations for the subsequent items in the sequence. Accordingly, the likelihood of a memory retrieval is highest for the very next item in the forward direction (lag distance = +1) and drops off (in a graded fashion) for more distal items (from +2 to +4). In the context of this task, the use of a TCM retrieval mode predicts the inverse in performance compared with free recall tasks because of interference. Specifically, performance on Skip OutSeq probe trials should be most difficult to detect for the shortest forward lag distance (+1) and improve at longer distances (+2, +3, or +4; Fig. 3B, right side) precisely because proximal items in a sequence (i.e., Skips with a short forward lag) are more likely to be retrieved (Howard and Kahana 2002; Kragel et al. 2015) and then falsely match up with an out of sequence probe image (thus be judged as InSeq; undetected).

We tested this prediction by examining performance across n-forward lag distances. First, all forward lags were performed better than response bias chance levels (Fig. 3C, blue bars; +1: 0.420 ± 0.178; $+1_{\text{vs. response bias}}$: $t_{(33)} = 10.609$, $p = 3.608 \times 10^{-12}$; +2: 0.665 ± 0.156; $+2_{\text{vs. response bias}}$: $t_{(33)} = 21.299$, $p = 7.417 \times 10^{-21}$; +3: 0.747 ± 0.248; $+3_{\text{vs. response bias}}$: $t_{(33)} = 15.343$, $p = 1.402 \times 10^{-16}$; +4: 0.765± 0.431; $+4_{\text{vs. response bias}}$: $t_{(33)} = 9.066$,

$p = 1.780 \times 10^{-10}$), suggesting that the use of a TCM retrieval mode does not completely interfere with OutSeq detection at the different forward lag distances. Second, subjects exhibited graded performance improvement as the skip distance increased ($F_{(3, 99)} = 13.790$, $p = 1.379 \times 10^{-4}$). We found that the identification of Skips with a +1 lag were the most difficult to detect compared with all other forward lags (*post hoc* LSD: +2: mean difference = 0.245 ± 0.029, $p = 1.218 \times 10^{-9}$, +3: mean difference = 0.327 ± 0.049, $p = 1.248 \times 10^{-7}$, +4: mean difference = 0.345 ± 0.079, $p = 1.186 \times 10^{-4}$). These results are consistent with TCM retrieval mode predictions (Fig. 3B, 3C). Detection of Skips with a +2 lag was significantly lower than Skips with a +3 lag (*post hoc* LSD: mean difference = 0.082 ± 0.038, p = 0.039). No significant difference in detection was observed, however, when comparing Skips with lags of +2 and +4 (*post hoc* LSD: mean difference = 0.100 ± 0.074, p = 0.187), or +3 and +4 (*post hoc* LSD: mean difference = 0.018 ± 0.074, p = 0.814), suggesting that performance approached asymptote. These behavioral results suggest that the participants' sequence memory was driven by the use of a TCM retrieval mode on Skips.

Repeats (reverse lags). OutSeq trials that repeated an item from earlier in the sequence (Fig. 3A; *n*-reverse; e.g., the second "A" in AB<u>A</u>DEF) can be solved by either the use of a TCM retrieval mode, a WM retrieval mode, or a mixture of the two (Fig. 3B, left side). Notably, the pattern of OutSeq detections across *n*-reverse lag distances should differentiate the two competing processes (Jayachandran et al. 2019). For Repeats, a TCM retrieval mode predicts that short backward lag distances (e.g., -2) would be the most difficult to detect due to heightened interference, while further *n*-reverse lag distances (e.g., -5) would be readily detectable as OutSeq. By contrast, a WM retrieval

mode predicts the opposite pattern because the most recently experienced items would be the most accessible and therefore easiest to detect.

We found that performance was better than response bias chance levels for all *n*-reverse lag distances (Fig. 3C, purple bars, -2: 0.859 ± 0.116; $-2_{\text{vs. response bias}}$: $t_{(33)} = 38.333$, $p = 6.058 \times 10^{-29}$; -3: 0.805 ± 0.171; $-3_{\text{vs. response bias}}$: $t_{(33)} = 24.138$, $p = 1.522 \times 10^{-22}$; -4: 0.782 ± 0.233; $-4_{\text{vs. response bias}}$: $t_{(33)} = 17.204$, $p = 4.821 \times 10^{-18}$; -5: 0.529 ± 0.507; $-5_{\text{vs. response bias}}$: $t_{(33)} = 4.996$, $p = 1.865 \times 10^{-5}$). As the *n*-reverse lag distance

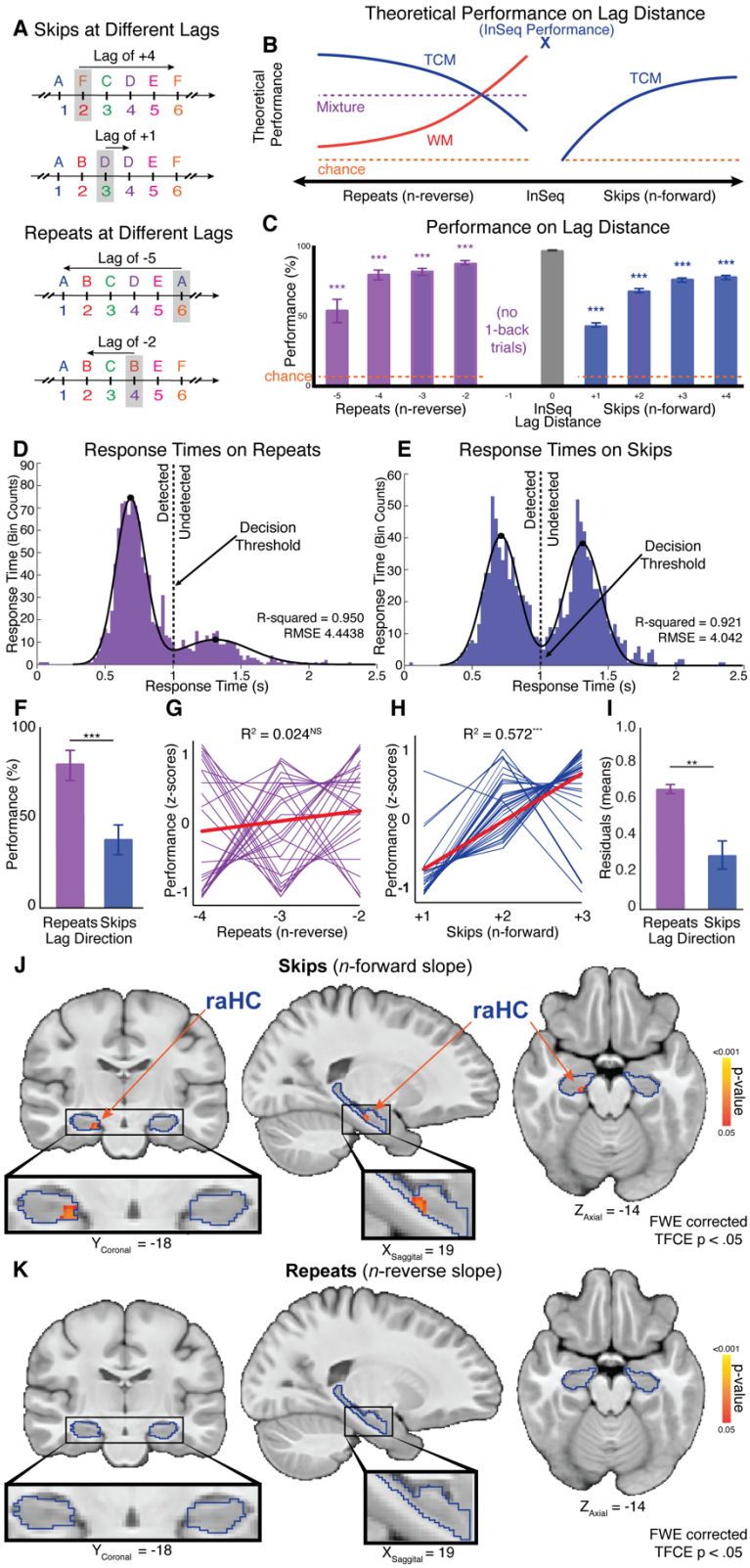

Figure 3. BOLD fMRI analysis indicates that the right anterior hippocampus tracks temporal context across forward lags**. A**, Skips and Repeats ocurred at different lags away from their InSeq position. **B**, theoretical predictions based on temporal context memory (TCM; blue lines) and working memory (WM; red line) retrieval modes for different lag distances on Repeats and Skips. A mixture of TCM and WM modes is shown by the dashed purple line. **C**, the mean performance accuracy for all participants on Repeats and Skips at different lags. Response times for both (**D**) Repeats (purple bars) and (**E**) Skips (blue bars) presented a bimodal distribution and were best fit using a bimodal Gaussian distribution (black line) indicating two distinct decisions (InSeq vs. OutSeq)**. F**, Overall performance on Repeats was higher than for Skips. **G**, Performance was flat on Repeats at different lags reflecting the use of a mixture of TCM and WM retrieval modes, **H**, and performance has a positive slope on Skips defining of TCM retrieval modes. **I**, there was significantly higher variability, measured by the averaged squared residuals per participant of the linear regression, in Repeats compared with Skips, which is thought to reflect the integration of variance from using both TCM and WM retrieval modes. Symbol(s): ns, not significant; *, $p < 0.05$, **, $p < 0.01$, *** $p < 0.001$. **J**, BOLD fMRI analysis of Skips with a linear contrast of -1, 0, 1 for lags of +1, +2, +3 respectively using the bilateral medial temporal lobe as a revealed significant activation in the raHC (right anterior Hippocampus). This activation pattern is unlikely due to general match/mismatch as we found no evidence of this in our brain region X retrieval mode interaction analysis. **K**, BOLD fMRI analysis of Repeats with a linear contrast of 1, 0, -1 for lags of -4, -3, -2 respectively using bilateral medial temporal lobe as a mask showed no significantly activated clusters.

increased, detection as OutSeq decreased ($F_{(3, 99)} = 9.760$, $p = 0.001$; Fig. 3C, purple bars), suggestive of the dominant use of a WM retrieval mode. Items with an *n*-reverse lag closest to their original position (e.g., ABC<u>B</u>EF; lag = -2) were easiest to detect as OutSeq compared with all other *n*-reverse lag positions (*post hoc* LSD lag -2 compared with: lag -3: mean difference = 0.055 ± 0.022, $p = 0.020$; lag -4: mean difference = 0.077 ± 0.033, $p = 0.025$; or lag -5: mean difference = 0.330 ± 0.084, $p = 4.262 \times 10^{-4}$). By contrast, items with an *n*-reverse lag farthest from their original position (e.g., ABCDE<u>A</u>; lag = -5) were the most difficult to detect as OutSeq compared with all other *n*-reverse lag positions (*post hoc* LSD lag -5 compared with: lag -4: mean difference = 0.253 ± 0.091, $p = 0.009$; lag -3: mean difference = 0.275 ± 0.091, $p = 0.005$; or lag -2: mean difference = 0.330 ± 0.084, $p = 4.262 \times 10^{-4}$). No significant differences in detection between -3 and

-4 *n*-reverse lags were observed (*post hoc* LSD: mean difference = 0.022 ± 0.035, p = 0.532). Taken together, performance at the *n*-reverse lag extremes (-2 and -5) supports the notion that the use of a WM retrieval mode certainly plays an important role in identifying Repeats, but the absence of a graded performance across *n*-reverse lags of -3 and -4 supports the idea that a combination of cognitive processes is being used. Overall, these analyses do not support the use of a TCM retrieval mode as an isolated process driving the identification of Repeats in this task.

A 2-term Gaussian curve (Fig. 3D-E, black line) fit best for the response time ditributions of both Repeats (Fig. 3D, purple bars; R-squared =0.950, RMSE = 4.4438, $x_{peak\ 1}$ = 0.688, $x_{peak\ 2}$ = 1.313) and Skips (Fig. 3E, blue bars; R-squared =0.9205, RMSE = 4.0416, $x_{peak\ 1}$ = 0.713, $x_{peak\ 2}$ = 1.313) compared to a 1-term Gaussian curve on Repeats (Fig. 1F; R-squared =0.8859, RMSE = 6.660, $x_{peak\ 1}$ = 0.688) and on Skips (Fig. 1F; R-squared =0.4198, RMSE = 10.796, $x_{peak\ 1}$ = 0.838) or a 3-term Gaussian curve on Repeats (Fig. 1F; R-squared =0.951, RMSE = 4.491, $x_{peak\ 1}$ =0.686, $x_{peak\ 2}$ = 1.313, $x_{peak\ 3}$ = 2.113) and on Skips (Fig. 1F; R-squared = 0.921, RMSE =4.087, $x_{peak\ 1}$ = 0.713, $x_{peak\ 2}$ = 1.313, $x_{peak\ 3}$ =2.363). The mean response times for detected Repeats was 0.710 ± 0.055 seconds, for undetected Repeats was 1.320 ± 0.142 seconds, for detected Skips was 0.729 ± 0.062 seconds, and for undetected Skips was 1.357 ± 0.113 seconds. These data suggest that two sequence decisions are being made on Repeats and Skips.

TCM Retrievals for Skips, but a Mixture of Retrieval Modes for Repeats

Differences in the overall ability to detect OutSeq probe trials, and the residuals from a lag-based linear regression model, helped to further elucidate the contributions of

either a TCM retrieval mode, a WM retrieval mode, or their combination. First, we predicted that the ability to detect OutSeq probes would be greater for Repeats than Skips because TCM and WM retrieval modes can both contribute to the evaluation of Repeats but not Skips (Fig. 3B, left, purple dashed line). Second, we predicted that a linear regression of Skip detections would positively increase across *n*-forward lags, whereas a similar analysis across *n*-reverse lags for Repeats would be essentially flat. Third, we predicted that the residuals from the linear regressions would be, highest on Repeats compared with Skips, reflecting the use of multiple retrieval modes, whereas Skips involve a single mode (i.e., TCM-based retrieval). To test these predictions, we compared the overall ability to detect the two probe trial types, calculated a linear regression based on the z-scores (accounting for individual baseline detection levels) across different lag positions, and averaged the squared residuals as a measure of detection variability across lags. Participants were significantly better at detecting Repeats ($M_{accuracy} = 0.786 \pm 0.166$) than Skips ($M_{accuracy} = 0.492 \pm 0.157$; $t_{(33)} = 14.435$, $p = 8.137 \times 10^{-16}$; Fig. 3F).

Consistent with our hypothesis, the linear regression in Skips positively increased across forward lags accounting for a large effect on performance (Fig. 3H; $R^2 = 0.572$, $\beta = 0.757$, $p = 3.711 \times 10^{-20}$), whereas a linear regression across reverse lags for Repeats had no significant slope (Fig. 3G; $R^2 = 0.024$, $\beta = 0.154$, $p = 0.139$). When quantifying variability, Repeats ($M_{residual} = 0.593 \pm 0.243$) were significantly more variable compared with Skips ($M_{residual} = 0.285 \pm 0.478$) across different lag positions (Fig. 3I; $t_{(30)} = 3.051$, $p = 0.004$). The patterns in OutSeq detection and variability further support the conclusion

that multiple retrieval modes likely contribute to identifying Repeats as OutSeq, while Skip detection is mediated more exclusively by a TCM retrieval mode.

HC Activations and TCM Retrievals

Converging evidence indicates that the medial temporal lobe, specifically the HC formation, plays a disproportionate role in the use of a TCM retrieval mode in the brain (Manns et al. 2007; Hsieh et al. 2014; Bladon et al. 2019). To test whether regions of the medial temporal lobe contribute to a TCM retrieval mode during Skip and Repeat probe trials, we looked for linear changes in activation across the different lag distances. We observed a significant activation cluster in the right anterior HC following small volume corrections (bilateral medial temporal lobe, FWE-tfce $p < 0.05$) that increased its activation across n-forward lags (Fig. 3J). The statistical significance of similar patterns of activation across n-reverse lags did not survive corrections for multiple comparisons (Fig. 3K). These results suggest that the right anterior HC contributes to a TCM retrieval mode during Skips.

Brain Region by Retrieval Mode Interaction Effect

After finding individual evidence supporting the mPFC contributes to sequence memory by the use of an ordinal retrieval mode and the right anterior HC by a TCM retrieval mode, we wanted to directly compare the mode-related activations (ordinal vs. TCM) across the regions that exhibited voxel-wise activations (right anterior HC vs. mPFC). A repeated-measures factorial ANOVA was conducted with brain region (anatomically defined right anterior HC vs. mPFC) and strategy (ordinal retrieval vs.

TCM retrieval modes) as within-subjects factors, and BOLD activations as the dependent measure. We observed greater activations in the mPFC in relation to the use of an ordinal retrieval relative to a TCM retrieval mode, and the opposite pattern in the right anterior HC, evidenced by a significant interaction effect (Fig. 4A. $F_{(1,31)} = 4.782$, $p = 0.036$).

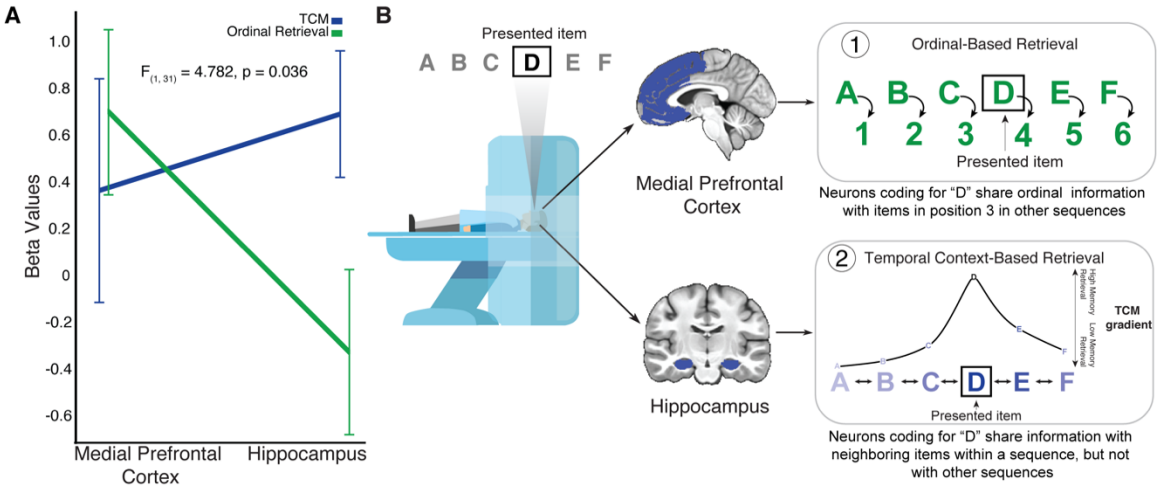

Figure 4. mPFC and HC retrieval mode interactions. **A**, there was a significant interaction effect between mode and brain region ($F_{(1,31)} = 4.782$, $p = 0.036$), where we observed greater activations in the mPFC for ordinal retrievals relative to TCM retrievals, and the opposite pattern in the right anterior HC. **B**, based on the results of the current experiment, **1**) the mPFC engages in ordinal-based retrieval calling on associations between items and their ordinal position (which could be represented elsewhere) and **2)** the HC engages in temporal context-based retrieval.

2.5 Discussion

The current study used different out of sequence probe trials during a memory task to test the concurrent use of distinct retrieval modes, adding to a growing literature on sequence memory as a fundamental component of episodic memory (Tulving 1984; 2002; Allen and Fortin 2013; Howard and Eichenbaum 2013; Eichenbaum 2017). Complementary behavioral results across the different out of sequence probe trials in the current task support the conclusion that memory for

sequences of events is supported by both ordinal and temporal context retrieval modes. The BOLD fMRI evidence showed that mPFC activations more strongly reflected the use of an ordinal retrieval mode, while activations in the HC better reflected a temporal context memory retrieval mode, thus dissociating the neurobiological substrates of two distinct processes contributing to sequence memory. While considerable evidence indicates that the mPFC and HC are involved in sequence memory, the current study provides new results that the mPFC and HC are concurrently engaged by retrieval modes in support of remembering *when* an event occurred. This evidence provides an important baseline for further investigation of how sequence memory is impaired in typical aging and diseases such as Alzheimer's Disease on the neurobiological level, especially since evidence implicates that the relative dependence on an ordinal retrieval mode increases with age while TCM dependence decreases (Bastin and Van der Linden 2010; Allen et al. 2015).

Ordinal Retrieval Modes in mPFC

Our results suggest that the positional information associated with retrieving memories in sequence is, at least partially, represented in the mPFC (e.g., Hsieh and Ranganath 2015), and/or that mPFC activations help engage these representations elsewhere such as within HC neurons (e.g., Allen et al. 2016). Ordinal Transfers were detected less often than both Repeats and Skips (Fig. 2B, see also Allen et al. 2014; 2015), but better than response bias chance levels. This suggests that multiple retrieval modes are being used, feasibly the concurrent ordinal retrieval modes and temporal context retrieval modes. These results are not totally surprising because mPFC has been

shown to be generally important to temporal order memory (Milner et al. 1985; Shimamura et al. 1990; DeVito and Eichenbaum 2011; Hsieh et al. 2015) and other semantic representations (Preston and Eichenbaum 2013; Hyman et al. 2012). Our study suggests that when an ordinal retrieval mode is strongly engaged, it interferes with the ability to detect Ordinal Transfers, supported by the fact that Ordinal Transfers went undetected at a very high rate and mPFC activation was high at those times.

Ordinal retrieval modes have also been demonstrated in rats (Allen et al. 2014), monkeys (Orlov et al. 2000; 2006) and humans (Allen et al. 2015; Hsieh et al. 2015). In fact, monkeys naturally categorize items within a sequence by their ordinal position which occurs early in the design by Orlov et al. (2000), and only later in trials do monkeys employ other strategies such as sequential associations for adjacent items and working memory (Orlov et al. 2000; 2006). Likewise, in humans it has been shown that multi-voxel patterns from the mPFC are significantly higher for objects that share the same position information, compared to objects in different positions (Hsieh et al. 2015), suggesting convergent patterns of activation reflect shared ordinal representations within mPFC (Tiganj et al. 2017) despite sensory differences in object identity. Taken together, prior research and the current study show compelling evidence that the mPFC helps remember *when* events occurred by engaging an ordinal retrieval mode. Notably, while the design of our study facilitated our ability to evaluate different retrieval modes using specific out of sequence probe trials, it is likely that the very presence of out of sequence probe trials and the order in which they are introduced impacted the emergence and utilization of these retrieval modes. Although we observed little changes in behavior throughout the task here, it will be worth exploring both behavioral and brain activation

patterns using versions of the sequence task that are designed to explicitly bias ordinal versus serial retrieval modes (Gudmundson et al. 2017).

Theoretically, an ordinal retrieval mode generated by mPFC would be input to the HC during episodic memory through indirect cortical or thalamic pathways (for review see Dolleman-van der Weel et al. 2019). The engagement of an ordinal retrieval mode in HC might then allow for the rapid formation of conjunctive item-position representations (e.g., 1^{st} – A, 2^{nd} – B, etc.; Fig. 4B), and provide sequential structure without an explicit need to represent the elapsing time between items (a useful form of neural compression for temporal information). There is indirect evidence that item-position representations are reflected in rodent CA1 neurons during spatial sequence tasks (Euston and McNaughton 2006), and direct evidence for conjunctive item-position representations during an analogous odor sequence task (Allen et al. 2016). Importantly, item-position representations are learned and retrieved *before* sequential item-item associations in non-human primates (Orlov et al. 2000), although this may be task specific. This raises the question whether episodic memories typically rely on an ordinal retrieval mode for recalling (or encoding) events with timelines. Subsequent replay events or other consolidation processes could either strengthen temporal context modes and/or weaken ordinal modes, although we suspect the former. Interestingly, in monkeys, ordinal transfers show graded interference over lag distances, suggesting they share similar properties with temporal context retrievals when studied in this way (Orlov et al. 2006), indicating two temporal dimensions may be complementary and normally integrated. Future neuroimaging studies in humans using ordinal transfers distributed across lag

distances will be useful for examine the neural activity when these processes are both contributing to retrieval patterns.

Temporal Context Retrieval Modes in HC

Consistent with the literature, our results show that the HC contributes to sequence memory through the use of a temporal context retrieval mode. The HC has been shown to be important for sequence memory (Hsieh et al. 2014; Goyal et al. 2018) but its precise contribution has remained an open question. According to TCM, the HC associates items in sequences through a drifting contextual representation (Howard et al. 2005; Polyn and Kahana 2008). As such, the presentation or retrieval of an item from a sequence elicits the retrieval of neighboring items that share a temporal context, decreasing in likelihood or strength for more distal items (Howard and Kahana 2002). According to this framework, a temporal context retrieval mode accounts for the increased likelihood that adjacent items in word lists are recalled (Howard and Kahana 2002). This pattern in free-recall performance predicted by temporal context memory has been validated in computational models (Howard and Kahana 2002), behavioral studies (Kahana 1996; Sederberg 2010; Morton and Polyn 2016), and neurobiological studies (Polyn and Kahana 2008; Jenkins and Ranganath 2010; Hsieh et al. 2014; Bladon et al. 2019). In the current sequence memory task, we reasoned that the presentation of InSeq items would elicit the retrieval of neighboring items that shared temporal contexts and lead to graded impairments in the detection of Skip probes. This is because, as the forward lag increased, the upcoming representations were less likely to be retrieved and thus less likely to interfere with an out of sequence determination. Similar patterns in

performance are observed in other tasks probing temporal memory (Allen et al. 2014; 2015; DuBrow and Davachi 2014).

The HC has shown activations consistent with the use of a TCM retrieval mode. Activation in the HC is elevated during the processing of overlapping compared to nonoverlapping sequences (Kumaran and Maguire 2006; Brown et al. 2010; Brown and Stern 2013). Population activity in CA1 drifts across both small- and large-time scales (Manns et al. 2007; Mankin et al. 2012; Ziv et al. 2013; Rubin et al. 2015; Mau et al. 2018). Additionally, HC lesions impair the discrimination of overlapping odor sequences (Agster et al. 2002). An fMRI study showed that HC multi-voxel pattern similarity was higher for pairs of adjacent trials that belonged to the same temporal context within a sequence compared to pairs of sequence items that bridged between sequences, even when the temporal distance between the pairs of items was similar (Hsieh et al. 2014). The same study observed that the HC carries information about the temporal context between items within a sequence, rather than information about the objects themselves (Hsieh et al. 2014). Specifically, Hsieh et al. (2014) demonstrated that when the same sequence item is repeated, hippocampal voxel patterns were dissimilar, unless the temporal context was reinstated. Our results add to this by showing that as Skips lag further away from their InSeq location, HC activity also increases closely matching predictions of TCM.

Limitations and Theoretical Considerations

While the use of specialized out of sequence probe trials provided important insight regarding different retrieval modes, and their related neurobiological substrates,

several limitations of the current study remain. First, the task was designed for cross species investigation (Allen et al., 2014), thus the timing of the task and self-paced design of the experiment precluded detailed item-based analyses at the neurobiological level (see intertrial intervals in Materials and Methods for relevant event timing). Our neuroimaging analysis thus, can only capture retrieval modes with uncertainties related to surrounding individual events. At the expense of repetitions of trials, future studies should include temporal jitter between sequence items to isolate signals at the different item positions. Second, similar to multivariate approaches, univariate approaches are subject to interpretational ambiguities (Hebart and Baker 2018; Ritchie et al. 2017). However, to avoid overfitting issues, especially with time-varying representations, we chose to use a univariate approach over a multivariate approach as it is better suited to our task design to differentiate retrieval modes using different out-of-sequence probe trials. Third, an in-sequence response bias could develop given the vast majority of individual items were in sequence. A response bias should impact all probe trial types similarly given their similar number of presentations. We did not observe evidence that performance was based on a response bias or changed over trials. All probe trial types were responded to better than chance and detailed response time analysis showed similar bimodal distributions across all conditions, notably lacking a rightward skew. While it would be helpful in the future to minimize a bias to hold, it does not change the overall interpretation of in sequence responses for any of our probe trial types. An additional limitation is that we are unable to cleanly isolate relative performance related brain activations and separate them from the retrieval mode activations on a given probe trial. This would be an interesting

question to analyze in a future study using a modified task design that explicitly manipulates difficulty on all probe trials.

Key questions remain concerning the interactions between ordinal and temporal context retrieval modes, and their related neurobiological constituents (mPFC and HC). While the current study did not include probe trials that investigated ordinal transfer and transpositions, future studies should examine these critical probe trial types and expect to see increased interactions between the mPFC and HC. mPFC-HC coupling may lead to conjunctive representations of temporal contexts and positional coding. As shown here, mPFC activation contributes to ordinal retrieval modes (Fig. 4B) which interacts with temporal contexts in the HC (Fig. 4B). In theory, this information could be merged allowing the formation of conjunctive temporal context and item-position association in HC neurons. Direct evidence for this latter possibility was provided by recent studies that showed HC neurons encode item-context and item-position conjunctions (Komorowski et al. 2009; Allen et al. 2016), suggesting that these conjunctive representations provide the neuronal basis for time and place integrations in episodic memory. However, future studies are required for examining mPFC-HC interdependent interactions directly in humans.

The results from our study highlight novel evidence that ordinal and temporal context retrieval modes both contribute to remembering items within a timeline. In particular, we showed that mPFC and HC activity differentially contribute to ordinal and TCM retrieval modes. Further experiments in both animals and humans are necessary to delineate the precise mechanisms by which the mPFC engages ordinal retrievals, and

how this process interacts with HC to integrate ordinality and temporal contexts in support everyday episodic memory.

CHAPTER 3

The midline thalamus across species: A review of the midline thalamus on anatomy, function, and involvement in neurological disorders.

3.1 Summary

The nuclei of the midline of the thalamus are critical structures involved in higher order cortico-thalamic-cortical networks that are important for cognition. These thalamic nuclei are key components in various cognitive functions including memory processes, stress regulation, arousal, and feeding behavior. Impairments of the midline thalamus are associated with neurological disorders including Alzheimer's Disease, schizophrenia, depression, and drug addiction (Braak and Braak, 1991a; 1991b; Neumeister et al., 2004; Greicius et al., 2007; Hsu and Price, 2009; Inutsuka et al., 2013; Hsu et al., 2014). Given the importance of the thalamic midline nuclei and their involvement in cognitive functions and neurological disorders, it is surprising that little is known about these structures in the human brain. The midline thalamic nuclei consist of four nuclei: The nucleus reuniens is located most ventral within the midline, dorsal to that lies the rhomboid nucleus, then the paraventricular nucleus and lastly the parataenial nucleus, located most dorsally. The current review will shed light on the limbic midline thalamus by first highlighting the importance of the midline thalamic nuclei; second discussing the gap in knowledge of the midline thalamic nuclei by describing the location of the midline thalamic nuclei in correspondence to adjacent nuclei and ventricles, third; summarizing the anatomical connectivity based on tracer studies in monkeys and rodents, and fourth; reviewing the functional involvement of the midline thalamic nuclei in cognitive behaviors and neurological disorders.

3.2 Introduction

The thalamus is a brain structure with an average size of about three cm in length in the middle of the brain near the third ventricle (Fig. 5; Tortora and Derrickson, 2008; Sherman, 2017). Traditionally, the thalamus was characterized as the central sensory and motor relay station of the brain, reciprocally communicating and relaying signals between cortical, subcortical, cerebellar regions, and the cortex (Sherman et al., 2006). The bilateral thalamus are paired in the middle of the brain by the massa intermedia (interthalamic adhesion) in about 96% of human brains (Tortora and Derrickson, 2008; Damle et al., 2017), and in about the remaining 4% the thalamus is not paired at the midline and separated by the third ventricle. The thalamus consists of paired oval subcortical masses of grey matter that are organized into cytoarchitectonically and functionally distinct nuclei, each concerned with receiving and projecting a characteristic type of efferent and afferent signal to a structurally and functionally distinct corresponding area of the ipsilateral cortex (Sherman et al., 2006; Tortora and Derrickson, 2008). Anatomically, based on their positions and functions, the thalamic nuclei can be divided in seven major groups; the anterior nuclei, the medial nuclei, the lateral nuclei, the ventral nuclei, the intralaminar nuclei, the reticular nuclei and the midline nuclei (Tortora and Derrickson, 2008).

Almost nothing is known about the midline thalamus in humans. Here, I aim to review current literature on the midline thalamus across species (humans, monkeys, and rodents) and aim to provide a snapshot of where current knowledge can lead us in the future of the investigation of the midline thalamus both in humans and non-human animals.

The midline thalamic nuclei are adjacent to the massa intermedia and adjacent to the third ventricle where the bilateral thalamus pair (Tortora and Derrickson, 2008). From dorsal to ventral, the midline thalamic nuclei consist of the parataenial nucleus (PT), paraventricular nucleus (PV), rhomboid nucleus (RH) and the nucleus reuniens (RE), with some variability across species (Fig. 5). Some studies include the intermediodorsal nucleus and the central medial nucleus of the thalamus in the dorsal midline thalamus (Pereira de Vasconcelos and Cassel, 2015), which are located more posterior compared to the four aforementioned nuclei, adjacent to the posterior boundary of RH, ventral boundary of PV, dorsal boundary of RE. However, the current review does not include this nucleus in the dorsal midline thalamus as these nuclei are more posterior in the brain compared to the dorsal-ventral stacked PT, PV, RH, RE nuclei.

The thalamic nuclei can be divided in two types of thalamic relays: first order nuclei that relay driver input from a subcortical brain structure, and the higher order nuclei that relay inputs from layer five of one cortical area to another cortical area (Sherman et al., 2006). The midline thalamic nuclei are higher order nuclei that are part of cortico-thalamo-cortical circuits in the brain (Sherman, 2017). The midline thalamic nuclei can be divided along the ventral and dorsal axis, where the ventral midline thalamus encompasses the more ventrally located RE, and the RH dorsal to that, and the dorsal midline thalamus encompasses PV (dorsal to RH), and the more dorsally located PT (Fig. 5).

The midline thalamic nuclei are critical to many functions including memory consolidation (Thielen et al., 2015), spatial working memory (Hallock et al., 2016; Viena et al., 2018), temporal organization of sequence memory (Jayachandran et al., 2019),

chronic stress regulation (Hsu et al., 2014), wakefulness (Hsu and Price, 2009; Inutsuka et al., 2013) and feeding behavior (Beas et al., 2020). Impairments of one or more of the midline thalamic nuclei have been shown to be involved in neurological diseases such as Alzheimer's disease (Braak and Braak, 1991a, 1991b), major depression (Neumeister et al., 2004; Greicius et al., 2007), stress (Hsu and Price, 2009; Hsu et al., 2014), and potentially drug relapse (Hsu and Price, 2009; Inutsuka et al., 2013; Hsu et al., 2014). The involvement of the midline thalamic nuclei in the aforementioned cognitive functions has made the midline thalamic nuclei a focus of rodent research (Vertes et al., 2007; Ramanathan et al., 2018; Dolleman-van der Weel et al., 2019; Jayachandran et al., 2019;); however, it is surprising how little these structures have been studied in the human brain. The purpose of the current review is to first, discuss the anatomical location of the four midline thalamic nuclei in reference to neighboring nuclei and ventricles in

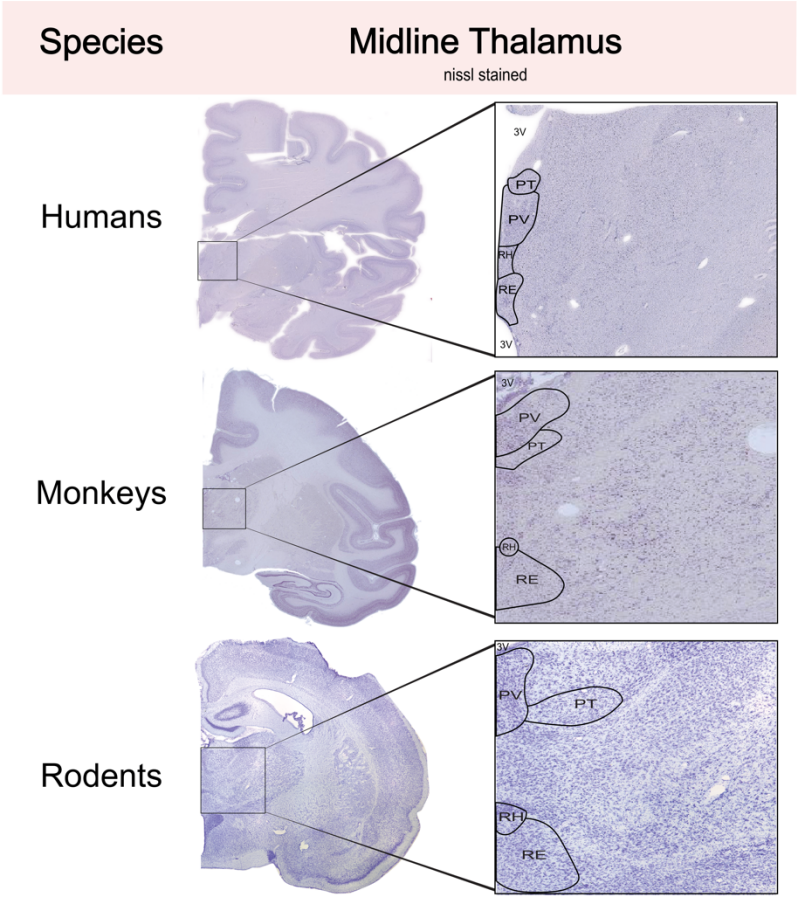

Figure 5. Midline thalamus in a Nissl stain in humans, monkeys, and rodents. The human brain slice and segmentation is from the Ding et al., (2016) atlas. The macaque brain slice is from Mikula et al., (2007), and the rat brain slice is from Viena et al. (2020).

humans; second, to provide a detailed review of the anatomical connectivity for the four midline thalamic nuclei in primates; and third, to discuss the involvement of these nuclei in various cognitive functions and to review associations of these nuclei with human neurological diseases. The review will draw from studies of the midline thalamic nuclei in humans and non-human primates (Amaral and Cowan, 1980; DeVito, 1980; Aggleton et al., 1986; Giménez-Amaya et al., 1995; Gabbot and Bacon, 1996; Saunders et al., 2005; Hsu and Price, 2007;2009; Hsu et al., 2014) and will discuss additional evidence from rodent studies (Wouterlood et al., 1990; Dolleman-Van der Weel et al., 1997; McKenna and Vertes, 2004; Vertes et al., 2006; Hoover and Vertes, 2012; Vertes et al., 2015).

Multiple names for the human midline thalamic nuclei create confusion.

The various nomenclatures and definitions for the human midline thalamic nuclei makes communication about these brain structures difficult (Mai and Majtanik, 2018). For example, RE was described in 1912 as reuniens nucleus (Malone, 1912). Years after that, RE has been called several different names including nucleus medialis posterior reuniens (Grüntal, 1934), nucleus centralis medialis (Sheps, 1945), and nucleus commissuralis (Hassler, 1959). Currently the nuclei of the midline thalamus still do not have an unequivocal nomenclature and are often thought to be part of the massa intermedia (interthalamic adhesion). The nuclei in the midline thalamus; RE, RH, PV, and PT, only have anatomical connections with ipsilateral neocortical areas and have distinct functions. There are no inter thalamic neural fibers exchanged between contralateral thalamic nuclei (Damle et al., 2017). The midline thalamic nuclei have

distinct functional connectivity patterns providing evidence that they are involved in distinct cortical systems.

Investigating midline thalamic nuclei connectivity in human brains is difficult.

In non-human animals, invasive techniques are used to investigate the connectivity of the midline thalamic nuclei that cannot be done in humans. Many connectivity studies use fluorescent tracers to investigate the anatomical connectivity of midline thalamic nuclei. In rodent and monkey tracer studies, after brain removal, brain sections are sliced and stained. In most studies, Nissl, chromatin, NeuN, calretinin and calbindin staining are used, after which sections are examined using bright field microscopy for Nissl and chromatin stains, or fluorescent microscopy for NeuN, calbinding and calretinin stains. Labeled fibers and injection sites are then identified and manually plotted using camera lucidae methods or other tracing techniques on representative schematic sections through the brain using cytoarchitectural differences and rodent and monkey brain atlases as references (Vertes et al., 2006; Hsu and Price, 2007, 2009; Jayachandran et al., 2019).

In human brains, tracing of tracts in post mortem brains can be done using injections of fluorescent dyes; however, this only works for distances of tens of millimeters (Behrens et al., 2003). As the human brain is significantly larger than a rat brain and the macaque brain (Passingham, 2009), postmortem fluorescent dye tracing methods will not allow tract tracing in long range projections between different cortical and subcortical regions. Using non-invasive and *in vivo* techniques such as functional magnetic resonance imaging (fMRI) and diffusion weighted imaging (DWI), it is now

possible to delineate individual sub nuclei, to test functional and structural connectivity patterns and to correlate task-based and resting state human fMRI analysis with the knowledge from post mortem human autopsy brain studies and experimental animal studies (Mai and Forutan, 2012). This anatomical and functional knowledge is important to provide basic information regarding the organization of the thalamus in the human brain. However, these methods provide challenges as there is a high amount of interindividual variability and structural deviations with factors such as age, as well as ambiguities in translating experimental results from non-human animal experiments to the human brain (Mai and Forutan, 2012). Even with these sophisticated tools, there are serious limitations in using these methods to investigate the midline thalamic nuclei due to their small size (~50 count 0.75mm isotropic voxels; Reagh et al., 2017), variability in nuclear size and location between individuals (Morel et al., 1997) and their proximal location to the cerebrospinal fluid filled third ventricle. A recent study has provided novel evidence regarding the connectivity and anatomy of the sub regions of the human thalamic nuclei using probabilistic tractography analyses on DWI obtained in a MRI machine (Lambert et al., 2017). In their research, they included the midline thalamus, including the PV; however, the RE, RH and PT were not mentioned in the segmentation methods. Mai and Majtanik (2018) also parcellated the human thalamus using a volumetric approach to characterize the subdivisions and determine relationships between the parcellation schemes of nine atlases of the human thalamus (Mai and Majtanik, 2018). They registered the 3D reconstructed atlases to standard brain space from the Montreal Neurological Institute and compared the different delineations of the nuclei of the different atlases (Mai and Majtanik, 2018). However, due to the small width of the

midline thalamic nuclei and inconsistencies in the delineation of these nuclei in the nine different atlases, the midline thalamus was excluded in the parcellation (Mai and Majtanik, 2018).

An additional factor that makes studying the small midline thalamic nuclei difficult in humans *in vivo* is that the thalamic nuclei are not paired by the massa intermedia in everyone (Tortora and Derrickson, 2008; Damle et al., 2017) and are separated by the medial third ventricle in the areas where they are not paired. This shows that there is a high level of interindividual variability in relative location of the midline thalamic nuclei. Although the location of the midline thalamic nuclei in the brain make it well suited for normalization (Mai and Forutan, 2012), the volume of these nuclei makes normalization difficult. Defining the midline thalamic nuclei using group level neuroimaging analyses is therefore difficult. Because the nuclei are small, vary in size and vary in exact coordinate location in each individual, using MRI provides difficulty as it could introduce error due to cerebrospinal fluid in the third ventricle or other brain tissue being averaged with the voxels containing the midline thalamic nuclei of a group of participants. This introduced error makes it hard to define detailed and precise locations and calls for investigation of these nuclei on an individual brain basis.

3.3 Anatomical location and organization

The thalamus is a bilateral subcortical structure located medially in the brain adjacent to the third ventricle. Fig. 6A shows coronal slices of the human brain with a zoomed in panel of the midline thalamic nuclei according to the Ding et al. (2016) coronal human brain atlas. The midline thalamic nuclei are located towards the midline

between the two hemispheres and are connected by the massa intermedia. The medial side of these nuclei is connected to the contralateral side and separated by the medial third ventricle in the areas where they are not paired. The most ventral midline thalamic nucleus is RE, above that is RH, followed by PV and the most dorsal midline thalamic nucleus is the PT (Fig. 5-6A). PT is the smallest nucleus in size of the four nuclei, next up in size is RH, then RE, and the largest nucleus of the four is the PV. The midline thalamic nuclei can be split up in a ventral group and a dorsal group based on anatomical location, connectivity, and function. The ventral midline thalamic nuclei consist of RE and RH, and mainly project to limbic cortical structures, particularly the medial prefrontal cortex (mPFC) and the hippocampus (HC), and are involved in functions involving these structures such as memory (Loureiro et al., 2012; Vertes et al., 2015), delayed discounted discrimination (Hembrook et al., 2012; Hallock et al., 2013), passive avoidance learning (Davoodi et al., 2011), memory precision and fear memory generalization (Xu and Sudhof, 2013). The dorsal midline thalamic nuclei consist of PV and PT, and mainly target limbic cortical structures such as the amygdala and nucleus accumbens and are involved in chronic stress regulation, arousal and wakefulness, feeding behavior, and when impaired they are associated with abnormal functions such as chronic stress, depressive disorder and drug seeking behavior (see chapter 3.5 and 3.6; Bubser and Deutch, 1999; Otake et al., 2002; Hamlin et al., 2009; Hsu et al., 2014).

In our current work (see Chapter 4; Reeders et al., in prep), we identified and segmented the midline thalamus based on strong connectivity patterns based on non-human animal tracer studies (Fig 6B-C). In this study (Reeders et al., in prep), we used probabilistic tractography analyses and k-means clustering on DWI data of 127 subjects

to segment the mask of the human midline thalamus. Briefly, using probabilistic tractography we obtained whole brain probabilistic connectivity maps with how often a streamline starting at a voxel of thalamus the made it to different cortical and subcortical brain regions. We then clustered the voxels of the thalamus together that had similar connectivity patterns (e.g., high connectivity to MTL, and low connectivity to cortex). We then extracted clusters of the thalamus with high connectivity to regions that the midline thalamus is known to have strong connectivity with in non-human animals (MTL, mPFC, nACC), and not to regions that the midline thalamus is known to have little to no connectivity with (superior frontal cortex, precentral gyrus, paracentral gyrus, post central gyrus, parietal cortex), based on non-human animal studies. This resulted in a midline thalamic mask with over 80% overlap in our dataset (Fig. 6B-C). Our results clearly distinguished voxels, that included the midline nuclei of the thalamus, PT, PV, RH and RE (Reeders et al., in prep). We further divided this midline thalamic mask based on the Ding et al., (2018) atlas into a dorsal midline thalamus mask (Fig 6D: Blue), including the PT and PV, and a ventral midline thalamus mask (Fig 6D: Pink), including the RE and RH (Reeders et al., in prep).

In the following section, the anatomical location of the midline nuclei will be described according to the human coronal brain atlas by Ding et al. (2016). This atlas was created using a 34 year old female brain and various techniques including DWI, MRI, specimen preparation, slabbing, sectioning, staining, and tissue scanning (Ding et al., 2016). They obtained 2716 slice sections in total, from where 679 were Nissl stained, and in turn from which 106 images were digitally scanned and traced for the digital atlas. For immunohistochemistry, they immunostained 339 sections for the calcium binding protein

parvalbumin and 338 sections for nonphosphorylated neurofilament proteins. They selected Nissl plates for the reference atlas. The final digital atlas contained 106 levels, with level 1 as the most anterior coronal slice, and level 106 as the most posterior coronal slice (Ding et al., 2016). The different levels contained sampling intervals of 0.4 – 1.0 mm medially in the brain (including the location of the thalamus), and sparser sampling intervals of 3.4 mm were applied to the most anterior and posterior cortical levels with few subcortical structures (Ding et al., 2016).

Nucleus Reuniens (RE).

RE is the largest of the two ventral midline thalamic nuclei and is the most ventral nucleus of the midline thalamic nuclei (Fig. 6A). The anterior part of the RE starts at level 29a and extends posteriorly to level 43a in the Ding et al. (2016) human coronal brain atlas. Anterior to the RE are the thalamic rhomboid nucleus and the paraventricular nucleus of the hypothalamus. In the most anterior coronal slice, RE shares boundaries with the RH dorsally, thalamic fasciculosis nucleus laterally, hypothalamic paraventricular nucleus ventrally and with the third ventricle towards the midline. As you navigate posterior in the brain, the RE extends ventral and the PV with RE connection is intervened by the central medial (CeM) nucleus of the thalamus replacing the location of the thalamic RH nucleus. More posterior in the brain, between the PV and CeM, appears the intermediodorsal nucleus of the thalamus. On the most posterior coronal slice the nucleus RE shares edges with the CeM on the dorsal side, the third ventricle on the medial side, the midbrain on the ventral side, and the magnocellular division of the ventral anterior nucleus of the thalamus on lateral side. Posterior of RE lies the

periventricular area of the thalamus. In the Ding et al. (2016) atlas, in 14 of the 15 slices the reuniens is paired with the contralateral RE.

Rhomboid nucleus (RH).

RH is a small cell group dorsal to RE. The anterior part of RH starts at level 27a in the Ding et al. (2016) coronal human brain atlas and extends posteriorly to level 31a. Anterior to RH is the stria medullaris of the thalamus. The most anterior coronal slice of RH shares boundaries with the third ventricle on the medial side, with the paraventricular and juxtaparaventricular area of the hypothalamus on the ventral side, with the fasciculosis nucleus of the thalamus on the lateral side and with PV on the dorsal side. In the most posterior coronal slice, RH shares boundaries with RE on the ventral side, third ventricle (and sometimes bilateral RH) on the medial side, PV on the dorsal side and the anteromedial nucleus on the lateral side. Posterior of RH is the central medial nucleus of the thalamus. In the Ding et al. (2016) atlas, the bilateral paired rhomboid nuclei share boundaries in three of the five slices.

Paraventricular nucleus (PV).

PV is the largest midline thalamic nucleus of the four midline thalamic nuclei. It is located ventral to PT, and dorsal to RH. The anterior part of the PV nucleus starts at level 27a in the Ding et al. (2016) human coronal brain atlas and extends posteriorly to level 47a. Anterior of PV is the stria medullaris of the thalamus. In the most anterior coronal slice PV nucleus shares boundaries with the RH on the ventral side, with the third medullaris of the thalamus on the dorsal side. In the most posterior coronal slice the PV

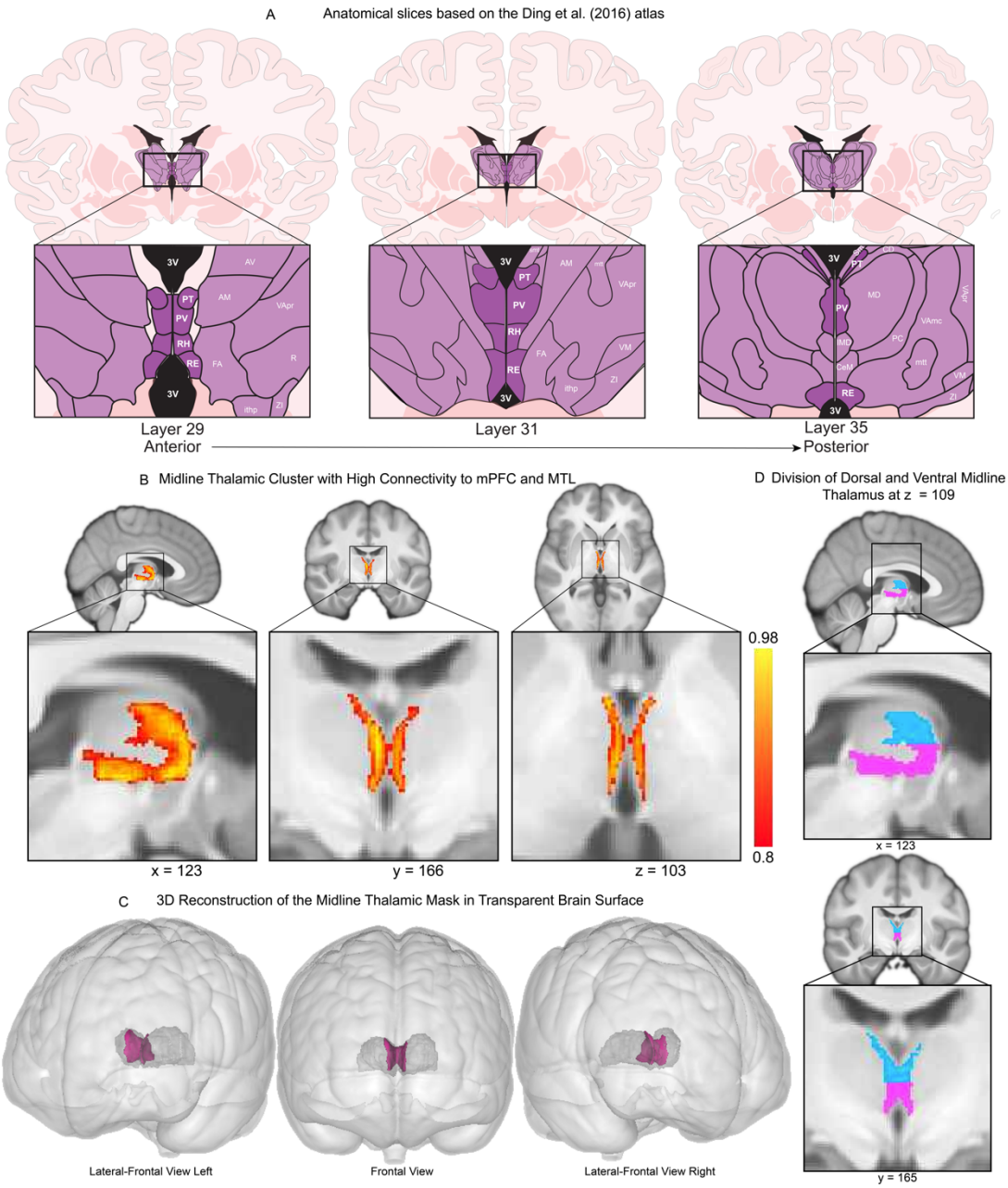

Figure 6. Midline thalamus identification in the human brain. **A,** Schematic representation of the midline thalamus in the human according to the Ding er al., (2016) atlas. Anterior in the brain, the midline thalamic nuclei of each hemisphere are paired together and are winged out where not paired. More posterior, the dorsal and ventral midline thalamic nuclei are separated. **B,** A mask of the midline thalamus with over 80% overlap of all participants (80% shown; Reeders et al., in prep). **C,** 3D rendering of the midline thalamus (pink) in the thalamus (dark grey) at 80% overlap in 127 subjects (Reeders et al., in prep). **D,** Division of the dorsal (blue; PT and PV) and ventral (pink; RH and RE) thalamus according to the Ding et al., (2016) atlas at z = 109. Where at the point of hemispheric attachment, 48% is dorsal midline thalamus and 52 is ventral midline thalamus.

shares boundaries with the PV on the dorsal side, anteromedial thalamic nucleus on the lateral side and the RE on the ventral side and with the third ventricle on the medial side. Posterior of the PV is the periventricular area of the thalamus. PV shared boundaries with the contralateral PV in nine of the 20 slices in the Ding et al. (2016) atlas.

Parataenial nucleus (PT).

PT is the smallest nucleus of the thalamic nuclei and is located most dorsal of the limbic thalamus. The anterior part of the PT nucleus starts at level 27a in the Ding et al. (2016) atlas and extends posteriorly to level 37a. Anterior of this nucleus is the stria medullaris of the thalamus. In the most anterior coronal slice, this nucleus shares boundaries with PV on the ventral, medial and lateral side, and with stria medullaris of the thalamus on the dorsal side. In the most posterior slice, the PT shares boundaries with the stria medullaris of the thalamus on the medial side and dorsal side, central dorsal nucleus and magnocellular (medial) division of medio dorsal nucleus on the lateral side and the PV nucleus on the ventral side. The bilateral parataenial nucleus shared boundaries in one of the ten slices Ding et al. (2016).

3.4 Efferents and afferents

The midline thalamic nuclei have a wide variety of connections for specific functions with multiple cortical areas. Despite the considerable evidence on systems of projections running between the midline thalamic nuclei and other cortical areas, the understanding of these connections in the human brain has remained not well understood and lacks detailed description and precision. Human tractography research in DWI has

shown that the most medial area of the thalamus is functionally connected with the medial orbitofrontal cortex, bilateral middle temporal gyrus, bilateral HC, posterior cingulate and retrosplenial cortex posteriorly (Lambert et al., 2017). In current research where we located and segmented the midline thalamus based on its connectivity to the mPFC (medial orbitofrontal and rostral ACC), MTL (hippocampus, parahippocampus, entorhinal cortex and amygdala) and to the nACC using probabilistic tractography in DWI data. However, more detailed anatomical connectivity patterns for the four individual midline thalamic nuclei in humans is lacking. Connections of the individual midline thalamic nuclei have been examined in macaque studies (Fig 7B; Amaral and Cowan, 1980; Aggleton et al., 1986; Hsu and Price, 2007, 2009), and more thoroughly examined in rodent studies (Fig. 7A; Wouterlood et al., 1990; Vertes et al., 1999; Krout and Loewy, 2000a; Otake et al., 2002; McKenna and Vertes, 2004; Vertes and Hoover, 2008; Hoover and Vertes, 2012; Li and Kirouac, 2012; Vasconcelos and Cassel, 2015; Vertes, 2015). The current section reviews the structural anatomical connectivity between the four midline thalamic nuclei (RE, RH, PV, and PT) and cortical and subcortical areas in primates, with additional findings from rodent studies to add on what has not been shown in primate research (Fig. 7).

Afferent projections to RE.

In primates, direct strong anatomical projections from PFC to RE, arise mainly from the medial areas (Amaral and Cowan, 1980; DeVito, 1980; Aggleton et al., 1986; Hsu and Price, 2007). In macaques, RE receives the densest projections from infralimbic cortex (IL; 25), and moderate-light projections from the prelimbic cortex (PL; 32), the

dorsal part of the anterior cingulate cortex (ACC; 24b), and lateral agranular insular area (lai) from the medial PFC network (Fig. 7B; Gabbott and Bacon, 1996; Hsu and Price, 2007). The macaque RE receives moderate projections from granular orbital cortex (area 13a and 13l), and moderate to light projections from orbital frontal cortex 12o from the orbital PFC network. RE receives moderate to light projections from rostral granular cortex 11l (Hsu and Price, 2007). These findings correspond to findings in rodent studies (Vertes, 2002: McKenna and Vertes, 2004). In macaques, RE also receives strong projections from the subiculum, presubiculum, and CA4/3 subfields of the HC (DeVito, 1980; Aggleton et al., 1986; Saunders et al., 2005; Hsu and Price, 2007). The input from HC to the RE appears most dense in the rostral and medial halves of the ipsilateral RE (Aggleton et al., 1986). In rodents, Re receives similar projections from the subiculum, and additionally receives input from cornu ammonis 1 (CA1; Wouterlood et al., 1990; Dolleman-Van der Weel et al., 1997; McKenna and Vertes, 2004). RE does not however receive any projections from the dentate gyrus in either the rodents or primates (Wouterlood et al., 1990: McKenna and Vertes, 2004). In rodents, the RE also receives input from entorhinal, perirhinal and retrosplenial cortices (Fig. 7A; McKenna and Vertes, 2004; Vertes et al., 2015), which has not yet been documented in primates. Furthermore in macaques, the RE received moderate projections from the basal, accessory basal and lateral nuclei of the amygdala (Aggleton and Mishkin, 1984; Hsu and Price, 2009), and moderate to light projections from the medial hypothalamus (Hsu and Price, 2009), which correspond to evidence found it rodents (Vertes, 2015). In rodents there are projections from the RE to the anterior, ventromedial, lateral, perifornical, posterior, supramammillary, and dorsal premammillary nuclei of the hypothalamus

(McKenna and Vertes, 2004). Additionally, findings in rodent studies showed that the rodent RE has inputs from the zona incerta, the ventral tegmental areas (VTA), peri aqueductal gray area (PAG), precommisural nucleus, parabrachial nuclei, laterodorsal tegmental nucleus dorsal and median raphe nuclei of the brainstem, claustrum, lateral septum, bed nucleus of stria terminalis (BNST), medial, lateral and magnocellular preoptic nuclei of the basal forebrain, the orbitomedial, insular cortices, the lateral habenula, and the lateral geniculate and paraventricular nuclei of the thalamus (McKenna and Vertes, 2004; Vertes, 2015). There is also evidence of widespread projections from the ectorhinal cortex of rodents to the RE (Vertes et al., 2015).

Efferent projections of RE.

In the macaque, the projections from RE to the PFC are the most dense to IL (area 25) and caudal part of insular cortical area (14c), moderate to medial frontal pole (area 10m) and moderate to light projections to PL (area 32), ACC (area 24), the rostral part of insular cortical area (14r), and lateral agranular insular areas (Iai) in the medial PFC network and orbital areas 13a,12o, 12l and medial agranular insular area (Fig. 7B; Hsu and Price, 2007). These findings in macaque research, correspond to findings in rodents (Fig. 7A; Hoover and Vertes, 2012; Vertes et al., 2015). Rodents, unlike macaques, also have light projections from the RE to posterior agranular, dysgranular and granular insular areas (Vertes et al., 2006). In rodents, RE also projects to the rostral retrosplenial cortex (RSC; Vertes et al., 2015) and the ectorhinal cortex (Vertes et al., 2006). In both the macaque and the rodent, the RE sends projections to the subiculum of the HC, and the entorhinal cortex (EC) (Amaral and Cowan, 1980; DeVito, 1980; Saunders et al., 2005;

Hsu and Price, 2009). In the rodent, RE fibers project to the stratum lacunosum-moleculare of CA1 of the dorsal and ventral HC as well as the molecular layer of the dorsal and ventral subiculum and parasubiculum (Wouterlood 1990; Vertes 2006); however, it has not been documented in primates if the CA1 of the HC also receives RE projections. Evidence from rodent research also showed that RE sends projections to the ventral CA1 that are 10 times stronger than those to the dorsal CA1 (Dolleman-Van der Weel et al., 1997; Hoover and Vertes, 2012; Varela et al., 2014). RE does not send projections to CA2, CA3 and the dentate gyrus of the HC in both rodents and macaques (Vertes et al., 2015). Hoover and Vertes (2012) showed evidence in rodents that cells sending projections to the HC are most dense in the rostral area of the RE, while the cells of the RE that project to the mPFC are located more laterally. They also showed that ten times more cells of the RE project to the ventral HC of the rodent, compared to the dorsal HC (Hoover and Vertes, 2012). Additionally, findings in rodent studies showed that the RE also projects heavily to the perirhinal cortex and the claustrum (Vertes et al., 2015). Moderate projections are also seen from the RE of rodents to the lateral and medial agranular areas of the motor cortex (Vertes et al., 2006). The macaque RE also sends moderate projections to lateral/middle hypothalamus, and light to moderate projections to the basal, accessory basal and lateral nuclei of the amygdala, the nACC, the rostro-medial caudate, and the putamen (Giménez-Amaya et al., 1995; Hsu and Price, 2009). The rodent RE also sends projections to these regions, but they are lighter than those in macaques (Vertes et al., 2006). There are also projections from the RE to the rodent piriform. However, the strength of these connections varies with denser projections to the anterior region and lighter projections to the posterior region. The opposite is observed in

RE projections to the rodent tania tecta, where dense projections are seen dorsally and light projections are seen ventrally (Vertes et al., 2006). Vertes et al. (2006) also showed that there is light labeling from the rodent RE to the somatosensory cortex, lateral septum, and anterior olfactory nucleus, as well as to several other regions in the hypothalamus, subthalamus, and thalamus. Among these regions are the supramammillary nucleus, the PV, anterodorsal, anteroventral, interanteromedial, intermediodorsal, mediodorsal and central medial nuclei of the thalamus as well as the lateral habenula and zona incerta. Light projections to the basal forebrain include the BNST, substantia innominata, the lateral, medial, median, and magnocellular preoptic nuclei, and the median septal and diagonal band nuclei (Vertes et al., 2006).

Afferent projections to RH.

The neuroanatomical connectivity of the RH is significantly less well-defined compared to the RE, especially in human and non-human primates. To the best of our knowledge, no afferent projections to the RH have been examined in primates. In rodents, despite some overlap, projections to RH are mostly different from those to RE. RH receives significant input from non-limbic sensory and motor structures (Vertes et al., 2015). In rodents, the RH also receives dense input from the PFC, specifically from IL, PL, ACC and most dense from the medial agranular cortex; however, RH has no inputs from the HC and few projections from the parahippocampus (Fig. 7A; Pereira de Vasconcelos and Cassel, 2015; Vertes, 2002; Vertes et al., 2015). The rodent RH receives subcortical projections from the forebrain, which arise most dense from the claustrum, substantia innominata and zona incerta, and to a lesser extent from the posterior and

lateral nuclei of the hypothalamus and amygdala. In rodents, RH also receives dense projections from the brainstem, specifically from the VTA, PAG, pedunculopontine tegmental nucleus, laterodorsal tegmental nucleus and the parabrachial complex. RH in rodents also receives input from the substantia nigra-pars reticulata, mesencephalic reticular formation, superior colliculus, and the anterior pretectal nucleus, which are more involved with motor functions (Vertes et al., 2015). The inputs the RH receives have yet to be studied in humans and non-human primates.

Efferent projections to RH.

In rodents, although RH afferents are different from RE, RH efferents are more similar to RE efferents. Whereas the projections from RE are more specific to limbic cortices, RH projections distribute to those cortices too, but also more widely to non-limbic cortex regions in rodents (Vertes et al., 2015). In rodents, the RH has dense projections to the PFC. Specifically, it has dense projections to the medial orbital, agranular medial cortex, ACC, IL, PL, the posterior agranular cortex, and the medial agranular motor cortex (Fig. 7A; Vertes et al., 2006). The rodent RH also sends dense projections to the CA1 of the HC, the subiculum, entorhinal cortex, retrosplenial cortex, perirhinal cortex, and temporal cortex (Vertes et al., 2006). The rodent RH specifically sends projections to the hippocampal CA1 (stratum lacunosum-moleculare) of the dorsal, but not ventral, hippocampus (Pereira de Vasconcelos and Cassel, 2015; Vertes, 2002). Interestingly, the RH has no inputs from the HC, but it does send dense projections to the HC in rodents (Vertes, 2015). These projections from RH to the HC, however, are significantly less dense compared to the projections from RE (Vertes et al., 2015).

Specifically, the medial and central region of the ventral striatum receives the densest innervations, and the lateral region of the ventral striatum and the shell of the nACC received medium to dense projections from RH (Giménez-Amaya et al., 1995). Interestingly, the RH sends the most dense projections to the medial and central regions of the ventral striatum out of the four midline thalamic nuclei (Giménez-Amaya et al., 1995). In rodents, other dense cortical targets of the RH are the primary and secondary somatosensory cortex, medial frontal pole, basolateral amygdala, claustrum, posterior parietal cortex, occipital cortex, dorsal and ventral agranular insular cortex, anterior piriform cortex, ventral anterior olfactory nucleus, BNST, caudate-putamen, endopiriform nucleus, lateral septum intermediate nucleus, substantia innominata, and the dorsal tania tecta (Vertes et al., 2006). The RH in rodents sends moderate projections to the medial agranular motor cortex, anterior piriform cortex, ventral anterior olfactory nucleus, BNST, caudate-putamen, endopiriform nucleus, lateral septum intermediate nucleus, and substantia innominata. Moderate labeling has also been seen in the ectorhinal cortex of rodents (Vertes et al., 2006). The RH in the rodent also sends light projections to the ventral tania tecta, posterior piriform, lateral frontal dysgranular/granular insular cortex, lateral agranular motor cortex, ventrolateral orbital cortex, posterior piriform cortex, anterior area of the amygdala, central amygdala, lateral and posterior amygdala, medial anterior olfactory nucleus, the diagonal band nucleus, ventral nucleus of the lateral septum, lateral and medial preoptic area, medial septal nucleus, ventral tania tecta, magnocellular preoptic nucleus, zona incerta, supramammillary nucleus, posterior nucleus and the lateral nucleus of the hypothalamus (Vertes et al., 2006). There are also light projections from the rodent RH to several

regions within the thalamus. These include the anteromedial nucleus, anteroventral nucleus, central medial nucleus, interanteromedial nucleus, intermediodorsal nucleus, medial and central part of the mediodorsal nucleus, lateral habenula, paraventricular nucleus, reticular nucleus, reuniens, and submedial nucleus (Vertes et al., 2006).

Afferent projections to PV.

The primate PV receives afferents from areas throughout the mPFC. PV receives most dense inputs from the IL, and less dense inputs from the PL and granular orbital surface (area 13 and 14; Fig. 7B; Hsu and Price, 2007; Passingham and Wise, 2012). There are also projections from the agranular insular cortex to PV (Hsu and Price, 2007, 2009). These incoming projections into the PV in macaques correspond to findings in rodent studies (Fig. 7A; Vertes et al., 2015). Rodent research has shown evidence of a dorsal to ventral gradient where the PL and IL send dense projections to PV, and medial agranular cortex and anterior cingulate send more moderate projections to PV (Li and Kirouac, 2008; Vertes and Hoover, 2008; Vertes et al., 2015). In the macaque, the PV receives dense projections from the lateral septum, nACC, and rostromedial caudate, as well as moderate to dense projections from the subiculum, presubiculum, entorhinal cortex and CA4/3 subfields of the HC (Aggleton et al., 1986; Hsu and Price, 2009). Previous studies have found that the projections from these structures terminate predominantly in the reuniens nucleus, anterior ventral, and lateral dorsal nuclei (Aggleton et al., 1986; McKenna and Vertes, 2004; Saunders et al., 2005; Hsu and Price, 2007) but there are still moderate projections going to PV. Projections from the entorhinal cortex to PV do not occur in rodents and appear to be unique in primates

(Aggleton et al., 1986; Saunders et al., 2005; Hsu and Price 2009). In rodents, the anterior PV receives more inputs from the hippocampal subiculum, especially from the ventral subiculum (Li and Kirouac, 2012; Hsu et al., 2014), and PL cortex, whereas the posterior PV receives more inputs from the PL, IL, and agranular cortex. PV also receives projections from the amygdala. The anterior part of the PV in the macaque receives inputs from the parvocellular part of the basal amygdaloid nucleus in the amygdala and the posterior part of PV receives projections from the central nucleus of the amygdala (CeA; Hsu and Price, 2009). This corresponds to rodent research (Vertes et al., 2015). In macaques, PV also receives dense projections from the dorsomedial nucleus of the hypothalamus. PV also receives projections from the lateral hypothalamic area, perifornical area, medial optic nucleus, ventromedial hypothalamic nucleus, suprachiasmatic and arcuate nucleus within the thalamus (Hsu and Price, 2009; Hsu et al., 2014). Very light projections are also seen from the lateral putamen and locus ceruleus to the PV in macaques (Hsu and Price, 2009). In rodents PV receives projections from supramammillary, tuberomammillary, lateral, dorsomedial, posterior, and parasubthalamic nuclei of the hypothalamus and the medial preoptic area and diagonal band nuclei (Goto and Swanson, 2004; Kirouac et al., 2005; Li and Kirouac, 2012; Vertes et al., 2015). The PV in macaques also receives projections from the midbrain. Specifically, PV receives dense projections from the dorsal raphe, and moderate projections from the median raphe, PAG, and parabrachial nucleus (Hsu and Price, 2009; Li and Kirouac, 2012). Consistent findings have been found in rodents, where additional projections have been found from the locus coeruleus, nucleus of the solitary tract, and ventral medulla (Vertes et al., 1999; Krout and Loewy, 2000a, 2000b; Otake et al., 2002;

Vertes et al., 2015). Vertes et al. (2015) also found projections from the BNST to the PV in rodents. Rodent research shows additional findings that PV receives projections from the brainstem, specifically from VTA, pontomesencephalic reticular formation, nucleus cuneiformis, nucleus of Darkeschewitsch, laterodorsal tegmental nucleus and pedunculopontine tegmental nucleus, (Krout and Loewy, 2000a, 2000b; Li and Kirouac, 2012; Vertes et al., 2015). Out of the four midline thalamic nuclei covered in this paper, PV uniquely received projections from the suprachiasmatic nucleus and the intergeniculate leaflet in rodents (Moga et al., 1995; Kawano et al., 2001; Alamilla et al., 2015).

Efferent projections from PV.

The PV in macaques sends dense projections to the medial prefrontal cortex, specifically PL, and IL, with less dense projections towards the frontal pole (10m; Fig. 7B; Hsu and Price, 2007). These findings are consistent with rodent findings (Fig. 7A; Li and Kirouac, 2008; Vertes and Hoover, 2008; Vertes et al., 2015). Rodents also have prominent projections from the PV to the dorsal peduncular and interstitial nucleus of the anterior commissure (Li et al., 2008). Along the gyrus rectus at the ventromedial corner of the frontal lobe, PV also sends dense projections to caudal areas of 14 but only sparse projections in more rostral areas (14r) and PV sends moderate to dense projections to inferior convexity area (12) and posteromedial agranular insular cortex (Hsu and Price, 2007). The rodent PV also has projections to the latter and to the granular insular cortex (Vertes et al., 2008; Vertes et al., 2015). In macaques, there are no projections from PV to the ACC (24; Hsu and Price, 2007). Rodents do have projections to the ACC but they are

light (Vertes et al., 2008; Vertes et al., 2015). This information adds to rodent data stating that PV has output to the dorsal agranular insular cortex (Li and Kirouac, 2008; Vertes and Hoover, 2008; Vertes et al., 2015). In a later experiment, Hsu and Price (2009) showed evidence that the dorsal midline thalamic nuclei (PV and PT) have the most dense outputs to the nACC, corresponding to findings in other macaque research (Giménez-Amaya et al., 1995) and rodent research (Giménez-Amaya et al., 1995; Li and Kirouac, 2008; Vertes and Hoover, 2008; Hsu and Price, 2009; Vertes et al., 2015). In turn, the nACC also has dense connections with the IL in the mPFC (Ferry et al., 2000), which in turn also has dense bidirectional connections with the PV (Hsu and Price, 2009), possibly forming a loop of communication (Hsu and Price, 2009). PV is unique from all the other thalamic nuclei because it is the only thalamic nucleus that projects to limbic structures such as the BNST, nACC, and IL, which are brain structures related to stress (Hsu et al., 2014). This is also true of the rodent PV (Vertes et al., 2008; Vertes et al., 2015). The macaque PV also projects to the caudate nucleus, which also receives projections from the mPFC (Ferry et al., 2000; Hsu and Price, 2009). The PV also projects to the ventral striatum, but has more dense projections to the medial regions than to the central and lateral regions (Giménez-Amaya et al., 1995). PV sends strong bidirectional connections to the amygdala, especially to the basal nucleus and the central nucleus of the amygdala (Aggleton et al., 1980; Mehler, 1980; Hsu and Price, 2009). These findings correspond to findings in rodents (Li and Kirouac, 2008; Vertes and Hoover, 2008; Vertes et al., 2015). Just like the RE, the PV also sends projections to the EC, especially the anterior regions of the EC, in both rodents and macaques (Hsu and Price, 2009).

Out of all the midline thalamic nuclei, the PV projects significantly the most to the hypothalamus. In the macaque, PV projects most dense to the rostral areas of the medial preoptic area and suprachiasmatic nucleus, and caudal parts of both the medial and lateral hypothalamus (Hsu and Price, 2009). Rodents also have projections from the PV to the medial preoptic area, but these projections are more moderate (Vertes et al., 2009; Vertes et al., 2015).

Findings in macaque research have also shown dense projections from the PV to the ammons horn, subicular complex, and PAG (Amaral and Cowan, 1980; Hsu and Price, 2009). Next to these dense projections in macaques, there are few projections from PV to the cellular part of the paraventricular hypothalamic nucleus, and dense projections to areas lateral to this hypothalamic nucleus (Hsu and Price, 2009). Findings from rodent studies showed evidence that PV has projections to suprachiasmatic, arcuate, and dorsomedial nuclei of the hypothalamus (Li and Kirouac, 2008; Vertes and Hoover, 2008; Vertes et al., 2015). There are also light projections from the PV to areas such as the globus pallidus, tania tecta, fusiform nucleus, ectorhinal cortex, piriform, and medial orbital cortex (Li et al., 2008; Vertes et al., 2008; Vertes et al., 2015). In macaques, there was only a little projection from the central part of the ventromedial hypothalamic nucleus (Hsu & Price, 2009), contrasting evidence from rodent studies (Moga et al., 1995). In macaques and rodents, PV also send projections to the lateral septum (Berendse and Groenewegen, 1990; Moga et al., 1995; Li and Kirouac, 2008; Vertes and Hoover, 2008; Hsu and Price, 2009; Vertes et al., 2015). Additionally, rodent literature also shows evidence of projections from PV to the ventral subiculum of the HC, claustrum, olfactory

tubercle, and dorsal striatum (Li and Kirouac, 2008; Vertes and Hoover, 2008; Vertes et al., 2015), which has not been documented in primates.

Afferent projections to PT.

PT in macaques receives dense projections from the medial PFC network. Specifically, from PL (area 32) and IL (area 25) (Fig. 7B; Hsu and Price, 2007). These findings are consistent with rodent data (Fig. 7A; Vertes, 2002). In macaques, the PT also has strong inputs from the presubiculum, raphe nuclei, PAG, and parabrachial nucleus. Both rodents and macaques have projections from the subiculum and parts of the septum to the PT (Vertes et al., 2015). PT also receives moderate to dense projections from the frontal pole (10m) and light to moderate projections from the lateral agranular insular area (lai). The macaque PT also receives moderate projections from the entorhinal cortex, dentate gyrus, CA3/CA4 and basal, accessory basal and lateral nuclei of the amygdala. Light projections have also been observed from the medial hypothalamus (Hsu and Price, 2007). Rodent studies have also identified several other regions that project to the PT. Some of the strongest projections to the PT arise from the claustrum, rostral agranular insular cortex, and medial/ventral orbital cortices (Vertes et al., 2015). Less strong projections are seen from the diagonal band nuclei, BNST, medial nuclei of amygdala, reticular thalamic nucleus, ZI, and parts of the hypothalamus (Vertes et al., 2015).

Efferent projections from PT.

Similar to the PV, the macaque PT has dense projections to areas in the mPFC, specifically the PL, IL, caudal and rostral areas of 14, area 12 and posteromedial

agranular insular cortex, and the PT sends less dense projections to the rostral areas, inferior convexity area (12), the posteromedial agranular insula cortex, orbitofrontal area

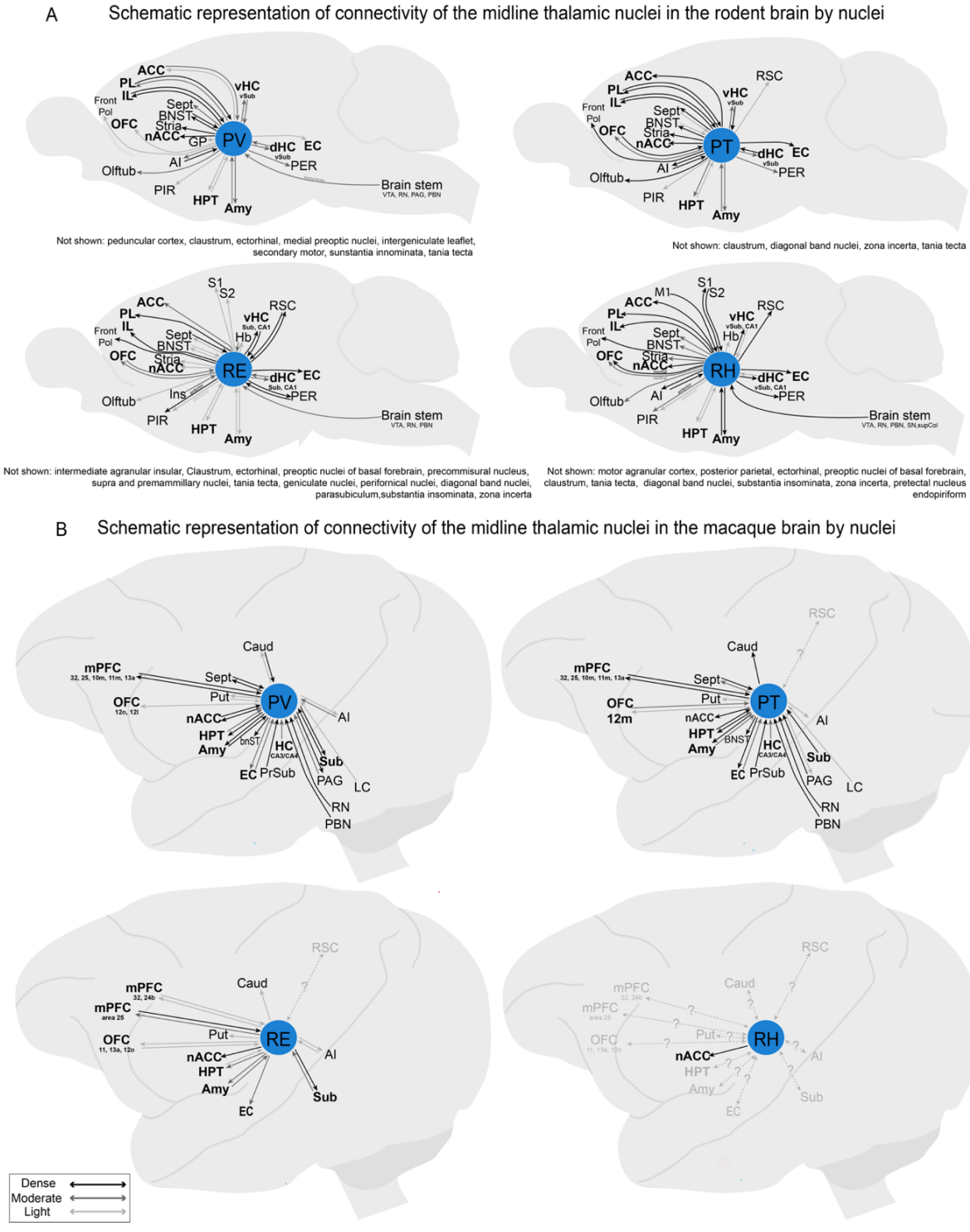

Figure 7. Schematic representation of known connectivity of the midline thalamic nuclei in rodents and macaques at different strengths. Note that although some variability between species can be expected, there is a large gap in knowledge between species, hence there is a less dense known connectivity profile of the macaque versus the rodent (shown in grey dashed line). Currently, the precise connectivity profile of the midline thalamic based on tracer studies is not known, however based on our previous work we have found there to be high connectivity to the mPFC (OFC, rostral ACC), MTL (HC, paraHC, EC, Amy) and nACC (Reeders et al., in prep).

projections to the BNST (Li et al., 2008; Vertes et al., 2008; Vertes et al., 2015). In macaques, similar to PV, PT does not send projections to ACC (Hsu and Price, 2007). On the contrary, rodent studies have found dense projections from the PT to the ACC (Vertes et al., 2008; Vertes et al., 2015). In macaques, just like RE and PV, PT also sends projection to EC (Hsu and Price, 2009). Anterior regions of the entorhinal cortex receive more dense connections from the PV and RE, and a less dense input from PT, and the posterior regions of EC receive more dense projections from PT and RE but less dense projections from PV (Insausti et al., 1987; Hsu and Price, 2009). This evidence suggests that different thalamic nuclei project to different subdivisions of the entorhinal cortex (Hsu and Price 2009). Rodent studies showed evidence that electrical stimulation of the midline thalamus results in an excitatory effect on the EC (Zhang and Bertram, 2002). In macaques, the PT has moderate projections to the basal, accessory basal and lateral nuclei of the amygdala, and light projections to the putamen, PAG, and lateral/middle hypothalamus (Giménez-Amaya et al., 1995; Hsu and Price, 2009). The PT also sends projections to the nucleus accumbens and medial regions of the ventral striatum, but not to lateral or central regions (Giménez-Amaya et al., 1995). Additionally, macaque research showed evidence for light projections from the PT to the rostro medial caudate, medial caudate and the medial preoptic area/anterior hypothalamus in macaques.

However this has not been found in all macaque subjects (Hsu and Price, 2009). Like the PV, but to a lesser extent, the PT also projects to lateral septum in macaques (Hsu and Price, 2009). This evidence corresponds to the PT efferents in rodent studies (Kelley and Stinus, 1984). Vertes et al. (2008, 2015) have also shown that there are dense projections from the PT in rodents to the olfactory tubercle and moderate projections to the perirhinal cortex, piriform, ventral subiculum, claustrum, and tania tecta. Lighter projections are also seen in the EC, retrospenial cortex, and nuclei of the amygdala (Li et al., 2008; Vertes et al., 2008; Vertes et al., 2015). The connectivity pattern of the PT suggests that this thalamic midline nucleus is an important link between limbic and striatal processing.

3.5 Functions involving the midline thalamus

Memory consolidation.

The midline thalamus has an important role in memory due to the connections it has with the HC and mPFC. The HC and mPFC are important structures for memory processing. The HC has direct projections to the mPFC but there are no direct projections from the mPFC to the HC in the rodent brain (Fig. 2A; Vertes et al., 2007). Furthermore, the HC to mPFC fibers are unidirectional and unevenly distributed over the HC in the rodent (Vertes et al., 2007; Hoover and Vertes, 2012). Therefore, for bidirectional communication between the mPFC and HC, another brain region is required (Thielen et al., 2015). The midline thalamus (RE and RH) has bidirectional connections to both the HC and mPFC in rodents (Fig. 8A; Vertes et al., 2007; Hoover and Vertes, 2012; Dolleman-van der Weel et al., 2019), and these findings are also evident in monkeys (Amaral and Cowan, 1980; DeVito, 1980; Aggleton et al., 1986; Hsu and Price, 2007,

2009; Aggleton, 2012;). The midline thalamus serves as a hub integrating the communication between the hippocampus and the mPFC, which is critical for memory processing in rodents (Thielen et al., 2015). This evidence suggests that midline thalamus therefore acts as an important structure closing the loop between HC and mPFC communication.

Human fMRI evidence suggests that the midline thalamus is functionally connected with the HC and mPFC during memory consolidation. During the initial stage of the classical model of systems consolidation the HC binds together distributed neocortical representations when recent memories are retrieved (Alvarez et al., 1994; Frankland and Bontempi, 2005). These neocortical representations code event features that are located in sensory representational areas located in posterior brain areas, and these areas are engaged during initial encoding (Alvarez et al., 1994). During the consolidation process, interconnectivity between these representational areas stabilizes, which allows the retrieval of remote memories to be hippocampally independent (Alvarez et al., 1994), and more neocortically represented. The mPFC comes to modulate the expression of memories that initially depended on the hippocampus in humans (Takashima et al., 2006) and rodents (Takehara-Nishiuchi and McNaughton, 2008). Recalling recent memories is hippocampally dependent, and recalling remote memories is associated with the mPFC (Frankland and Bontempi, 2005). Thielen et al. (2015) showed evidence supporting a model where the midline thalamus acts as a hub which links the mPFC, HC, and posterior representational cortex during retrieval of memories at initial stages of consolidation in humans, extending the classical models of systems consolidation by the addition of the role of the midline thalamic nuclei (Thielen et al.,

2015). They found that there is an increase in functional connectivity between the midline thalamus, the HC, mPFC and posterior parahippocampal cortex during retrieval of two hour old memories that might have undergone initial consolidation (Thielen et al., 2015). This increase in functional connectivity weakened over the course of three months. A subsequent analysis showed increasing functional connectivity between the mPFC and the same posterior parahippocampal region that showed a strong connectivity with the midline thalamus in the first analysis (Thielen et al., 2015). These results suggest that during the short sleep prior to day one, the offline consolidation process has caused initial steps of consolidation, but the memories have not yet fully consolidated. Retrieval of partly consolidated memories may require more HC-mPFC cooperation, as compared with memories that are still fully HC dependent or already neocortically represented (Thielen et al., 2015). With time the role of the midline thalamus and the HC appear to diminish such that connectivity between the mPFC and a specific representational area is associated with successful retrieval (Thielen et al., 2015).

Another theory based on rodent research states that the midline thalamic nuclei may control the dispersion of activity providing the appropriate activation level necessary to carry out cognitive processes like memory consolidation (Pereira de Vasconcelos et al., 2015). The midline thalamus is involved in adjusting the activity level of cortical structures relevant to memory processing. Findings in mice research showed that the mPFC controls hippocampal activation levels during memory encoding via the nucleus reuniens, where the interaction determines how specific or generalized a memory trace becomes (Xu and Südhof, 2013). Xu and Südhof (2013) suggested that increased hippocampal activation allowed less prominent memory features to be incorporated into

the overall memory of an event, creating a more specific memory. The opposite is suggested for the mPFC. The neocortex abstracts common features from multiple memories, creating more generalized memories (Xu and Südhof, 2013). This data suggests that when memories become consolidated, it becomes neocortically represented and the memories become more generalized. Connecting the functional fMRI data to this theory, this theory would suggest that to retrieve these partly consolidated memories, the mPFC utilizes the midline thalamus to increase HC activity and the posterior parahippocampal cortex to reinstate the specific memory trace (Thielen et al., 2015). The increase of the midline thalamus compensates for the loss of specificity due to the memories not being fully consolidated yet. After the consolidation process is finished, the memories will be neocortically represented in the mPFC and the functional coupling between the mPFC and the HC using the midline thalamus decreases (Thielen et al., 2015).

Taken together, evidence suggests that the RE is critical for closing the communication loop between the mPFC and HC (fig. 8A) necessary for memory consolidation. Once a memory has been fully consolidated, it becomes hippocampally independent, and more neocortically represented, not needing this communication loop as much.

Spatial working memory.

Spatial working memory is the maintenance of locations and spatial relations between objects over a brief temporal delay. Ventral midline thalamic nuclei are critical in spatial working memory (Dolleman-van der Weel et al., 2019) and work together with

the HC and mPFC during spatial working memory processes (Fig 8A). RE is an important anatomical link between the HC and mPFC, and as such is crucially involved in spatial working memory functions that recruit both structures (Hallock et al., 2016; Viena et al., 2018). Viena et al. (2018) examined the role of RE in spatial working memory and executive functioning following reversible inactivation of RE with either muscimol or procaine. They found that after inactivation of RE spatial working memory was impaired in rodents (Viena et al., 2018). Additionally, they found that rodents with inactivated RE showed impaired win-shift strategy as well as severe spatial perseveration, where rats re-entered incorrect arms of a spatial memory maze during correction trials, despite the absence of reward (Viena et al., 2018). This data suggests that RE is critical to spatial working memory, behavioral flexibility, and response strategy. Another study showed evidence that RE and RH are necessary for delayed alternation tasks, but not in continuous alternation (Layfield et al., 2015). Inactivation of RE and RH produces impairments in behavior on delayed alternation tasks, supporting the theory that RE and RH are orchestrators of interactions between the HC and mPFC during working memory.

Accumulating evidence shows the importance of the ventral midline nuclei in spatial working memory and the synchrony between the mPFC and HC. However, more research needs to be done to investigate more specific effects of RE and RH in spatial working memory and mPFC-HC synchronization. The specific role of RE and RH needs to be investigated to better understand the synchronizing effect these nuclei have on the mPFC-HC theta oscillations (Dolleman-van der Weel et al., 2019). Research also needs to be done on how the RE and RH affect the mPFC and HC independently and at different times during spatial working memory.

Temporal organization of memory.

Temporal organization of time is a critical aspect of episodic memory. Many of our experiences occur in the same places but the temporal patterns are distinct (Dolleman-van der Weel et al., 2019). How we remember temporal sequences of occurring events is fundamental to episodic memory (Allen et al., 2014). Accumulating evidence has shown that mPFC and HC are key players in memory for sequences of events (Ekstrom and Bookheimer, 2007; Devito and Eichenbaum, 2011; Reeders et al., 2021). In the temporal order of events during sequences, the brain will both play back events that have just occurred and think in the future for the anticipation of upcoming events. A recent rodent study showed that RE is critical to remembering sequences of events (Jayachandran et al., 2019). They used synaptic silencing to suppress activity from the mPFC to the RE prior to sequence memory testing after the rats had been trained to memorize the sequences (Jayachandran et al., 2019). They found that inactivating the mPFC projections to the RE heavily impaired sequence memory in rats but showed no impairments on other behaviors such as speed of running (Jayachandran et al., 2019). This evidence suggests that the RE is not solely involved in memory consolidation and spatial working memory, but that the RE is also involved in the organization of the temporal aspect of memory for sequences of events.

Chronic Stress Regulation.

Rodent studies showed that the PV is consistently activated following a wide variety of stressors including conditioned fear, sleep deprivation, foot shock, forced

swimming, and handling (Cullinan et al., 1995; Bhatnagar and Dallman, 1998; Bubser and Deutch, 1999; Otake et al., 2002; Spencer et al., 2004; Hsu et al., 2014;). That a variety of stressors activate the PV suggests that this nucleus is part of a common mechanism that is activated regardless of the stressor type (Hsu et al., 2014). Non-human primate and rodent studies have shown that PV has strong projections to the amygdala, BNST , nACC, and IL cortex and ACC of the PFC (Fig. 8B; Otake et al., 2002; Hsu and Price, 2007, 2009). These brain regions have been shown to be involved in the regulation of stress, mood and motivation (Bubser and Deutch, 1999). Projections from PV to these brain regions may represent pathways by which the PV can influence structures that regulate stress (Hsu et al., 2014). Rodent immunohistochemistry studies showed evidence that c-Fos, a molecular marker of increased neuronal activity in response to stress, in the PV has a strong and consistent increase in levels after exposure of psychological and physical stressors (Cullinan et al., 1995; Spencer et al., 2004; Dunn, 2005; Hsu and Price, 2009). Other rodent studies found that following mild foot shock, neurons that were activated by stress in the PV project to CeA and basolateral nucleus of the amygdala (BLA), nACC, and the medial prefrontal cortex (Bubser and Deutch, 1999). Similarly, following forced swimming, neurons in PV activated by stress project to the CeA in the amygdala (Zhu et al., 2011). Without direct connections to the hypothalamic paraventricular nucleus, the thalamic PV contributes to a parallel system in regulating the hypothalamic pituitary adrenal (HPA) axis.

The HPA axis is responsible for the neuroendocrine adaptation component of the stress response, and the hypothalamic paraventricular nucleus is a critical player in the initiation of HPA axis response (Bhatnagar et al., 2002), and its secretion of

glucocorticoid is critical for homeostasis of stressful conditions (Otake et al., 2002). However, the thalamic PV has only very light projections to this the hypothalamic paraventricular nucleus (Li and Kirouac, 2008). Due to this lack of connections with the hypothalamus paraventricular nucleus, Otake et al. (2002) investigated the activation of the PV in response to stress and its afferents using retrograde tracing combined with Fos immunohistochemistry after immobilization stress in rodents. They found that immobilization stress induces c-Fos protein expression in PV afferents from several areas known to be involved in the response to stressors, including the ventrolateral medulla, PAG, locus coeruleus, parabrachial nucleus, dorsal raphe, and the nucleus of the solitary tract. These brain regions have important inputs to the HPA axis (Otake et al., 2002). The lack of direct connections between the thalamic PV and the hypothalamic paraventricular nucleus, as well as the stress related input to the thalamic PV from these brain regions suggest that there is a system parallel that regulates the HPA axis via pathways through the aforementioned brain structures (Otake et al., 2002). This suggests that the PV is critical for habituation and facilitation of the HPA axis during chronic stress.

In rodents, the posterior PV is critical during chronic stress, for habituation and also facilitation of the HPA axis (Bhatnagar and Dallman, 1998; Bhatnagar et al., 2002, 2003). Rodent lesion studies showed evidence that the PV plays a unique role in adaptation to chronic stress, both neuroendocrine and behavioral; however, it does not adapt to acute stress without repeating preceded stress (Bhatnagar and Dallman, 1998; Bhatnagar et al., 2002, 2003). Rats exposed to repeated days of stress showed habituation of the HPA axis to a stressor if it is of the same type as the previous stressor (Bhatnagar et al., 2002). However, HPA axis stress response is often enhanced if the following

stressor is a different type compared to the previous stressor (Bhatnagar et al., 2002). This evidence suggests that the PV has the ability to habituate to the repeated stress response in chronic stress, and activate to a novel, potentially threatening, stressor (Bhatnagar and Dallman, 1998; Bhatnagar et al., 2002). A later study showed that this was also the case in young rat pups, where the PV was activated by repeated handling but not acute handling (Fenoglio et al., 2006), suggesting that activation of PV in chronic stress occurs throughout the lifespan.

The PV is innervated by neurotransmitter systems that are involved in abnormal stress response and mood disorder such as anxiety, depression and substance abuse (Hsu et al., 2014). These neurotransmitter inputs include orexins (ORX), corticotropin-releasing hormone (CRH), dopamine, serotonin, norepinephrine and endogenous opioids (Kirouac et al., 2005; Sánchez-González et al., 2005; Vogt et al., 2008; Hsu and Price, 2009) . Additionally, stressful stimuli create a stress response by increasing cortisol and increasing wakefulness. After a stressor stimuli, CRH stimulates the release of ORX and this circuit contributes to activation and maintenance of arousal associated with the stress response (Winsky-Sommerer et al., 2004). Connections of the PV and its innervation by serotonin, ORX and CRH suggest that the PV may relax stress signals between the midbrain and hypothalamus with the nucleus accumbens, basal amygdala, and infralimbic cortex, as part of a circuit that manages stress and possibly is related to stress related psychopathologies (Hsu and Price, 2009). In conclusion, the evidence presented suggests that the PV receives strong inputs from neurotransmitter systems and systems including the PAG, dorsal raphe, and parabrachial nucleus, that are activated in response to stressors, and potentially transmits these signals to output structures including agranular

insular cortex, CeA and BLA nuclei in the amygdala, nACC, BNST and IL (Fig. 8B). These specific afferents and efferents of the PV contribute importantly to the role of PV in stress response and regulation and could be involved in stress related disorders such as anxiety and depression. While this evidence supports the critical role PV has in chronic stress regulation, the exact mechanisms remain to be determined and more research is necessary.

Wakefulness and arousal.

Studies have shown that dorsal midline thalamus is critical for controlling wakefulness and arousal (Hsu and Price, 2009; Inutsuka et al., 2013; Luo et al., 2018; Ren et al., 2018). PV participates both in arousal in relation to the sleep-wake cycle, and in arousal related to salient stimuli and events independent of the sleep-wake cycle (Ren et al., 2018; Barson et al., 2020). Ren et al. (2018) found that glutamatergic neurons of the PV exhibited high activities during wakefulness using *in vivo* fiber photometry or multichannel electrophysiological recordings in mice. When suppressing the PV, there is a reduction in wakefulness, and when activated, there is an induced transition from sleep to wakefulness, even after general anesthesia (Ren et al., 2018).

Animals with chronic PV lesions showed a decrease in wakefulness during the dark phase, with a reduction in duration of wakefulness episodes and an increase in NREM sleep, whereas lesion of the PV did not affect wakefulness during the light phase (Ren et al., 2018). Additionally, chemogenetic inhibition of the downstream pathway of PV neurons to nACC, which also participates in control of wakefulness (Fig. 8C; Luo et al., 2018), significantly reduced wakefulness (Ren et al., 2018). Suppressing of the

upstream pathway of lateral hypothalamus (Li and Lecea, 2014) to PV, also decreased wakefulness (Ren et al., 2018). This demonstrates that the PV to nACC and the lateral hypothalamus to PV pathways have influence on the control wakefulness. Moreover, PV has two distinct cell types, where the posterior PV signal aversive states, and the anterior PV modulate arousal (Gao et al., 2020).

The midline thalamus also has many ORX neurons, which regulate many vital body functions, including wakefulness and sleep cycles (Hsu and Price, 2009; Inutsuka et al., 2013). ORX neurons are at high density in the hypothalamus and the brainstem, but can also be found in high density in the midline thalamus, specifically PV (Hsu and Price, 2009; Inutsuka et al., 2013). Interestingly, in the macaque, the PV has the highest concentration of ORX fibers in the brain (Peyron et al., 1998; Kirouac et al., 2005; Hsu et al., 2014). The PV receives dense innervation from hypothalamic ORX neurons in macaques (Hsu and Price, 2009) and rats (Peyron et al., 1998; Marcus et al., 2001). In rodents, the action of the ORX fibers are depolarizing, and excite the post synaptic PV neurons via OR_2X receptors to coordinate sleep-wakefulness signals (Ishibashi et al., 2005). When ORX neurons are activated by ORX, they maintain a long, consolidated wake period (Inutsuka et al., 2013). PV also receives dense innervations from norepinephrinergic, serotonergic, and cortico-releasing hormone brain regions in humans, non-human primates, and rodents (Baldo et al., 2003; Saper et al., 2005; Hsu and Price, 2009). The effect of these innervations of ORX neurons on norepinephrinergic and serotonergic cell groups promotes wakefulness and helps maintain a stable wake-sleep (Hsu and Price, 2009). Absence of ORX in the wake-sleep system results in narcolepsy

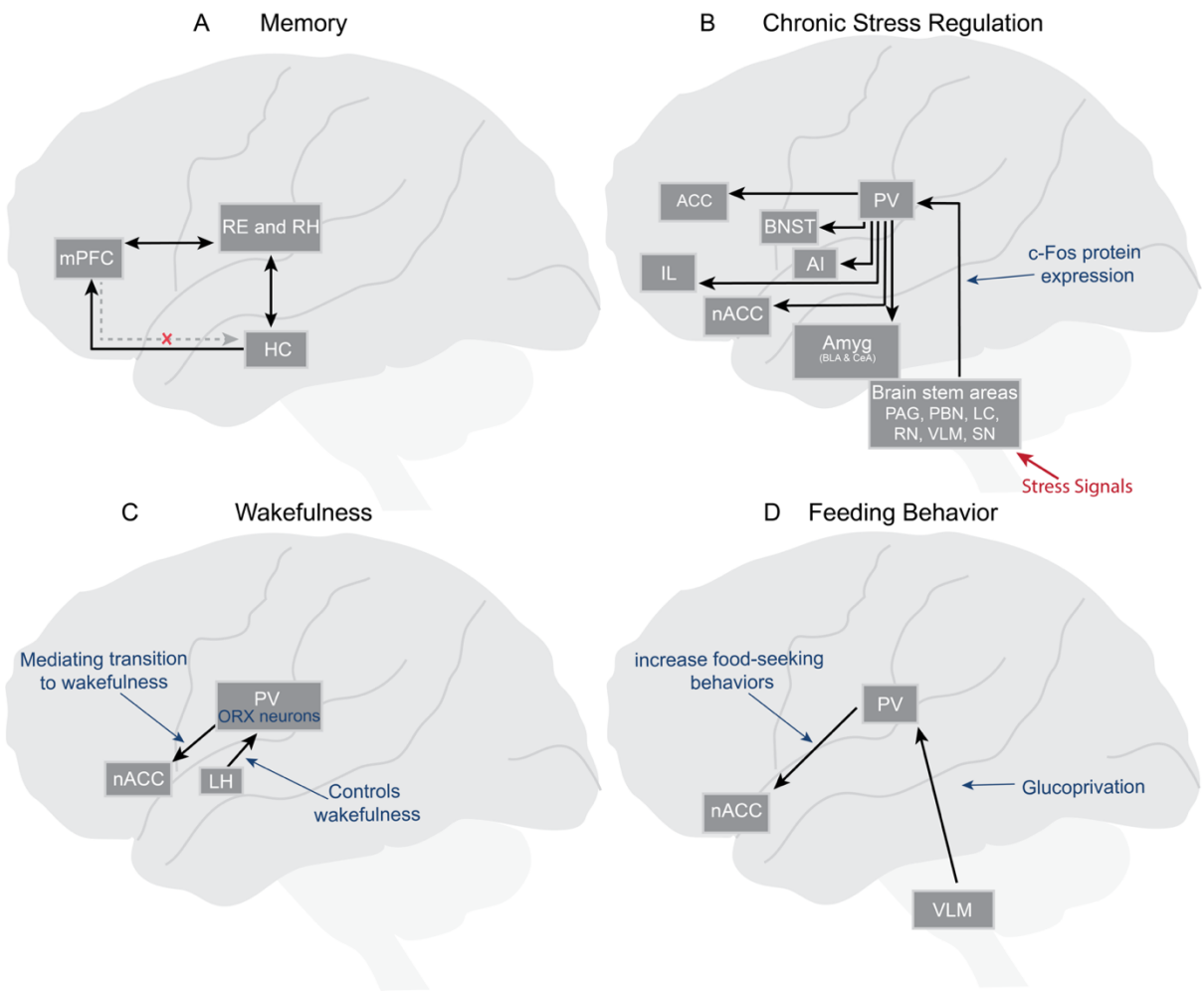

Figure 8. Schematic and simplistic representation of circuits involved in the memory, chronic stress regulation, wakefulness and feeding behavior. **A,** The HC and mPFC are critical for memory. The HC has direct projections to the mPFC, but there are no/very little direct return projections. The midline thalamus closes this communication loop necessary for memory processes. **B,** the PV is a mediator in chronic stress regulation. The idea is that the PV receives signals from regions known to be involved in response to stressors including the PAG, C, PBN, RN, VLM and SN. The PV then potentially transmits these signals to output structures including agranular insular cortex, CeA and BLA nuclei in the amygdala, nucleus accumbens, BNST and IL. These specific afferents and efferents of the PV contribute importantly to the role of PV in stress response and regulation. **C,** The PV is also involved in wakefulness. The lateral hypothalamus sends signals to the PV controlling wakefulness, and the PV sends ORX projections to the nucleus accumbens mediating the transition to wakefulness. **D,** The PV is also important for feeding behavior. The VLM sends dense projections to the PV with glucoprivation signals, and in turn the PV sends send signals to the nucleus accumbens to increase food seeking behavior.

and unstable wake-sleep cycles (Burlet et al., 2002). Mice with inactivated ORX genes exhibit narcolepsy behavior (Chemelli et al., 1999; Sutcliffe and de Lecea, 2000) and humans with narcolepsy have significantly reduced levels of ORX peptides in their cerebrospinal fluid (Sutcliffe and de Lecea, 2000). This evidence suggests that ORX neurons maintain proper wakefulness level for survival and that the PV has an important role communicating the signals regarding wakefulness from ORX neurons to its proper target cortex.

Appetite and feeding behavior

Research has also revealed that the PV is involved in reward and food-seeking behavior through homeostatic responses. Beas et al. (2020) showed that in rodents the PV is particularly important in counter-regulatory responses to glucoprivation, highlighting the PV's role in homeostasis. In glucoprivation, there is a lowering of blood glucose levels that triggers feelings of hunger. When blood glucose levels decrease, the PV is involved in a mechanism that promotes food-seeking to restore blood glucose levels to their homeostatic level. PV neurons projecting to the nACC are especially important in this response since they are functionally and anatomically connected to the ventrolateral medulla (VLM), which is a key regulator in this homeostatic response (Beas et al., 2020). In fact, the VLM has very dense connections to the PV (Phillipson and Bohn, 1994; Card et al., 2006; Beas et al., 2020), which in turn has dense connections to the nACC, a structure that is highly influential in reward seeking behaviors (Meffre et al., 2019; Otis et al., 2019; Beas et al., 2020). The nACC s involvement in reward-seeking explains its role in glucoprivation, since food-seeking and consumption are types of reward-seeking

behavior and are both activated when glucose levels are abnormally low. These strong VLM-PV connections facilitate the activation of PV- nACC projections, which has been shown to increase food-seeking behavior (Beas et al., 2020). However, it is important to make a distinction between food-seeking and consummatory behavior since PV- nACC neuronal activity varies with both. In a rodent study by Beas et al. (2020), activation of the PV- nACC pathway was linked to food-seeking behavior while decreased activation was linked to consummatory behavior. This finding is consistent with other studies that also showed this bidirectional modulation of the PV- nACC neurons (Reed et al., 2018; Otis et al., 2019). Thus, the VLM regulates food-seeking behavior through the activation of PV neurons that project to the nACC. In fact, the inhibition of PV- nACC projecting neurons results in a significant decrease in rodent feeding behavior, highlighting the essential role of the PV in this homeostatic response (Beas et al., 2020). This VLM-PV-nACC circuit is specific to glucoprivic responses and has not been shown to regulate other kinds of food-seeking behaviors, such as those associated with food restriction (Beas et al., 2020).

Kelley et al. (2005) showed that the PV is also involved in other food-seeking behaviors in rodents, specifically those associated with "overeating." Based on multiple studies, they propose that the PV is part of an arcuate-LH-PV-striatal axis that modulates feeding behaviors when energy requirements have been satisfied. Through this axis, hypothalamic information can reach the striatum via the PV (Kelley et al., 2005). The critical role of the PV in this circuit can be attributed to its function as an interface between signals from the lateral hypothalamus (LH), circadian oscillators, and behavioral state-regulating neurons (Kelley et al., 2005). These PV afferents are key in modulating

ingestive behavior since the LH receives and integrates both behavioral and metabolic information related to arousal and energy balance from the arcuate nucleus (Elmquist et al., 1999). More specifically, the LH has orexin-coded neurons which influence arousal levels, especially during goal-directed behavior. The PV then conveys these signals to cholinergic interneurons in the striatum which relay this information to behavioral action systems, orchestrating food-seeking behavior (Kelley et al., 2005). Most afferent projections of the striatal cholinergic interneurons come from the midline thalamus, especially from the PV (Kelley et al., 2005). Thus, input from the PV promotes feeding, even beyond energy needs, by stimulating the release of enkephalin from striatal output neurons. This ensures future energy availability through fat reserves (Kelley et al., 2005). Several other studies have also shown a great thalamic influence on these cholinergic interneurons (Dube et al., 1988; Lapper and Bolam, 1992). Evidently, the PV has a significant influence on ingestive behaviors through the regulation of cholinergic interneuron activity.

3.6 Midline thalamus is involved in multiple neurological disorders

Although very little is known about impairment or dysfunction of the midline thalamic nuclei and the associations with neurological disorders and symptoms, it has been suggested that the impairment of the midline thalamic nuclei is involved in Alzheimer's Disease (Braak and Braak 1991b; Ryan et al., 2013; Aggleton et al., 2016), Schizophrenia (Byne et al., 2009; Lisman et al., 2010), depression (Drevets et al., 1997; Brody et al., 2001; Pizzagalli et al., 2003; Hsu and Price, 2009;), drug relapse and addiction (Hamlin et al., 2009; Hsu and Price, 2009; James et al., 2010; Li and Kirouac,

2012), and others that are beyond the scope of the current review, including epilepsy (Bertram et al., 2001), autism (Ray et al., 2005) and Korsakoff's syndrome (Visser et al., 1999).

Alzheimer's Disease.

Alzheimer's Disease (AD) is a chronic progressive neurodegenerative disease that gradually worsens over time. Clinical symptoms of AD include impairments in memory, language, visuospatial orientation, and higher executive function. Non-cognitive changes include personality changes, decreased judgment ability, wandering, psychosis, mood disturbance, agitation, and sleep abnormalities (Schachter and Davis, 2000). Braak and Braak (1991a) studied in detail the involvement of the HC in the human brain in AD and also found evidence of other brain areas involved in AD including the thalamus (Braak and Braak, 1991b). Postmortem human AD brain slices showed evidence of amyloid plaques and neurofibrillary tangles in the thalamus. While amyloid deposition in the thalamus was variable and spread throughout, the pattern of neurofibrillary changes provided a more specific pattern of deposit in different nuclei of the thalamus (Aggleton et al., 2016). Amyloid plaques were present across numerous thalamic nuclei, unlike neurofibrillary tangles which were more restricted to specific areas. During earlier stages of AD, the parataenial nucleus of the midline thalamus displayed a significant number of neurofibrillary tangles (Braak and Braak, 1991b; Aggleton et al., 2016). By later stages of Alzheimer's disease (stage 5 and 6), neurofibrillary changes were also prominent in RE, PV and other thalamic nuclei. The thalamic neurofibrillary tangles were found on thalamic nuclei that have reciprocal connections with the HC (Aggleton et al., 2016).

The subiculum also shows significant decrease in cells and increase in neurofibrillary tangles in Alzheimer's disease (Hyman et al., 1990). During the progression of Alzheimer's Disease there is an interruption of the connection of the hippocampal formation due to the tangles, and presumably this includes the connection with the midline thalamic nuclei (Hyman et al., 1990; Aggleton et al., 2016). This also suggests that the midline thalami nuclei are critical for the communication and synchronization of the mPFC-HC and is important for memory consolidation.

Human neuroimaging studies showed findings that the thalamus is one of the earliest sites of amyloid deposition (Ryan et al., 2013). They also found evidence that the volume of the thalamus was reduced, but not of the hippocampus volume (Lee et al., 2013; Ryan et al., 2013), indicating that the thalamus is significantly involved in AD. Neuroimaging findings also showed reduced hippocampal functional connectivity with areas including the thalamus in patients with an increased risk of Alzheimer's disease (carriers of the APOE4 allele; Li et al., 2014).

Animal research also showed evidence for early pathological progression of Alzheimer's disease. Studies in transgenic mice showed that amyloid plaques first appear in the subiculum, and then in mamillary bodies and the thalamus, followed by the dentate gyrus and HC CA fields (Wilcock et al., 2008; Rönnbäck et al., 2012). However, the precise location or which thalamic nuclei was not specified (Aggleton et al., 2016). Further research needs to be done to examine the detailed anatomical specificity of these thalamic locations of where the amyloid-β plaques manifest, and how the neuropathology of this disease affects brain systems causing the cognitive impairments.

Cognitive impairment in AD may be related to mPFC impairments, or to impairments in communication between the HC and mThal with the mPFC. A positron emission tomography (PET) study indicated that memory deficits in early AD were due to a reduction in activity in the PFC and HC (Harrison et al., 2016). Additionally, early-stage AD ApoEε4 carriers exhibited decreased functional connectivity between the HC and mPFC. (Wang et al., 2015). Resting state fMRI found that there was also reduced functional connectivity between the HC and mPFC. However, changes in functional and structural connectivity between the midline thalamus and the mPFC is not known.

Schizophrenia

The thalamus provides a nodal link for multiple functional circuits that are impaired in schizophrenia (Byne et al., 2009). Post mortem studies have shown that patients with schizophrenia have high dopamine concentrations in various subcortical regions, and also increased dopamine receptor densities (Davis et al., 1991). A direct effect on the thalamus in response to typical antipsychotics would be expected selectively to the anterior, medial, midline and intralaminar nuclei because, as reviewed above, these nuclei have the greatest density of dopamine receptors (Byne et al., 2009). However, very little is known about midline thalamic involvement in abnormal cortical synchronization in schizophrenia.

Cortical synchronization patterns have been shown to be altered in schizophrenia (Uhlhaas and Singer, 2010). A study showed that there was reduced coherence between the HC and mPFC, accompanied by working memory impairments, in a genetic mouse model of schizophrenia (Sigurdsson et al., 2010). However, RE was not studied. RE is a

critical link because it closes the communication loop between the HC and mPFC and is necessary for this synchronization. Since the HC and mPFC need the RE to communicate bidirectionally, the RE is potentially involved in this coherence reduction associated with Schizophrenia. Dysfunction in prefrontal cortex, hyperactivity in thalamus, and hyperactivity in ventral hippocampus have been proposed to underlie the psychotic symptoms of schizophrenia (Zimmerman and Grace, 2016). However, the idea that hyperactivity in RE could lead to overdrive of subicular activity and aberrantly high ventral tegmental dopamine neuron activity has not been established. Rodent studies showed that NMDA receptor antagonist works in interaction with dopamine to produce delta frequency bursting in the thalamus (Olney et al. 1991; Umbricht et al., 2000). RE is among the most activated thalamic nuclei by NMDA receptors. RE has strong projections to the HC that excite the CA1 region (McKenna and Vertes, 2004). Experiments indicate that such activation can lead to excitation of dopaminergic cells of the ventral tegmental area (Floresco et al., 2001). When this happens, there will be an increase in dopamine levels in the thalamus. This will increase the activation of RE and send more signals to VTA, creating a loop of signals. A predisposition to schizophrenia is a NMDA receptor block (Lisman et al., 2010). If only this block is present the loop activity stays low, and if only stress is present without the NMDA receptor block, the loop activity will also stay very low. However, when both the NMDA receptor block and stress are active, it will throw the loop into a positive feedback, producing maximal activity (Lisman et al., 2010). This activity keeps persisting, even when stressors are removed. This demonstrated the bistable properties of the system in a situation where the NMDA receptor block is present. In conclusion, according to a model by Lisman et al. (2010),

schizophrenia occurs when the thalamus, HC and VTA are active in a loop, and they

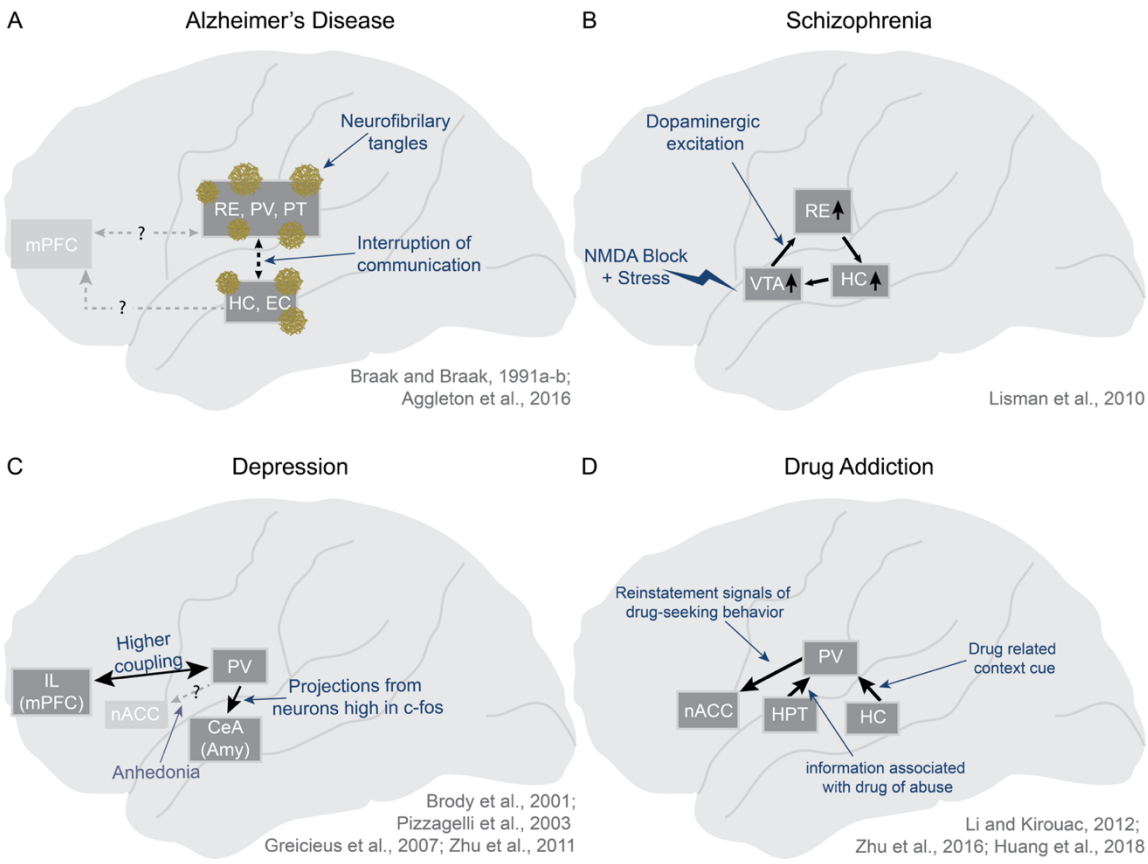

Figure 9. Schematic and simplified circuit models involved in neurological disorders. **A,** During the progression of Alzheimer's Disease there is an interruption of the connection of the hippocampal formation due to the tangles, and presumably this includes the connection with the midline thalamic nuclei. It is unknown whether and how this would affect the mPFC-midline thalamus – HC circuit that is critical to memory processes. **B,** A predisposition to Schizophrenia is a NMDA receptor block. When this block is present in combination with stress, the nucleus reuniens goes in hyperactivity, and can lead to overdrive of subicular activity, and in turn increase signals to the VTA forming a positive feedback loop (Lisman et al., 2010). **C,** The role of PV in chronic stress and based on its connectivity suggests it may play a crucial role in stress related psychopathology such as depression. There is abnormal higher coupling between the PV and IL in depressed individuals compared to healthy individuals (Greicius et al., 2007). This abnormal activity In PV may also influence the nucleus accumbens and may be responsible for anhedonia in depression (pizzagalli et al., 2003). **D,** In drug addiction the idea is that the hypothalamus sends drug related signals to the PV, the HC sends drug related context cue information to the PV. The PV processes this information and sends projections to the nucleus accumbens with signals associated with reinstatement of drug-seeking behavior.

become hyperactive under basal conditions. However, this computational model needs to be replicated and investigated in animal models.

Major Depression

There is substantial evidence that increased sensitivity to stress is an important risk factor for depression (Hasler et al.,2004). The role of PV in regulating chronic stress combined with its connectivity pattern and neurochemical input suggests it may play a role in clinical disorders and stress related psychopathology such as depression (Hsu and Price, 2009). As mentioned earlier in the stress regulation section, the PV receives stressZrelated signal from the hypothalamus, dorsal raphe, parabrachial nuclei, and PAG and has influence over the amygdala, nACC and IL of the mPFC. These structures all are key players in mood disorders and clinical conditions related to stress or abnormal reactions to stress such as depression (Hsu and Price, 2009; Hsu et al., 2014).

Furthermore, abnormal activity in PV in depression may intensify or maintain negative emotional effects caused by chronic stress by contributing to higher IL activity in the mPFC (Drevets et al., 1997; Brody et al., 2001; Pizzagalli et al., 2003). As mentioned before, PV has strong structural connectivity with IL cortex. The IL exhibits abnormal activity functional neuroimaging studies during depression (Drevets et al., 1997; Mayberg et al., 1999; Brody et al., 2001; Pizzagalli et al., 2003), which shows reversal after successful treatment of depression using fluoxetine treatment, which is an antidepressant serotonin reuptake inhibitor (Mayberg et al., 1999; Brody et al., 2001). In a human PET study, Drevets et al. (1997) showed that in depressed individuals there was an abnormal reduction in blood flow and rate of glucose metabolism in the IL cortex

compared to healthy controls. This evidence suggests that there was a lower metabolic rate in IL in depressed individuals. Another human electroencephalogram (EEG) and PET study showed that melancholia in depression resulted in reduced activity in IL, with increased inhibitory delta activity and decreased glucose metabolism (Pizzagalli et al., 2003). In that same study they showed that after treatment with tricyclic antidepressants, subjects with the largest reduction in depression severity showed the lowest post-treatment IL delta activity (Pizzagalli et al., 2003).

Evidence shows that there is abnormal activity of PV in individuals with depression. However, the specific role of the PV in relation to stress regulation and the onset of depression is poorly understood. One hypothesis is that the involvement of PV depends on whether the stressor presented leads to habituation or facilitation, e.g. an acute stressor can facilitate the onset of depression when there are already high levels of chronic stress present (Hammen, 2005, 2009). Then, in turn, a dysregulated HPA axis due to high levels of chronic stress is often associated with depression, and in part could be associated with the inability of PV to respond adaptively to the chronic stress. This view is supported by the observation using fMRI that there is an increase in midline thalamic activity and abnormal higher coupling between midline thalamus and IL of the mPFC in individuals with depression compared to healthy individuals (Neumeister et al., 2004; Greicius et al., 2007). Researchers suggested that in depressed individuals, the activity in the thalamus is excessively coupled to the IL, which is more involved in affective functions, at the cost of the more dorsal anterior cingulate cortex, which is more involved in cognitive functions (Greicius et al., 2007). Abnormal PV activity may also influence

the nucleus accumbens and may be responsible for anhedonia in depression (Pizzagalli et al., 2003).

Additionally, serotonin dysfunction is also associated with depression. In a human PET study, tryptophan depletion was used to measure decreased serotonin function which is associated with major depressive disorder (Neumeister et al., 2004). They showed that depressed patients in remission have increased thalamic metabolism in the midline of the thalamus, anterior cingulate, and orbitofrontal cortex, after tryptophan depletion, but not after sham depletion (Neumeister et al., 2004). This tryptophan depletion was associated with an increase in regional cerebral glucose usage in the medial thalamus, cingulate cortex, OFC, and ventral striatum in patients with remitted depression (Neumeister et al., 2004). This evidence suggests that tryptophan depletion is associated with a serotonin system dysfunction, which is associated with depression, and identifies a circuit that includes the midline thalamus with a role in the pathology of depressive disorder.

Pharmacological treatments affect PV and depressive-like behaviors.

The PV is studied in many rodent models of depression, targeting the PV with lesions or pharmacological manipulations. In one study, after rodents were forced to swim, there were increased c-fos levels, which were correlated to their freezing behavior (Zhu et al., 2011). Additionally, they found that PV neurons that projected to the amygdala CeA had an increase in c-fos. These results suggest that the PV-CeA pathway is involved in depressive like behavior such as freezing (Zhu et al., 2011). Additionally, according to Smith et al. (1999), studies in nonhuman primates and pigs have found that selective serotonin reuptake inhibitors (SSRI), radiolabeled for use in PET or SPECT

(single-photon emission computed tomography), have been shown to accumulate to a high degree in the midline thalamic nuclei (Smith, 1999). This suggests that serotoninergic neurotransmission to the midline thalamic nuclei, particularly PV, may be involved in the antidepressant effects of SSRIs (Hsu et al., 2014). Another study investigated the pharmacological effects of desipramine, a tricycling antidepressant, on brain regions including the PV. They found that PV was of the structures that showed reduced c-Fos levels after the pharmacological administration, which also led to a reduced level of depressive behavior (Beck and Fibiger, 1995). Similarly, a study using olfactory bulbectomized rats, which is used as a model of depression, studied the effect of the administration of chronic fluoxetine treatment, a SSRI, on stress sensitive areas including the PV (Roche et al., 2007). They found that after chronic treatment, there was reduced c-fos expression in the PV, amygdala, HC and dorsal raphe, and the rodents showed reduced depressive like behaviors (Roche et al., 2007). Taken together, these studies suggest that the PV is involved in multiple rodent models of depression and is affected by the pharmacological treatments. Future studies should focus on selectively targeting the PV with pharmacological treatment or with lesions to investigate the specific role this nucleus has in non-human animal models of depression.

Drug Addiction

Studies have shown that PV is activated by acute and repeated drugs of abuse (Hamlin et al., 2009), and context cues that are associated with the drug of abuse (Brown et al., 1992; Rhodes et al., 2005; Dayas et al., 2008; Barson et al., 2015; Chisholm et al., 2019) such as signal for sugar water (Igelstrom et al., 2010), or during foot shock (Beck

and Fibiger, 1995; Yasoshima et al., 2007), and also when they are placed in an environment associated with conditioned taste aversion (Yasoshima et al., 2007). In turn, studies have shown that lesioning the PV can lead to emotionally correlated behaviors such as conditioned taste aversion (Yamamoto et al., 1995) and drug seeking behavior (James et al., 2010; Hamlin et al., 2009; Browning et al., 2014). Evidence that the PV has an important role in negative and positive charged emotional behavior is accumulating; however, the precise mechanisms on how exactly the PV is involved in both negative and positive charged behavior is still undetermined.

The PV has inputs to the amygdala, nucleus accumbens, prefrontal cortex and other brain areas that are involved in expressing negative or positive emotional states (Hamlin et al., 2009; Zhu et al., 2011). The idea is that when the PV receives information from the hypothalamus that has an association with an event that is emotionally charged, it would provide excitatory input to the amygdala, nucleus accumbens, prefrontal cortex and other brain areas involved in emotional states activating them. Consistent with this view, rodent studies have shown that lesioning or inactivating PV neurons reduce reinstatement of drug seeking behaviors such as expressing drug-seeking behavior after being primed with cocaine (James et al., 2010), conditioned place preference induced by cocaine (Browning et al., 2014), and moving to an environment that is cocaine-induced (Marchant et al., 2010; Young and Deutch, 1998). The hypothalamus sends projections such as ORX signals or a signal containing information associated with drug of abuse to the PV, and the PV will in turn send projections to the nucleus accumbens. However, the PV to nACC pathway is thought to be involved in addictive behaviors motivated by

negative reinforcement, rather than craving induced addictive behavior (Zhu et al., 2016; Huang et al., 2018; Hill-Bowen et al., 2020).

Projections from the PV to the nACC have also been shown to be involved in the reinstatement of extinguished alcohol-seeking behavior induced by context, but receive contextual cues coming from the subiculum (Hamlin et al., 2009; Hsu and Price, 2009; Li and Kirouac, 2012). This evidence suggests that the PV is activated by exposure to drugs and to drug associated contexts and cues. This activation of the PV with possible cue information coming from the subiculum are what leads to drug seeking behavior. Therefore, while the hypothalamus sends drug related signals to the PV, the HC sends drug related context cue information to the PV. The PV processes this information and sends projections to the nucleus accumbens with signals associated with reinstatement of drug-seeking behavior (Fig. 9D)

ORX has also been shown to be involved in reward seeking, drug relapse and drug addiction (Harris et al., 2005; Inutsuka et al., 2013). Evidence also shows that ORX is involved in mediating stress-induced reinstatement of drug-seeking behavior (Boutrel et al., 2005). The nucleus accumbens is well known for its involvement in substance abuse (Deadwyler et al., 2004). PV, IL and the shell of the nucleus accumbens have high levels of ORX fibers (Ferry et al., 2000; Baldo et al., 2003; Hsu and Price, 2009), and these structures have bidirectional connections with each other, potentially forming a circuit involved in reward seeking and drug abuse. These brain regions are also involved in chronic stress and depression, and often these diseases are comorbid (Hsu and Price, 2009).

3.7 Conclusion.

The midline thalamic nuclei, and their complex circuits, are part of higher order cortico-thalamic-cortical networks that are important for cognition. The midline thalamic nuclei receive a wide array of afferents from limbic related sites in the brainstem and forebrain and have specific projections to limbic cortical and subcortical structures. While the dorsal midline thalamic nuclei are primarily involved in functions related to affective functions such as chronic stress control, and the ventral midline thalamic nuclei are more involved in cognitive function such as memory, the entire midline thalamus projects specifically to limbic subcortical and cortical areas (Vertes et al., 2016).

Although there is rich anatomical, functional, and behavioral data on the midline thalamic nuclei, the knowledge on their precise involvement in functions and neurological disorders is far from complete. First the smaller nuclei, PT and RH, are often studied in combination with their bigger neighbor, PV and RE, respectively. Isolating these nuclei in studies would be of great advantage to understanding their specific anatomical, functional and behavior roles. On the other side, the ventral and dorsal thalamic nuclei groups are often studied in isolation, and in very different research domains investigating different research questions. Therefore, whether the ventral and dorsal nuclei have similar involvement in specific functions is not known.

Additionally, very little is known about the midline thalamus in the human brain due to the difficulty identifying these small nuclei. The results of our recent study (Reeders et al., in prep) will aid in the identification and segmentation of the midline thalamus in the human brain *in vivo*. This can aid in the investigation of the involvement

of the midline thalamus in various of functions and disorder using fMRI data, and the investigation of differences in anatomical connectivity in relation to development, aging, and neurological disorders.

CHAPTER 4

Finding the midline thalamus in the human brain using medial temporal lobe and medial prefrontal cortex connectivity

4.1 Summary

The midline thalamus is critical to the coordination of many higher-order cortico-thalamic-cortical networks. For example, the midline thalamus has been shown to be essential to cognition at the intersection of executive function and memory and associated with several neurological disorders including Alzheimer's disease, epilepsy, and depression. Based on specific patterns of anatomical connectivity in rodents and macaques, four midline thalamic nuclei have been identified including: paratenial nucleus (PT), paraventricular nucleus (PV), rhomboid nucleus (RH), and the nucleus reuniens (RE). However, almost nothing is known about the midline thalamic nuclei in humans *in vivo*. This is due, in part, to the difficulty in identifying the midline thalamus with current imaging technologies. Here, we identified and segmented the midline thalamus *in vivo* by using probabilistic tractography and *k*-means clustering with diffusion weighted imaging data. Thalamic nuclei were clustered across participants based on cortical and subcortical connectivity profiles informed by rodent and macaque tracer studies. This approach revealed a midline thalamic cluster that is well connected to the agranular medial prefrontal cortex, nucleus accumbens (nACC), and medial temporal lobe and located directly adjacent to the third ventricle. We further subdivided the human midline thalamus into a dorsal midline thalamic region, which we believe includes the PV and PT, and a ventral midline thalamic region, which includes the RH and RE. These are important divisions due to their unique anatomical connectivity and different contributions to cognitive functions – only explored in rodents to date. Ultimately, this connectivity-based identification and segmentation method can be used to help

characterize the involvement of the midline thalamus in vivo both structurally and functionally in both healthy and neurological brain pathologies.

4.2 Introduction

The midline thalamus consists of medial nuclei, adjacent to the third ventricle, that are essential to an array of cognitive functions including emotional processing, memory consolidation, decision making, and stress regulation (Li and Kirouac, 2008; Hsu et al., 2014; Thielen et al., 2015). Dysfunction in the midline thalamus has been directly implicated in numerous neurodegenerative and psychiatric disorders including Alzheimer's disease, schizophrenia, epilepsy, major depression, and others (Braak and Braak, 1991a, 1991b; Bertram et al., 2001; Neumeister et al., 2004; Aggleton et al., 2016). Anatomically, midline thalamic nuclei form canonical higher order cortico-thalamo-cortical circuits in the brain (Sherman, 2017), most notable for connecting the medial temporal lobe (MTL), especially the hippocampus (HC), with the medial prefrontal cortex (mPFC; Herkenham, 1978; Wouterlood et al., 1990; Dolleman-Van Der Weel and Witter, 1996; Van Der Werf et al., 2002; McKenna and Vertes, 2004; Hoover and Vertes, 2012; Varela et al., 2014). Despite the importance of the midline thalamus, surprisingly little is known about the connectivity and function of these nuclei in humans, due to the difficulty in localizing the boundaries of these nuclei in vivo. Here, we use a data driven technique to identify the midline thalamus in vivo in humans, based on its known connectivity profile from macaque and rodent research. Localizing the midline thalamus using its connectivity patterns provides the opportunity to implement this

segmentation in future functional and structural human MRI studies to investigate clinical neurodegenerative disorders associated with the midline thalamic nuclei.

The midline thalamus has been most extensively studied in rodents and can be separated into four separate nuclei including the nucleus reuniens (RE), rhomboid nucleus (RH), paraventricular nucleus (PV), and paratenial nucleus (PT) based on histologically determined connectivity and cytoarchitectural features. Both in humans and non-human animals, these nuclei are often combined into ventral- and dorsal regions. In humans, the ventral midline thalamus comprises the RE and RH, where RE is situated above the third ventricle and RH located immediately dorsal to RE. The dorsal midline thalamus comprises the PV and PT, where the PT is dorsal to PV, just below the third ventricle. In rodents, it is unclear whether and how the midline thalamus should be divided functionally, and how subregions may interact forming a single unit that curves around the third ventricle (Viena et al., 2020).

The midline thalamic nuclei are most commonly characterized by their anatomical connectivity profiles in rodents (Amaral and Cowan, 1980; DeVito, 1980; Aggleton et al., 1986; Gabbott and Bacon, 1996; McKenna and Vertes, 2004; Hsu and Price, 2007; Passingham and Wise, 2012; Vertes, 2002; Vertes et al., 2015; Laubach et al., 2018) and macaques (Amaral and Cowan, 1980; DeVito, 1980; Aggleton et al., 1986; Hsu and Price, 2007; 2009; Passingham and Wise, 2012). In this study we used connectivity profiles from prior rodent and macaque studies to inform our identification of the midline thalamus in in humans in vivo using patterns of anatomical connectivity derived from diffusion weighted imaging (DWI) probabilistic tractography. While these circuits have

been studied most often in rodents, similar pathways are presumed to exist in primates, which are together summarized below.

The midline thalamic nuclei all share bidirectional connectivity with the agranular mPFC in both macaques and rodents (Amaral and Cowan, 1980; DeVito, 1980; Aggleton et al., 1986; Gabbott and Bacon, 1996; McKenna and Vertes, 2004; Hsu and Price, 2007; Passingham and Wise, 2012; Vertes, 2002; Vertes et al., 2015; Laubach et al., 2018). In macaques, the strongest bidirectional connections are with the infralimbic (IL) and prelimbic (PL) areas of the mPFC (Amaral and Cowan, 1980; DeVito, 1980; Aggleton et al., 1986; Hsu and Price, 2007; Passingham and Wise, 2012). For RE, PV and PT this corresponds with rodent data (Vertes et al., 2015), but this has not been investigated in RH in macaques yet. All four nuclei have connectivity with the anterior cingulate cortex (ACC) in rodents (Gabbott and Bacon, 1996; Vertes, 2002; McKenna and Vertes, 2004). ACC connectivity corresponds for RE and PV in macaques (Hsu and Price, 2007), but has not yet been investigated for PT and RH in primates. Additionally, PT, PV, RH, RE all have strong projections to the nucleus accumbens (nACC) in both rodents (Kelley et al., 1984; Vertes et al., 2006; 2008; Parsons et al., 2007; Li et al., 2008; Vertes et al., 2015) and macaques (Hsu and Price, 2009). However, it should be noted that only one study showed tracer projections from nACC to PV in macaques (Hsu and Price 2009).

All four midline thalamic nuclei also have strong connections with the hippocampal formation in both macaques and rodents, especially the subiculum, presubiculum and CA4 subregions (DeVito, 1980; Aggleton et al., 1986; Gabbott and Bacon, 1996; Saunders et al., 2005; Vertes et al., 2006; Hsu and Price, 2007; 2009; Vertes et al., 2015). In rodents the strongest connectivity between midline thalamic nuclei

and the hippocampal formation is observed between the CA1 and RE (Wouterlood et al., 1990; Dolleman-Van der Weel et al., 1997; McKenna and Vertes, 2004). A similar bias in anatomical connectivity strength between the CA1 and RE has not yet been found in primates. RE does not receive any projections from the dentate gyrus in either rodents or primates (Wouterlood et al., 1990; McKenna and Vertes, 2004). In rodents it has been shown that RE, in particular, completes the connectivity loop between the mPFC and HC, as the HC has direct projections to mPFC, but there are no return monosynaptic projections (Laroche et al., 2000; Hoover & Vertes, 2007), making this structure crucial for bidirectional mPFC and HC communication. For a full structural connectivity profile in rodents, please see Vertes et al., (2015) and Dolleman van der Weel et al., (2019), and in macaques please see Amaral and Cowan (1980) and Hsu et al. (2007, 2009, 2014).

These connectivity profiles have driven work on their functions. PV is connected with many brain regions implicated in emotion regulation and therefore has been studied in drug addiction (Hsu and Price, 2009; Inutsuka et al., 2013; Hsu et al., 2014), emotional memory (Padilla-Coreano et al., 2012; Domonte et al., 2015; Penzo et al., 2015), sleep-wake cycles (Hsu and Price, 2009; Inutsuka et al., 2013) and in its unique role in the response to chronic stress (Hsu et al., 2014). A recent study by Kato et al., (2019) found that modulation of the activity in PV neurons affected the firing patterns in neurons in the mPFC (Kato et al., 2019). Specifically, chronic presynaptic inhibition of PV neurons increased the number of firing interneurons in mPFC resulting in more active behavior, whereas long term activation of PV neurons caused hypoactivity episodes (Kato et al., 2019). These findings suggest that proper synaptic transmission of PV to mPFC might have important roles in depression. The PT has most often been studied combined with

PV. While the precise function of the PT exclusively is uncertain, its connectivity profile suggests that it may act as a gateway for multimodal information to the limbic system to select an appropriate response (Vertes and Hoover, 2008) including feeding behavior (Kelley et al., 2005), and may also be involved in consolidated fear conditioning (Padilla-Correano et al., 2012). Additionally, the outputs from PV to nACC may be involved in arousal states in rodents (Parsons et al., 2007). The nACC shell received dense innervation from dopamine neurons from the PV (Parsons et al., 2007). Using electrical stimulation of the PV dopamine neurons on the dopamine levels in the nACC shell, Parsons et al., (2007) found that stimulation of PV evoked large oxidation current changes in the shell of the nucleus accumbens, suggesting that glutamate release from PV can act on ionotropic glutamate receptors in the nACC to induce a dopamine efflux. This modulation of dopamine levels in the nACC may be linked to arousal or stressful situations (Parsons et al., 2007).

RE is connected to many limbic regions and has been most commonly studied in memory consolidation (Thielen et al., 2015), spatial working memory (Hallock et al., 2013; Viena et al., 2018), goal directed spatial navigation (Ito et al., 2015), temporal organization of sequence memory (Jayachandran et al., 2019), contextual fear memory (Xu and Südhof, 2013) and behavioral flexibility (Viena et al., 2018). RH has most often been studied in combination with RE in rodents and not in detail in primates, and therefore little is known regarding functions exclusive to RH. However, in combination with RE, RH has been shown to be involved in contextual fear memory persistence (Quet e al., 2020), fear extinction (Ramanathan et al., 2018), spatial memory persistence (Loureiro et al., 2012), anxiety-like avoidance behavior (Linley et al., 2021) in rodents.

RH and RE also have been shown to induce plasticity by coordinated synaptic transmission to the prefrontal cortex in rodents (Banks et al., 2021).

The midline thalamic nuclei are integral to normal cognitive processing. The involvement of the midline thalamic nuclei in various disorders has made the midline thalamus a focus of rodent research (Vertes et al., 2007; Ramanathan et al., 2018; Dolleman-van der Weel et al., 2019; Jayachandran et al., 2019). Impairments of one or more of the midline thalamic nuclei has been shown to be involved in neuropsychological diseases including Alzheimer's disease, chronic stress, epilepsy, and drug-seeking behavior.

In Alzheimer's disease, large numbers of extracellular amyloid deposits occurred in almost all thalamic nuclei (Braak and Braak, 1991b), while neurofibrillary tangles deposit in the midline thalamic nuclei, especially RE, as early as in the third of the six stages of the disease (Braak and Braak ,1991a). The PV and RE of the midline thalamus contained numerous neurofibrillary tangles and neuropil threads compared to other regions of the thalamus in Alzheimer's disease (Braak and Braak 1991b). These severe changes due to Alzheimer's disease are confined only to the limbic midline thalamic nuclei (Braak and Braak, 1991b). A recent study (Walsh et al., 2020) investigating rodent amyloid pathology models showed that there are alterations of the likelihood that RE neurons produce burst firing after hyperpolarization compared to controls. Additionally, they also showed that action potential waveforms of RE neurons are also altered (Walsh et al., 2020). These alterations to the intrinsic membrane properties of RE neurons are likely to have important consequences for learning and memory.

The midline thalamus has been shown to play a role in seizure modulation in limbic epilepsy. Hazra et al. (2016) has linked increased c-fos immunoreactivity, a marker for neuronal activity, in RE to cortical epileptiform activity in mice. Bertram et al. (2001), showed that the midline thalamus has seizure activity onset linked to seizure onset in the HC and that there is consistent neuronal loss in the midline thalamic nuclei similar to neuronal loss and atrophy seen in hippocampal sclerosis in human medial temporal lobe epilepsy. Additionally, there are changes in physiology in the midline thalamic neurons of epileptic rodents which result in hyperexcitability (Bertram et al., 2001).

The midline thalamus has been shown to play a critical and unique role in regulating behavioral and physical adaptions to severe and chronic stress (Hsu et al., 2014) and impairments are associated with depressive symptoms (Kato et al., 2019). Specifically, the PV may mediate stress-induced changes in mood and behavior through the amygdala, bed nucleus of the stria terminalis (BNST), nACC, and subgenual anterior cingulate cortex (sgACC) (Hsu et al., 2014). Additionally, PV has a critical role in chronic stress regulation through orexin inputs (Hsu et al., 2014). In chronic stress, but not acute stress, PV is critical for habituation and facilitation of the HPA axis in rodents (Bhatnagar et al., 2000; 2002; Hsu et al., 2014). In a recent study, evidence was found that long-term activation of PV neurons by designer receptors exclusively activated by designer drugs hM3Dq increased the frequency of depression-like episodes (Kato et al., 2019) In a human PET, evidence showed that in patients with remitted depressive disorder to controls, tryptophan depletion was associated with increased regional glucose metabolic blood flow in the midline thalamus (Neumeister et al., 2004). In depressed

human subjects, activity in the midline thalamus shows increased functional connectivity with the subgenual cingulate, a brain region associated with affective behaviors, and decreased functional connectivity in the dorsal anterior cingulate, a brain region associated with cognitive behaviors, which normalized with depression treatment of sertraline (Anand et al., 2005; Greicius et el., 2007).

Accumulating evidence also indicates that the PV mediates drug-seeking behavior. The PV receives major hypothalamic orexin projections, which have been shown to modulate reward function, including drug-seeking behavior (Mahler et al., 2012; Matzeu et al., 2018) and regulate arousal, wakefulness and appetite. Orexin neurons express dynorphin, which in contrast to orexin, promotes depressive-like behaviors and is involved in mediating the effects of stress (Matzeu et al., 2018). PV has been shown to express both orexin and k-opioid receptors (Matzeu et al., 2018). This suggests that orexin and dynorphin have a functional interaction in the PV (Matzeu et al., 2018).

Given the midline thalamus is implicated in many neurological disorders, it is therefore surprising that very little is known about the midline thalamus in humans both anatomically and functionally. In a recent study, Kark et al., (2021) showed that the PV is functionally connected during rest to many of the regions it is structurally connected to in non-human animals including the HC, amygdala and mPFC, and that it is integrated into the default mode network which has associations with episodic memory and self-referential thought (Andrews-Hanna et al., 2010). Another report by Reagh et al. (2017) found that a thalamic area located on top of the third ventricle, identified as RE, mediated correlations between the anterior hippocampus and the medial prefrontal cortex during

recognition judgments in line with its role in rodent memory. These initial studies provide a foundation for functional roles of the midline thalamic nuclei in the human brain. Structural connectivity of the midline thalamic nuclei in the human brain and their functional involvement in cognitive functions and neurodegenerative disorders in humans has yet to be investigated in detail.

The paucity of data on the human midline thalamus is due, in part, to the small size, location next to ventricles, and lack of clear boundaries in local cell type and tissue densities makes it difficult to identify with *in vivo* imaging technologies in humans (e.g. MRI). Here, we attempt to delineate the borders of midline thalamus in humans by using DWI and probabilistic tractography to produce voxel clusters with similar connectivity profiles and co-registering them across subjects. This approach takes advantage of the known connectivity profiles of the midline thalamus in non-human primate and rodent studies. The results of this approach provide stereotypical midline thalamus coordinates in humans based on highly overlapping connectivity profiles across individual subjects. This method can pave the path for future studies investigating the involvement of the midline thalamus in various functions, and neurocognitive disorders.

4.3 Methods

Participants & Image Acquisition

The WU-Minn dataset from the Human Connectome Project (HCP; Van Essen et al., 2013) were obtained through "connectome in a box" (www.store.humanconnectome.org). We selected the first 127 participants from the HCP dataset. Ages ranged from 22 to 35 years old (M = 29.000, SD = 3.432) from which 72

were female. Participants were scanned on a customized Siemens 3T "Connectome Skyra" at Washingtoon University in St. Louis, using a 32-channel Siemens head coil. The structural image had an acquisition time of 7:40 min (repetition time; TR = 2400 ms, echo time; TE = 2.14 ms, inversion time, TI = 1000 ms, flip angle = 8°, FOV = 224x224 mm, voxel size = 0.7 mm isotropic, BW of 210 Hz/Px). The diffusion weighted images included 6 runs of approximately 9 minutes and 50 seconds. There were 3 different gradient tables. Each table was acquired once with right-to-left and left-to-right phase encoding polarities, respectively. Each table has approximately 90 diffusion weighting directions plus 6 b=0 acquisitions interspersed throughout each run. Diffusion weighting consisted of 3 shells with b = 1000, 2000 and 3000 s/mm^2 interspersed. The sequence was a spin-echo EPI (TR = 5520 ms, TE = 89.5 ms, flip angle = 78°, FOV = 210x180 mm, matrix = 168x144 mm, and refocusing flip angle of 160 degrees). There were 111 slices and were 1.25 mm thick with 1.25 mm isotropic voxels. The multiband factor was 3 and 0.78 ms of echo spacing was used. Phase partial Fourier was 6/8.

Data Processing and Analysis.

Preprocessing. HCP data was preprocessed by the HCP. Using the structural images, they produced an undistorted "native" structural volume space for each participant, performed a bias field (B1) correction, and lastly registered the native structural volume to Montreal Neurological Insititute (MNI) space. Freesurfer (5.3.0-HCP) was used to segment the volume into predefined structures, reconstruct white and pial cortical surfaces, and perform standard folding based surface registration to the surface atlas (fsaverage). Their diffusion preprocessing included normalization of the b0 image intensity across six diffusion series using the "topup" tool (Andersson et al., 2003),

removing EPI distortions. FSL's EDDY algorithm was used for eddy-current-induced correction and motion correction. Next, they did gradient nonlinearity correction and removed spatial distortion and mean b0 image was corrected from distortion. Bvalue and bvector deviation were calculated. They registered the mean b0 to native volume T1w with FLIRT and bbregister and transformation of diffusion data, gradient deviation, and gradient directions to 1.25 mm structural space. Brain mask was based on the segmentation output from FreeSurfer.

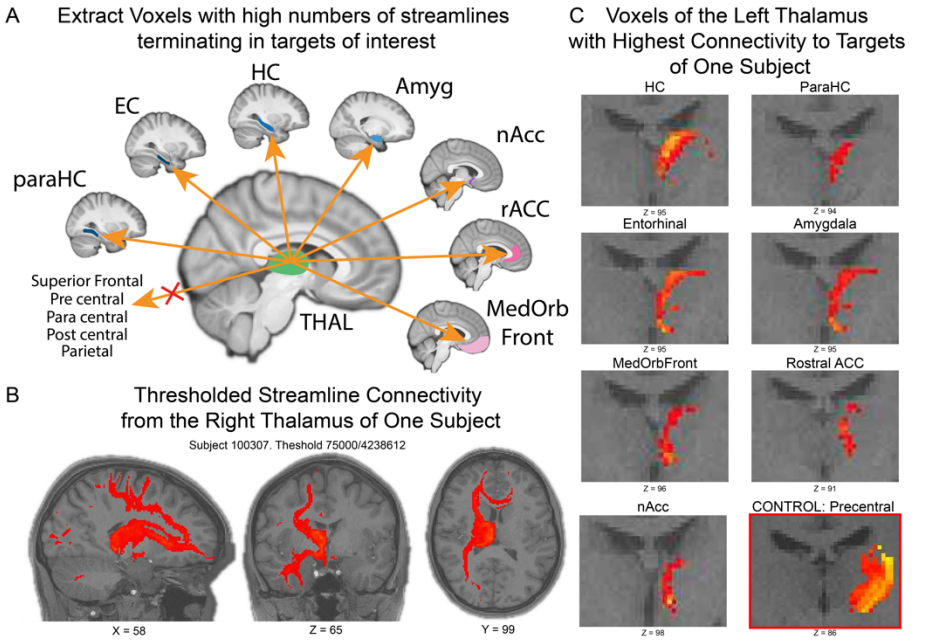

Figure 10. Fiber tracking using probabilistic tractography on DWI data. **A,** Seed region was the whole thalamus, and target regions of interest were the hippocampus, parahippocampus, entorhinal cortex, amygdala rostral anterior cingulate cortex and the medial orbital frontal gyrus. Our control regions were the superior frontal cortex, precentral gyrus, paracentral gyrus, post central gyrus, parietal cortex). **B,** Streamline density maps showed that the whole thalamus had strong connectivity to the MTL regions and the mPFC regions and some Occipital region. Cut off: 75000 from 4238612 total. **C,** When looking at which voxels of the thalamus had the highest connectivity our regions of interest after probabilistic tractography to, we found that continuously the midline voxels were revealed. Thresholding hippocampus 4000/24992 y = 94, parahippocampus 500/6132 y = 94, entorhinal cortex 1700/9721 y = 95, amygdala 3000/24440 y=95, medial orbitofrontal cortex 900/17783 y = 96, rostral anterior cingulate 15/64 y = 91, nucleus accumbens 300/4919 y=98. Connectivity to control regions showed high connectivity with lateral posterior regions: e.g. Precentral gyrus 8000/19528 y = 86.

Probabilistic Tractography analysis Next, we used Bayesian Estimation of Diffusion Parameters (BEDPOSTX) to model crossing fibers within each brain voxel and to create a fitting of the probabilistic diffusion model on corrected data. The results of BEDPOSTX were the basis of all subsequent probabilistic tractography based analyses. The thalamus of both hemispheres was separately used as seed regions for probabilistic tractography with ipsilateral cortical and subcortical targets obtained from Freesurfer. We used ProbtrackX to run probabilistic tractography on the data. Briefly, ProbtrackX produces sample streamlines, starting from a voxel within the seed region, and then iterates between 1) drawing an orientation from the voxel-wise bedpost distributions and 2) taking a step in the direction of diffusion orientation and 3) checking for any termination criteria (see below). These sample streamlines will then be used to investigate how often a streamline from each voxel of the thalamus ends up in one of the target regions. This streamline distribution can be thought of as an estimated connectivity distribution.

We sampled 25000 voxel-wise principal diffusion directions (streamlines) from each voxel in the seed region (the whole thalamus), each time computing a streamline through these local samples to generate a *probabilistic streamline* from the distribution on the location of the true streamline. The termination criteria where either when a streamline hit a voxel in the target mask, or 2) reaching 5000 steps; and restriction criteria were that the streamline random walks could not go backward to the previous voxel make and are only allowed to make movements greater than 90 degrees away from the current step. FMRIB's Diffusion Toolbox (FDT) was then used to create a *connectivity distribution.* Primarily, we recorded the target destination of each random walk for every

thalamic voxel. We used anatomical derived from Freesurfer anatomical regions of interest (surfer.nmr.mgh.harvard.edu) using their aparc+aseg files. Cortical and subcortical target files were binarized, transformed using a nearest neighbor interpolation, and resampled to DWI resolution prior to running the ProbtrackX algorithm. Masks of the ventricles were used as avoid masks. Next, we made a voxel by target matrix with the frequency of how often each voxel in the thalamus made it to each specific ipsilateral target which were entered into the k-means clustering algorithm.

K-means clustering. The voxel by target (a.k.a., feature) multidimensional data was entered into a *k*-means clustering algorithm using scikit-learn (https://scikit-learn.org/stable/), which clusters data by separating samples into n groups of equal variances, minimizing inertia (within-cluster sum-of-squares) we constrained the solution to 8 clusters. Voxels with similar target patterns of connectivity based on how many times their random walks made it to the set of targets are grouped together into a k-means cluster. K-means clusters with connectivity profiles that preferentially included high connectivity to targets of interest and minimal connectivity with targets of non-interest were used to select k-means clusters that matched the connectivity profile informed by the non-human animal studies. Targets of interest were medial temporal lobe regions (hippocampus, parahippocampus, entorhinal cortex, and amygdala), nucleus accumbens and medial prefrontal cortex regions (medial orbitofrontal cortex, rostral anterior cingulate cortex; Fig. 10A). These mPFC labels correspond to agranular cortex Broddmann areas 14 (orbital prefrontal cortex), 25 (infralimbic cortex), 32 (prelimbic cortex) and 24 (anterior cingulate gyrus) according to Passingham and Wise (2012). Targets of non-interest included superior frontal cortex, precentral gyrus, paracentral

gyrus, post central gyrus, parietal cortex (Fig. 10A). The resulting k-means clusters that met our target/non-target criteria were binarized and normalized to the MNI template, averaged across our sample, and thresholded to select voxels that only exhibited 80% or greater overlap across all participants. We divided the resulting thresholded midline thalamus mask based on Ding et al., (2016) atlas into a dorsal midline thalamus mask (upper 48% of pairing height in the most anterior slice where the midline thalamus pairs) and ventral midline thalamus mask (lower 52% of the pairing height of the most anterior slice where the midline thalamus pair). The dorsal midline thalamus mask includes the PT and PV, and the ventral midline thalamus mask includes the RH and RE. This results in three masks per hemisphere that can be used for further analyses including fMRI or structural connectivity analyses: a full midline thalamus mask, a dorsal midline thalamus mask, and a ventral midline thalamus mask.

4.4 Results

We identified the human midline thalamus by segmenting thalamic voxels based on their anatomical connectivity profile informed by previous studies in rodents and macaques. Using probabilistic tractography and k-means clustering analyses on DWI data we illuminated voxels within the thalamus with direct, structural connections with temporal lobe regions (hippocampus, parahippocampus, entorhinal cortex and amygdala), mPFC regions (medial orbitofrontal cortex and rostral anterior cingulate) and the nucleus accumbens, but not to non-target regions (superior frontal cortex, precentral gyrus, paracentral gyrus, post central gyrus, parietal cortex). These connectivity results correspond well to structural connectivity in non-human animals (Amaral and Cowan,

1980; DeVito, 1980; Aggleton et al., 1986; Gabbott and Bacon, 1996; Vertes, 2002; McKenna and Vertes, 2004; Hsu and Price, 2007; Passingham and Wise, 2012; Vertes et al., 2015; Laubach et al., 2018).

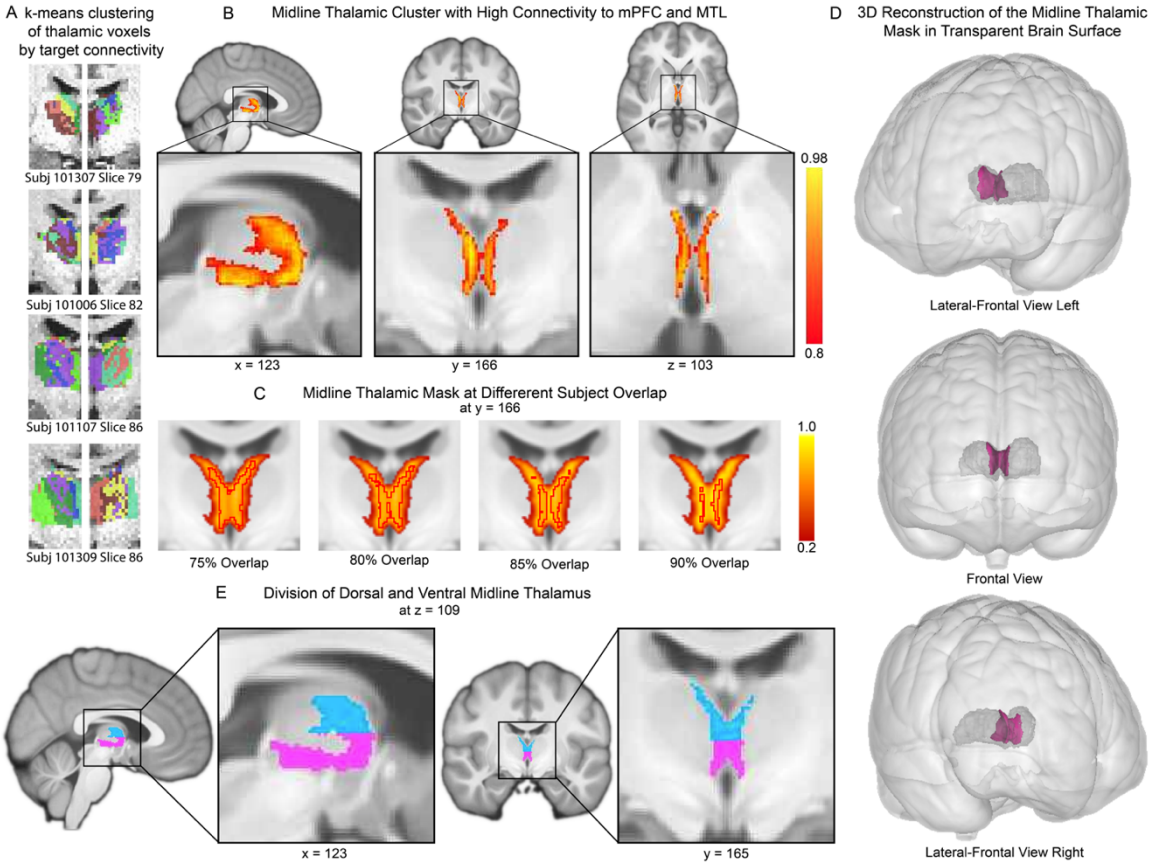

Figure 11. Midline thalamic mask in the human brain. **A,** Clustering of thalamic voxels with similar connectivity profiles revealed a midline thalamic cluster. Colors are arbitrary. **B,** When extracting the cluster with high connectivity to MTL and mPFC and not our control regions, we obtained a mask of the midline thalamic mask with over 80% overlap of all participants (80% shown). **C,** Midline thalamic mask with different overlap in 127 subjects ranging from 75% overlap (left) to 90% overlap (right). **D,** 3D rendering of the midline thalamus (pink) in the thalamus (dark grey) at 80% overlap in 127 subjects. **E,** Division of the dorsal (PT and PV) and ventral (RH and RE) thalamus according to the Ding et al., 2016 atlas at z = 109. Where at the point of hemispheric attachment, 48% is dorsal midline thalamus, and 52% is ventral midline thalamus.

As a qualitative check we examined the topology of the probabilistic tractography streamline density maps (fdt-map) for several representative participants to assess which target regions at a gross level exhibited the greatest anatomical connectivity with the entire thalamus (left and right separately). Using arbitrary thresholding, the results showed that the streamlines appeared to terminate in the medial regions of the PFC, regions of the MTL and to medial regions of the occipital lobe to a lesser extent and largely avoided the lateral cortical regions (e.g. Fig. 10B; Subject 100307, right thalamus, thresholded at 75000 out of a max 4238612, Coordinates: x=60, y = 99, z=71, best observed in the coronal and axial slices).

We also looked at which voxels of the thalamus had the highest numbers of streamlines terminating in specific targets of interest in a representative participant (Fig. 10C). Different numbers of total streamlines ended up in each target region (hippocampus, parahippocampus, entorhinal cortex, amygdala, medial orbitofrontal cortex, rostral anterior cortex, and nucleus accumbens), but when using an arbitrary threshold (varying per target) to investigate which thalamic voxels had the highest number of streamline terminate in the target of interest, all target regions of interest revealed that voxels along the midline of the thalamus had the highest numbers of streamlines ending up in our targets of interest (Fig. 1C; Subject 100307; Thresholding for the hippocampus 4000/24992 y = 94, para hippocampus 500/6132 y=94, entorhinal cortex 1700/9721 y = 95, amygdala 3000/24440 y=95, medial orbitofrontal cortex 900/17783 y = 96, rostral anterior cingulate 15/64 y = 91, nucleus accumbens 300/4919 y=98.), and all control regions revealed highest connectivity with more lateral and posterior regions of the thalamus (Fig. 10C. pre-central gyrus shown: 8000/19528 y =

86). These results show that the midline region of the thalamus for individual subjects have the highest connectivity with our target regions of interest compared to the rest of the thalamus.

Next, following the application of the k-means algorithm, clusters at the midline of the thalamus were evident in every subject (Fig. 11A; for example, the yellow cluster in Subj 101006 right image). We isolated specific K-means clusters from each participant based on whether specific target features from MTL (hippocampus, parahippocampus, entorhinal cortex or amygdala) or mPFC (orbitofrontal cortex, rostral anterior cingulate) or nACC and not to any of the non-target regions contributed to those clusters. Target and non-target regions were based on non-human animal research, we hypothesized that this would result in the segmentation of the cluster at the midline of the thalamus. Our results clearly distinguished voxels, that included the midline nuclei of the thalamus (putative PT, PV, RH and RE) (Fig 2B, 2D). The relative location of the midline thalamic clusters qualitatively was reproducible across subjects. As expected, although relative positions of the midline thalamic clusters were preserved across subjects, there was variability in the precise location of borders and of the volume per subject. Although some variability, the overlap of the midline thalamic mask was high between subject – we obtained an overlap of over 80% (overlap of 80% shown in Fig. 11B, 2D, overlap of 75-90% shown in Fig. 11C) in 127 participants.

Based on anatomical considerations, the dorsal and ventral midline thalamus were split according to an atlas provided by Ding et al., (2016). According to the Ding et al., (2016) atlas, a dorsal/ventral division should be set on the coronal slice where the midline thalamic nuclei paired from both hemispheres. In the Ding et al., (2016) atlas, the dorsal

midline thalamus measured 48% of the entire height of the coronal slice of the midline thalamic nuclei, and the ventral midline thalamus measured 52% of the entire height of the coronal slice of the midline thalamic nuclei. We applied these percentages to divide our midline thalamic sample into a dorsal mask (blue) which measured 52% of the height of the entire midline thalamus on the coronal slice where both midline thalami pair, and a ventral mask (purple) measuring 48% of the height of the entire midline thalamus on the coronal slice where both midline thalami pair (Fig. 11E).

4.5 Discussion

Here, we show an anatomical identification and segmentation of the midline thalamus in humans in vivo based on its known connectivity profile in non-human animals using probabilistic tractography and k-means clustering on diffusion weighted imaging data.

The midline thalamus is critical for everyday cognitive functions and impairment of this region is associated with serious cognitive disorders including memory impairments, poor regulation of chronic stress, depressive-like symptoms and drug seeking behaviors. However, due to the size, location and unclear borders, the midline thalamic nuclei have not gotten a lot of attention in human research. It is important, to have a data-driven and readily reproducible method for identifying this region in human MRI studies, so that the midline thalamus can be further investigated. The method proposed here based on anatomical connectivity obtained from a combination of probabilistic tractography and k-means clustering can be used for future studies that include the midline thalamus as their region of interests implementing a data driven

masking procedure. Being able to locate and mask in vivo the midline thalamus in humans based on known connectivity profiles provides the opportunity to objectively investigate this region and its functional and structural implications in behavior, cognition, and anatomy studies and to further investigate the involvement of this region in neurological disorders.

One specific motivator for this study, was evidence that neurofibrillary tangles were confined to the midline thalamus in humans with Alzheimer's Disease (AD), and that this was associated with severe behavioral changes and symptoms (Braak and Braak, 1991b). Additionally, the midline thalamic neurons show alterations in action potential waveform in animal AD models (Walsh et al., 2020). We are interested in investigating structural connectivity-based alterations in the midline thalamic-medial prefrontal – hippocampal circuit in patients at different stages Alzheimer's disease, and required an objective data driven approach to identify the midline thalamus for this investigation. Additionally, investigating the midline thalamus in functional MRI or connectivity DWI studies in AD, or other neurological disorders including drug addiction, depression, schizophrenia, and epilepsy, would be of great importance to the study and understanding of those disorders, perhaps aiding in future diagnostic methodologies.

Probabilistic tractography is a sophisticated and powerful modality to investigate white matter connectivity in vivo in the human brain. Based on non-human animal studies, and post-mortem human brain studies, we know that axons are organized into major white matter fiber bundles. Using probabilistic tractography, we can calculate estimations of white matter fiber bundle probability using the DWI MRI information and reconstruct these white matter fiber pathway distributions. Briefly, probabilistic

tractography uses the information from BedpostX to take intra-voxel crossing of fibers into account. It then estimates the pathway originating at a voxel in the seed region (the thalamus), and outputs quantitative information about the probability of a white matter tract passing through voxels in the brain. It then repeats this streamlining analysis many times per seed voxel and will repeat this process for every voxel in the seed region. Using termination criteria in this analysis, we can obtain quantitative information about the probability that a seed voxel has structural connectivity with a target region.

Multiple studies have used probabilistic tractography to segment the human thalamus with different research questions as the main driver (Behrens et al., 2003; Traynor et al., 2010; Akram et al., 2018; Middlebrooks et al., 2018). Bherens et al. (2003) were one of the first to use probabilistic tractography to identify specific connections between the human thalamus and cortex, providing a quantitative demonstration of reliable inference of anatomical connectivity between human grey matter structures. This was later followed up with a study showing multi-fiber tractography offers significant advantages in sensitivity when tracking non-dominant fiber populations, while not dramatically changing dominant pathway tractography results (Behrens et al., 2007). Additionally, Traynor et al., (2010), build on this and showed that this the method described in Behrens et al., (2007) had very high reproducibility, even when using slightly different starting voxel conditions, and that thalamic segmentation was also very reproducible when multiple datasets from the same subject were processed using six cortical target regions (Traynor et al., 2010). In a more clinical application setting, Middlebrooks et al., (2018) have used probabilistic tractography obtained thalamic parcellations to predict tremor improvements following thalamic deep brain stimulation.

Additionally, Akram et al., (2018) used probabilistic tractography to identify the ventral intermediate nucleus and the dentato-rubro-thalamic tract in patients that will undergo thalamic deep brain stimulation for tremors.

However, as almost nothing is known about the midline thalamus in humans, no one has focused on this brain region, and we have not found a study identifying the midline thalamus based on its connectivity profile. In this study, we provide an identification and segmentation method to identify the midline thalamus, for the further investigation of neurological disorders. The main interest of the current study was to find an evidence-based modality to identify the midline thalamus in humans in vivo. The k-means clustering algorithm and the extraction of the midline thalamus based on its connectivity profile provided by non-human animals is, to the best of our knowledge, the first attempt using this specific method to extract the midline thalamus in humans in vivo.

Although this method is great for many reasons, including it being non-invasive, in-vivo and can be used in whole brain analyses, it does not come without limitations. The first limitation is that the probabilistic streamlines do not represent individual axons, because the resolution of MRI data is not high enough. Instead, it is an estimation of larger bundles of axons. A second limitation is that probabilistic tractography is an indirect measure of white matter pathways. Using DWI and BedpostX, we can measure the diffusion of water molecules, and with that information we can observe diffusion paths in voxels. Therefore, probabilistic tractography uses an indirect measure of diffusivity which is highly correlated to fiber tracking (Behrens et al., 2003). Using probabilistic tractography, we cannot infer true fiber distributions and pathways, but probability estimates of possible fiber pathways based on principle direction

measurements. Additionally, it is impossible to define polarity of the tract, and therefore the direction (e.g. midline thalamus to HC, vs HC to midline thalamus. Third, probabilistic tractography is sensitive primarily to major pathways, and will not always detect small pathways with small inflections. Probabilistic tractography is also prone to error as MRI has a relatively low signal to noise ratio compared to invasive tract tracing methods such as tracer studies. Although our results correspond well with evidence found in non-human literature, further validation is desirable. For example, the same dataset could be analyzed using multiple tract tracing techniques including manganese-enhanced magnetic resonance imaging (Pautler et al. 1998). Additionally, our DWI, probabilistic tractography and kmeans clustering technique could be replicated in addition to investigate real fiber pathways in non-human primates.

Dyrby et al., (2007) has quantitatively and qualitatively assessed the anatomical validity and reproducibility of in vitro multi-fiber probabilistic tractography against two invasive tracers in the porcine brain. In their study, they used postmortem DWI to ensure that most of the sources known to degrade the anatomical accuracy in vivo DWI did not influence the tracking results (Dyrby et al., 2007). They demonstrated that probabilistic tractography reliably detected specific pathways, concluding that DWI probabilistic tractography offers precision in the investigation of structural connectivity (Dyrby et al., 2007). Although the relative location of our midline thalamic mask we found corresponds well with the schematic human atlas by Ding et al., (2016) and macaque and rodent studies, further validation of our methodology is desirable. For example, this study could be replicated to find the midline thalamus in humans or pigs, and then compared to

postmortem cytoarchitectonic boundaries using staining or tracers of the same subjects that were scanned for comparison.

This method has obvious clinical applications, as it could help characterize neuropsychological brain disorders, by for example investigating alterations and changes in the streamline connectivity between these regions or the size of the midline thalamus mask in subjects with dementia and at different stages of Alzheimer's disease. These measures can in turn be correlated with cognitive and behavioral performances with the use of e.g., memory tasks, learning tasks, mood disorder measures, and cognitive impairment measures. Another future direction of interest could be to investigate correlations between myelination of the cortex, with the streamline connectivity in the mPFC-mThal-HC circuit in aging, to see if there is degradation of both these measures as people age.

CHAPTER 5

CONCLUSION

This dissertation examined the role of medial prefrontal cortex (mPFC) and the hippocampus (HC) in episodic memory, and provides a novel approach to identify the midline thalamus mediating mPFC-HC interactions in humans.

First, this dissertation provides evidence that the mPFC and HC are concurrently engaged in different memory retrieval modes in support of remembering *when* an event occurred. This evidence suggests that the mPFC is active in memory retrieval when using an ordinal retrieval mode, where items of a sequence are associated with an ordinal position within the sequence (1^{st}, 2^{nd}, 3^{rd}). The evidence also shows that the HC is active in memory retrieval when using a temporal context retrieval mode, where items that have a temporal association (e.g., items are closer together in time) are remembered together. Taken together, this suggests that there are separate neurobiological substrates of two distinct memory retrieval processes contributing both to how we remember events in the order they happened. This novel evidence provides an important baseline for further investigation of how sequence memory is impaired in typical aging and diseases such as Alzheimer's Disease on the neurobiological level, especially since evidence implicates that the relative dependence on an ordinal retrieval mode increases with age while TCM dependence decreases (Bastin and Van der Linden 2010; Allen et al. 2015).

Second, this dissertation provides a detailed cross species framework for understanding the midline thalamus in humans and its pathology. Since the mPFC and HC do not have strong bidirectional connections, they are reliant on the midline thalamus for bidirectional communication. In the second study, I review in detailed the anatomy and connectivity of the midline thalamus with the rest of the brain comparing the extensive anatomical evidence in rodents with the available evidence in monkeys and

humans. This study also reviews the midline thalamic models of memory, stress regulation, wakefulness and feeding behavior, and midline thalamic pathology models of neurological disorders including Alzheimer's Disease, schizophrenia, depression, and drug addiction.

Third, this dissertation provides a novel approach for the identification of the midline thalamus in humans *in vivo* using fiber tracing and clustering methods in DWI data using knowledge gleaned from non-human animals' connectivity studies. The results revealed a midline thalamic cluster that is well connected to the agranular medial prefrontal cortex, nucleus accumbens, and medial temporal lobe and located directly adjacent the third ventricle. These findings provide an important tool for the further investigation of the midline thalamus in humans. Furthermore, this method allows for investigation of functional and connectivity differences in individuals with neurological disorders.

Overall, this work provides new evidence on 1) complementary function roles of the mPFC and HC in sequence memory, 2) a cross-species anatomical framework for understanding the midline thalamus in humans and neurological disorders, and 3) a new approach for non-invasive identification of the midline thalamus in humans *in vivo*. In conclusion, this work provides a new fundamental understanding of mPFC-midline thalamic-HC circuit in humans and tools for its non-invasive study in human disease.

REFERENCES

Aggleton JP. 2012. Multiple anatomical systems embedded within the primate medial temporal lobe: Implications for hippocampal function. Neurosci. Biobehav. Rev. 36(7), 1579–1596.

Aggleton, JP, Desimone, R, and Mishkin, M. 1986. The origin, course, and termination of the hippocampothalamic projections in the macaque. J. Comp. Neurol. 243, 409–421.

Aggleton JP, and Mishkin M. 1984. Projections of the amygdala to the thalamus in the cynomolgus monkey. J. Comp. Neurol. 222(1), 56–68.

Aggleton JP, Desimone R, Mishkin M. 1986. The origin, course, and termination of the hippocampothalamic projections in the macaque. J. Comp. Neurol. 243(3), 409–421.

Aggleton JP, Pralus A, Nelson AJD, Hornberger M. 2016. Thalamic pathology and memory loss in early Alzheimer's disease: moving the focus from the medial temporal lobe to Papez circuit. Brain. 139(pt 7), 1877–1890.

Aggleton JPP, Burton, MJJ, Passingham REE. 1980. Cortical and subcortical afferents to the amygdala of the rhesus monkey (Macaca mulatta). Brain Res. 190(2), 347–368.

Agster KL, Fortin NJ, Eichenbaum H. 2002. The hippocampus and disambiguation of overlapping sequences. J Neurosci 22(13):5760-5768.

Akram H, Dayal V, Mahlknecht P, Georgiev D, Hyam J, Foltynie T, Limousin P, De Vita E, Jahanshahi M, Ashburner J, Behrens T, Hariz M, Zrinzo L. 2018. Connectivity derived thalamic segmentation in deep brain stimulation for tremor. Neuroimage Clin. 18: 130-142.

Alamilla J, Granados-Fuentes D, Aguilar-Roblero R. 2015. The anterior paraventricular thalamus modulates neuronal excitability in the suprachiasmatic nuclei of the rat. Eur. J. Neurosci. 42(10), 2833–2842.

Allen TA, Fortin NJ. 2013. The evolution of episodic memory. Proc Natl Acad Sci U S A 110 (suppl 2):10379-10386.

Allen TA, Morris AM, Mattfeld AT, Stark CEL, Fortin NJ. 2014. A sequence of events model of episodic memory shows parallels in rats and humans. Hippocampus. 24(10), 1178-1187.

Allen TA, Morris AM, Fortin NJ, Stark CEL. 2015. Memory for sequences of events impaired in typical aging. Learn Mem 22(3): 138–148.

Allen TA, Salz DM, McKenzie SA, Fortin NJ. 2016. Nonspatial sequence coding in CA1 neurons. J Neurosci 36(5): 1547-1563.

Alvarez P, Squire LR, Rutters F, Tendolkar I, Jensen O, Zwarts MJ, McNaughton BL, Fernández G. 1994. Memory consolidation and the medial temporal lobe: a simple network model. Proc. Natl. Acad. Sci. 91(15), 7041–7045.

Amaral DG, Cowan WM. 1980. Subcortical afferents to the hippocampal formation in the monkey. J. Comp. Neurol. 189(4), 573–591.

Anand A, Li Y, Wu J, Gao S, Bukhari L, Mathews VP, Kalnin A, Lowe MJ. 2005. Antidepressant effect on connectivity of the mood-regulating circuit: an fMRI study. Neuropsychopharmacology. 30(7): 1334-1344.

Andrews-Hanna JR, Reidler JS, Sepulcre J, Poulin R, Buckner RL. 2010. Functional-anatomic fractionation of the brain's default network. Neuron 65: 550-562.

Avants BB, Epstein CL, Grossman M, Gee JC. 2008. Symmetric diffeomorphic image registration with cross-correlation: Evaluating automated labeling of elderly and neurodegenerative brain. Med Image Anal 12(1):26-41.

Baldo BA, Daniel RA, Berridge C.W, Kelley AE. 2003. Overlapping distributions of orexin/hypocretin- and dopamine-beta-hydroxylase immunoreactive fibers in rat brain regions mediating arousal, motivation, and stress. J. Comp. Neurol. 464(2), 220–237.

Banks PJ, Warburton EC, Bashir ZI. 2021. Placticity in prefrontal cortex induced by coordinated synaptic transmission arising from reuniens/rhomboid nuclei and hippocampus. Celebral Cortex Communications. 2(2): 1-16.

Barson JR, Ho HT, Leibowitz SF. 2015. Anterior thalamic paraventricular nucleus is involved in intermittent access ethanol drinking: role of orexin receptor 2. Addict. Biol. 20(3), 469–481.

Barson JR, Mack NR, Wen-Jun G. 2020. The paraventricular nucleus of the thalamus is an important node in the emotional processing network. Front. Behav. Neurosci. 14:598469: 1-9.

Bastin C, Van der Linden M. 2005. Memory for temporal context: Effects of ageing, encoding instructions, and retrieval strategies. Memory 13(1): 95-109.

Beas, SB, Xinglong G, Leng Y, Koita O, Rodriquez-Gonzalez S, Kindel M, Matikainen-Ankney BA, Larsen RS, Kravitz AV, Hoon MA, Penzo MA. 2020. A ventrolateral medulla-midline thalamic circuit for hypoglycemic feeding. Nat Commun. 11(6218): 1-13.

Beck CHM, Fibiger HC. 1995. Conditioned fear-induced changes in behavior and in the expression of the immediate early gene c-fos: with and without diazepam pretreatment. J Neurosci. 15(1), 709-720.

Behrens TEJ., Johansen-Berg H., Woolrich MW, Smith SM, Wheeler-Kingshott CAM, Boulby PA, Barker GJ, Sillery EL, Sheehan K, Ciccarelli O, Thompson AJ, Brady JM, Matthews PM. 2003. Non-invasive mapping of connections between human thalamus and cortex using diffusion imaging. Nat. Neurosci. 6(7): 750–757.

Benoit RG, Gilbert SJ, Frith CD, Burgess PW. 2012. Rostral prefrontal cortex and the focus of attention in prospective memory. Cerebral Cortex 22(8):1876-1886.

Berendse HW, Groenewegen HJ. 1990. Organization of the thalamostriatal projections in the rat, with special emphasis on the ventral striatum. J. Comp. Neurol. 299(2), 187–228.

Bertram EH, Mangan PS, Zhang D, Scott CA, Williamson JM. 2001. The midline thalamus: alterations and a potential role in limbic epilepsy. Epilepsia 42(8): 967–978.

Bhatnagar S, and Dallman M. 1998. Neuroanatomical basis for facilitation of hypothalamic-pituitary-adrenal responses to a novel stressor after chronic stress. Neuroscience. 84(4), 1025–1039.

Bhatnagar S, Huber R, Lazar E, Pych L, Vining C. 2003. Chronic stress alters behavior in the conditioned defensive burying test: role of the posterior paraventricular thalamus. Pharmacol. Biochem. Behav. 76(2), 343–349.

Bhatnagar S, Huber R, Nowak N, Trotter P. 2002. Lesions of the posterior paraventricular thalamus block habituation of hypothalamic-pituitary-adrenal responses to repeated restraint. J. Neuroendocrinol. 14(5), 403–410.

Bhatnagar S, Viau V, Chu A, Soriano L, Meijer OC, Dallman MF. 2000. A cholecystokinin-mediated pathway to the paraventricular thalamus is recruited in chronically stressed rats and regulates hypothalamic-pituitaryadrenal function. J. Neurosci. 20(14), 5564–5573.

Bladon JH, Sheehan DJ, De Freitas CS, Howard MW. 2019. In a temporally segmented experience hippocampal neurons represent temporally drifting context, but not discrete segments. J Neurosci 39(35):6936-6952.

Boutrel B, Kenny PJ, Specio SE, Martin-Fardon R, Markou A, Koob GF, de Lecea L. 2005. Role for hypocretin in mediating stress-induced reinstatement of cocaine-seeking behavior. Proc. Natl. Acad. Sci. U. S. A. 102(52), 19168–19173.

Braak H, and Braak E. 1991a. Neuropathological staging of Alzheimer-related changes. Acta Neuropathol. 82(4), 239–259.

Braak H, and Braak E. 1991b. Alzheimer's disease affects limbic nuclei of the thalamus. Acta Neuropathol. 81(3), 261–268.

Brody AL, Saxena S, Stoessel P, Gillies LA, Fairbanks LA, Alborzian S, Phelps ME, Huang SC, Wu HM, Ho MK, Au SC, Maidment K, Baxter Jr LR. 2001. Regional brain metabolic changes in patients with major depression treated with either paroxetine or interpersonal therapy: preliminary findings. Arch. Gen. Psychiatry. 58(7), 631–640.

Brown E, Robertson G, Fibiger H. 1992. Evidence for conditional neuronal activation following exposure to a cocaine-paired environment: role of forebrain limbic structures. J Neurosci. 12(10), 4112–4121.

Browning JR, Jansen HT, Sorg BA. 2014. Inactivation of the paraventricular thalamus abolishes the expression of cocaine conditioned place preference in rats. Drug Alcohol Depend. 134, 387–390.

Brown TI, Stern CE. 2013. Contributions of medial temporal lobe and striatal memory systems to learning and retrieving overlapping spatial memories. Cereb Cortex 24(7):1906-22.

Brown TI, Ross RS, Keller JB, Hasselmo ME, Stern CE. 2010. Which way was I going? Contextual retrieval supports the disambiguation of well learned overlapping navigational routes. J Neurosci 30(21):7414 –7422.

Bubser M, and Deutch AY. 1999. Stress induces Fos expression in neurons of the thalamic paraventricular nucleus that innervate limbic forebrain sites. Synapse. 32(1), 13–22.

Burlet S, Tyler CJ, Leonard CS. 2002. Direct and indirect excitation of laterodorsal tegmental neurons by hypocretin/orexin peptides: Implications for wakefulness and narcolepsy. J Neurosci. 22(7), 2862-2872.

Byne W, Hazlett EA, Buchsbaum MS, Kemether E. 2009. The thalamus and schizophrenia: Current status of research. Acta Neuropathol. 117(4), 347–368.

Card JP, Sved JC, Craig B, Raizada M, Vazquez J, Sved AF. 2006. Efferent projections of rat rostroventrolateral medulla C1 catecholamine neurons: implications for the central control of cardiovascular regulation. J. Comp. Neurol. 499(5), 840-859.

Chemelli RM, Willie JT, Sinton CM, Elmquist JK, Scammell T, Lee C, Richardson JA, Williams SC, Xiong, Y., Kisanuki Y, Fitch TE, Nakazato M, Hammer RE, Saper CB, Yanagisawa M. 1999. Narcolepsy in orexin knockout mice: molecular genetics of sleep regulation. Cell. 98(4), 437–451.

Chisholm A, Iannuzzi J, Rizzo D, Gonzalez N, Fortin É, Bumbu A, Batallán Burrowes AA, Chapman CA, Shalev U. 2019. The role of the paraventricular nucleus of the thalamus in the augmentation of heroin seeking induced by chronic food restriction. Addict. Biol. 25(2), e12708.

Cox RW. 1996. AFNI: software for analysis and visualization of functional magnetic resonance Neuroimages. Comput Biomed Res 29(3):162-173.

Cullinan WE, Herman JP, Battaglia DF, Akil H, Watson SJ. 1995. Pattern and time course of immediate early gene expression in rat brain following acute stress. Neuroscience. 64(2), 477–505.

Dale AM, Fischl B, Sereno MI. 1999. Cortical surface-based analysis. I. Segmentation and surface reconstruction. Neuroimage 9(2):179-194.

Damle N, Ikuta T, John M, Peters BD, Derosse P, Malhotra AK, Szeszko PR, Peters JJ, Struct B, Author F. 2017. Relationship Among Interthalamic Adhesion Size, Thalamic Anatomy and Neuropsychological Functions in Healthy Volunteers HHS Public Access Author manuscript. Brain Struct Funct. 222(5), 2183–2192.

Davis KL, Kahn RS, Ko G, Davidson M. 1991. Dopamine in schizophrenia: A review and reconceptualization. Am. J. Psychiatry. 148(11), 1474–1486.

Davoodi FG, Motamedi F, Akbari E, Ghanbarian E, Jila B. 2011. Effect of reversible inactivation of reuniens nucleus on memory processing in passive avoidance task. Behav. Brain Res. 221(1), 1–6.

Dayas CV, McGranahan TM, Martin-Fardon R, Weiss F. 2008. Stimuli Linked to Ethanol Availability Activate Hypothalamic CART and Orexin Neurons in a Reinstatement Model of Relapse. Biol. Psychiatry. 63(2), 152–157.

Deadwyler SA, Hayashizaki S, Cheer J, Hampson RE. 2004. Reward, memory, and substance abuse: functional neuronal circuits in the nucleus accumbens. Neurosci. Biobehav. Rev. 27(8), 703–711.

DeVito JL. 1980. Subcortical projections to the hippocampal formation in squirrel monkey (Saimiri sciureus). Brain Res. Bull. 5(3), 285–289.

Devito LM, and Eichenbaum H. 2011. Memory for the order of events in specific sequences: contributions of the hippocampus and medial prefrontal cortex. J. Neurosci. 31 (9), 3169–3175.

Ding SL, Royall JJ, Sunkin SM, Ng L, Facer BAC, Lesnar P, Guillozet-Bongaarts A, McMurray B, Szafer A, Dolbeare TA, Stevens A, Tirrel L, Benner T, Caldejon S, Dalley RA, Dee N, Lau C, Nyhus J, Redin M, Riley ZL, Sandman D, Shen E, can der Kouwe A, Varjabedian A, Wright M, Zollei L, Dang C, Knowles JA, Koch C, Phillips JW, Sestan N, Wohnoutka P, Zielke HR, Hohmann JG, Jones AR, Bernard A, Hawrylucz MJ, Hof P, Fischl, Lein ES. 2016. Comprehensive cellular-resolution atlas of the adult human brain. J. Comp. Neurol. 524 (16): 3127-3481.

Dolleman-van der Weel MJ, Griffin AL, Ito HT, Shapiro ML, Witter MP, Vertes RP, Allen TA. 2019. The nucleus reuniens of the thalamus sits at the nexus of a hippocampus and medial prefrontal cortex circuit enabling memory and behavior. Learn. Mem. 26(7), 191–205.

Dolleman-Van der Weel MJ, Lopes da Silva FH, Witter MP. 1997. Nucleus reuniens thalami modulates activity in hippocampal field ca1 through excitatory and inhibitory mechanisms. J. Neurosci. 17(14), 5640–5650.

Dolleman-Van Der Weel MJ, Witter MP. 1996. Projections from the nucleus reuniens thalami to the entorhinal cortex, hippocampal field CA1, and the subiculum in the rat arise from different populations of neurons. J Comp Neurol. 364(4): 637-650.

Do-Monte FH, Quinones-Laracuente K, Quirk GJ. 2015. A temporal shift in circuits mediating retrieval of fear memory. Nature. 519:460-463.

Drevets WC, Price JL, Simpson JR, Todd RD, Reich T, Vannier M, Raichle ME. 1997. Subgenual prefrontal cortex abnormalities in mood disorders. Nature. 386(6627), 824–827.

Dube L, Smith AD, Bolam JP. 1988. Identification of synaptic terminals of thalamic or cortical origin in contact with distinct medium-size spiny neurons in the rat neostriatum. J. Comp. Neurol. 267(4), 455-471.

Dubrow S, Davachi L. 2014. Temporal memory is shaped by encoding stability and intervening item reactivation. J Neurosci 34(42):13998-14005.

Dubrow S, Davachi L. 2013. The influence of context boundaries on memory for the sequential order of events. J Exp Psychol Gen 142(4):1277-1286.

Dunn AJ. 2005. Handbook of Stress and the Brain - Part 2: Stress: Integrative and Clinical Aspects (Elsevier).

Dyrby TB, Søgaard LV, Parker GJ, Alexander DC, Lind NM, Baaré WFC, Hay-Schmidt AH, Eriksen N, Pakkenberg B, Paulson OB, Jelsing J. 2007. Validation of in vitro probabilistic tractography. Neuroimage. 37(4):1267-1277.

Ehlers CL, Reed TK, Henriksen SJ. 1986. Effects of Corticotropin-Releasing Factor and Growth Hormone-Releasing Factor on Sleep and Activity in Rats. Neuroendocrinology. 42(6), 467–474.

Eichenbaum H. 2014. Time cells in the hippocampus: a new dimension for mapping memories. Nat Neurosci 15:732-744.

Eichenbaum H. 2017. On the integration of space, time and memory. Neuron 95(5):1007-1018.

Eichenbaum H, Yonelinas A, Ranganath C. 2007. The medial temporal lobe and recognition memory. Annu Rev Neurosci 30:123-152.

Ekstrom AD, and Bookheimer SY. 2007. Spatial and temporal episodic memory retrieval recruit dissociable functional networks in the human brain. Learn. Mem. 14(10), 645–654.

Elmquist JK, Elias CF, Sper CB. 1999. From lesions to leptin: hypothalamic control of food intake and body weight. Neuron. 22(2), 221-232.

Euston DR, McNaughton BL. 2006. Apparent encoding of sequential context in rat medial prefrontal cortex is accounted for by behavioral variability. J Neurosci 26(51):13143-13155.

Fenoglio KA, Brunson KL, Baram TZ. 2006. Hippocampal neuroplasticity induced by early-life stress: functional and molecular aspects. Front. Neuroendocrinol. 27(2), 180–192.

Ferry AT, Öngür D, An X, Price JL. 2000. Prefrontal cortical projections to the striatum in macaque monkeys: Evidence for an organization related to prefrontal networks. J. Comp. Neurol.

Floresco SB, Todd CL, Grace AA. 2001. Glutamatergic afferents from the hippocampus to the nucleus accumbens regulate activity of ventral tegmental area dopamine neurons. J. Neurosci. 21(13), 4915–4922.

Fortin NJ, Agster KL, Eichenbaum HB. 2002. Critical role of the hippocampus in memory for sequences of events. Nat Neurosci 5:458-462.

Frankland PW, Bontempi B. 2005. The organization of recent and remote memories. Nat. Rev. Neurosci. 6, 119–130.

Gabbott PLA, Bacon SJ. 1996. Local Circuit Neurons in the Medial Prefrontal Cortex. J. Comp. Neurol. 636(4), 609–636.

Gao C, Leng, Y, Ma J, Rooke V, Rodriguez-Gonzalez S, Ramakrishnan C, Deisseroth K, Penzo MA. 2020. Two genetically, anatomically and functionally distinct cell types segregate across anteroposterior axis of paraventricular thalamus. Nat Neurosci. 23, 217-228.

Giménez-Amaya J.M, McFarland NR, De Las Heras S, Haber SN. 1995. Organization of thalamic projections to the ventral striatum in the primate. J. Comp. Neurol. 354(1), 127–149.

Goto M, and Swanson LW. 2004. Axonal projections from the parasubthalamic nucleus. J. Comp. Neurol. 469(4), 581–607.

Gorgolewski K, Burns CD, Madison C, Clark D, Halchenko YO, Waskom ML, Ghosh SS. 2011. Nipype: a flexible, lightweight extensible neuroimaging data processing framework in python. Front Neuroinform 5:13.

Goyal A, Miller J, Watrous AJ, Lee SA, Coffey T, Sperling MR, Sharan A, Worrell G, Berry B, Lega B, Jobst BC, Davis KA, Inmann C, Sheth SA, Wanda PA, Azzyat Y, Das SR, Stein J, Gorniak R, Jacobs J. 2018. Electrical stimulation in hippocampus and entorhinal cortex impairs spatial and temporal memory. J Neurosci 38(19):4471-4481.

Greicius MD, Flores BH, Menon V, Glover GH, Solvason HB, Kenna H, Reiss AL, Schatzberg AF. 2007. Resting-state functional connectivity in major depression: abnormally increased contributions from subgenual cingulate cortex and thalamus. Biol Psychiatry. 62(5), 429-437.

Grill-Spector K, Kushnir T, Hendler T, Edelman S, Itzchak Y, Malach R. 1998. A sequence of object-processing stages revealed by fMRI in the human occipital lobe. Hum Brain Mapp 6(4):316-328.

Grüntal E. 1934. Der Zellbau im Thalamus der Säuger und dem Menschen. Eine beschreibend und vergleichend anatomische Untersuchung. J. Fur Psychol. Und Neurol. 46, 41–112.

Gudmundson A, Stark SM, Stark CEL. 2017. Item-item and item-position strategy use in a cross-species sequence memory task. SfN Abstracts.

Hallock HL, Wang A, Griffin AL. 2016. Ventral midline thalamus is critical for hippocampal–prefrontal synchrony and spatial working memory. J. Neurosci. 36(32), 8372–8389.

Hallock HL, Wang A, Shaw CL, Griffin AL. 2013. Transient inactivation of the thalamic nucleus reuniens and rhomboid nucleus produces deficits of a working-memory dependent tactile-visual conditional discrimination task. Behav Neurosci. 127(6), 860-866.

Hamlin AS, Clemens KJ, Choi EA, McNally GP. 2009. Paraventricular thalamus mediates context-induced reinstatement (renewal) of extinguished reward seeking. Eur. J. Neurosci. 29(4), 802–812.

Hammen C. 2005. Stress and depression. Annu. Rev. Clin. Psychol. 1, 293–319.

Hammen C. 2009. Adolescent depression: Stressful interpersonal contexts and risk for recurrence. Curr Dir Psychol Sci. 18(4), 200–204.

Harris GC, Wimmer M, Aston-Jones G. 2005. A role for lateral hypothalamic orexin neurons in reward seeking. Nature. 437(7058), 556–559.

Harrison TM, Burggren AC, Small GW, Bookheimer SY. 2016. Altered memory-related functional connectivity of the anterior and posterior hippocampus in older adults at increased genetic risk for Alzheimer's disease. Hum Brain Mapp. 37(1):366–380.

Hasler G, Drevets W, Manji H. Charney DS. 2004. Discovering endophenotypes for major depression. Neuropsychopharmacol. 29, 1765-1781.

Hassler R. 1959. Anatomy of the thalamus, in Introduction to Stereotaxic Operations with an Atlas of the Human Brain. (Gierg Thieme Verlag).

Hazra A, Corbett BF, You JC, Aschmies S, Zhao L, Li K, Lepore AC, Marsh ED, Chin J. 2016. Corticothalamic network dysfunction and behavioral deficits in a mouse model of Alzheimer's disease. Neurobiol aging. 44: 96-107.

Hebart MN, Baker CI. 2018. Deconstructing multivariate decoding for the study of brain function. Neuroimage. 180(pt A):4-18.

Hembrook JR, Onos KD, Mair RG. 2012. Inactivation of ventral midline thalamus produces selective spatial delayed conditional discrimination impairment in the rat. Hippocampus. 22(4), 853–860.

Herkenkam M. 1978. The connections of the nucleus reuniens thalami: Evidence for a direct thalamo-hippocampal pathway in the rat. J Comp Neurol. 177(4):589-609.

Hill-Bowen LD, Flanner JS, Poudel R. 2020. Paraventricular thalamus activity during motivational conflict highlights the nucleus as a potential constituent in the neurocircuitry of addiction. J. Neurosci. Res. 40(4), 726-728.

Holsboer F, von Bardeleben U, Steiger A. 1988. Effects of intravenous corticotropin-releasing hormone upon sleep-related growth hormone surge and sleep EEG in man. Neuroendocrinology. 48(1), 32–38.

Hoover WB, Vertes RP. 2007. Anatomical analysis of afferent projections to the medial prefrontal cortex in the rat. Brain Struct Funct. 212(2): 149-179.

Hoover WB, and Vertes RP. 2012. Collateral projections from nucleus reuniens of thalamus to hippocampus and medial prefrontal cortex in the rat: A single and double retrograde fluorescent labeling study. Brain Struct. Funct. 217(2), 191-209.

Howard MW, Eichenbaum H. 2013. The hippocampus, time and memory across scaled. J Exp Psychol 142(4):1211-1230.

Howard MW, Kahana MJ. 2002. A distributed representation of temporal context. J Math Psychol 46(3):269-299.

Howard MW, Fotedar MS, Datey AV, Hasselmo ME. 2005. The temporal context model in spatial navigation and relational learning: toward a common explanation of medial temporal lobe function across domains. Psych Rev 112(1):75-116.

Howard MW, Viskontas IV, Shankar KH, Fried I. 2012. Ensembles of human MTL neurons "jump back in time" in response to a repeated stimulus. Hippocampus 22(9):1833-1847.

Hsu DT, and Price JL. 2007. Midline and intralaminal thalamic connections with the orbital and medial prefrontal networks in macaque monkeys. J. Comp. Neurol. 504(2), 89–111.

Hsu DT, and Price JL. 2009. The paraventricular thalamic nucleus: Subcortical connections and innervation by serotonin, orexin, and corticotropin releasing hormone in macaque monkeys. J. Comp. Neurol. 512(6), 825–848.

Hsu DT, Kirouac GJ, Zubieta J, Bhatnagar S. 2014. Contrubutions of the paraventricular thalamic nucleus in the regulation of stress, motication, and mood. Front. Behav. Neurosci. 8(73), 1–10.

Hsieh LT, Gruber MJ, Jenkins LJ, Ranganath C. 2014. Hippocampal activity patterns carry information about objects in temporal context. Neuron 81(5):1165-1178.

Hsieh LT, Ranganath C. 2015. Cortical and subcortical contributions to sequence retrieval: Schematic coding of temporal context in the neocortical recollection network. Neuroimage 121:78-90.

Huang AS, Mitchell JA, Haber SN, Alia-Klein, N, Goldstein RZ. 2018. The thalamus in drug addiction: from rodents to humans. Phil. Trans. R. Soc. 373, 20170028.

Hyman BT, Van Hoesen GW, Damasio AR. 1990. Memory-related neural systems in Alzheimer's disease: an anatomic study. Neurology. 40(11), 1721–1730.

Hyman JM, Ma L, Balaquer-Ballester e, Durstewitz D, Seamans JK. 2012. Contextual encoding by ensembles of medial prefrontal cortex neurons. Proc Natl Acad Sci U S A 109(13): 5086-5091.

Igelstrom KM, Herbison AE, Hyland BI. 2010. Enhanced c-Fos expression in superior colliculus, paraventricular thalamus and septum during learning of cue-reward association. Neuroscience. 168(3), 706–714.

Insausti R, Cowan WM, Salk T, Diego S. 1987. The Entorhinal Cortex of the Monkey: 11. Cortical Afferents. 264(3), 356-395.

Inutsuka A, Yamanaka A, Vaudry H, De Lecea L. 2013. The physiological role of orexin/hypocretin neurons in the regulation of sleep/wakefulness and neuroendocrine functions. Front Endocrinol. 4(18): 1-10.

Ishibashi M, Takano S, Yanagida H, Takatsuna M, Nakajima K, Oomura Y, Wayner MJ, and Sasaki K. 2005. Effects of orexins/hypocretins on neuronal activity in the paraventricular nucleus of the thalamus in rats in vitro. Peptides. 26(3), 471–481.

Ito HT, Zhang SJ, Witter MP, Moser EI, Moser MB. 2015. A prefrontal-thalamo-hippocampal circuit for goal directed spatial navigation. Nature. 522:50-55.

James MH, Charnley JL, Jones E, Levi EM, Yeoh JW, Flynn JR, Smith DW, Dayas C V. 2010. Cocaine and amphetamine-regulated transcript (CART) signaling within the paraventricular thalamus modulates cocaine-seeking behaviour. PLoS One. 5(9), e12980.

Jayachandran M, Linley SB, Schlecht M, Mahler SV, Vertes RP. 2019. Prefrontal pathways provide top-down control of memory for sequences of events. Cell Rep. 28(3), 1–15.

Jenkins LJ, Ranganath C. 2010. Prefrontal and medial temporal lobe activity at encoding predicts temporal context memory. J Neurosci 30(46):15558-15565.

Jenkins LJ, Ranganath C. 2016. Distinct neural mechanisms for remembering when an event occurred. Hippocampus 26(5):554-559.

Kahana MJ. 1996. Associative retrieval processes in free recall. Mem and Cogn 24(1):103-109.

Kalm K, Davis MH, Norris D. 2013. Individual sequence representations in the medial temporal lobe. J Cogn Neurosci 25(7):1111-1121.

Kark SM, Birnie MT, Baram TZ, Yassa MA. 2021. Functional connectivity of the human paraventricular thalamic nucleus: Insights from high field functional MRI. Front Integr Neurosci. 15(662293): 1-18.

Kato TM, Fuimori-Tonou N, Mizukami H, Ozawa Keiya, Fuisawa S, Kato T. 2019. Presynaptic dysregulation of the paraventricular thalamic nucleus causes depression-like behavior. Scientific Reports. 9(16506):1-9.

Kawano J, Krout KE, Loewy A. 2001. Suprachiasmatic nucleus projections to the paraventricular thalamic nucleus of the rat. Thalamus Relat. Syst. 1(3), 197-202.

Kelley AE, Baldo BA, Pratt WE. 2005. A proposed hypothalamic-thalamic-striatal axis for the integration of energy balance, arousal, and food reward. J. Comp. Neurol. 493(1), 72-85.

Kelley AE, Stinus L. 1984. The distribution of the projection from the parataenial nucleus of the thalamus to the nucleus accumbens in the rat: An autoradiographic study. Exp. Brain Res. 54(3), 499–512.

Kesner RP, Gilbert PE, Barua LA. 2002. The role of the hippocampus in memory for the temporal order of a sequence of odors. Behav Neurosci 116(2):286-290.

Kirouac GJ. 2015. Placing the paraventricular nucleus of the thalamus within the brain circuits that control behavior. Neurosci Biobehav Rev. 56, 315-329.

Kirouac GJ. 2021. The paraventricular nucleus of the thalamus as an integrating and relay node in the brain anxiety network. Front. Behav. Neurosci. 15:627633.

Kirouac GJ, Parsons MP, Li S. 2005. Orexin (hypocretin) innervation of the paraventricular nucleus of the thalamus. Brain Res. 1059(2), 179-188.

Komorowski RW, Manns JR, Eichenbaum H. 2009. Robust conjunctive item-place coding by hippocampal neuros parallels learning what happens where. J Neurosci 29(31):9918-9929.

Kragel JE, Morton NW, Polyn SM. 2015. Neural activity in the medial temporal lobe reveals the fidelity of mental time travel. J Neurosci 35(7):2914-2926.

Krout KE, and Loewy AD. 2000a. Parabrachial nucleus projections to midline and intralaminar thalamic nuclei of the rat. J. Comp. Neurol. 428(3), 475–494.

Krout KE, and Loewy AD. 2000b. Periaqueductal gray matter projections to midline and intralaminar thalamic nuclei of the rat. J. Comp. Neurol. 424(1), 111–141.

Kumaran D, Maguire EA. 2006. An unexpected sequence of events: Mismatch detection in the human hippocampus. PLoS Biol 4(12):2372-2382.

Lambert C, Simon H, Colman J, Barrick TR. 2017. Defining thalamic nuclei and topographic connectivity gradients in vivo. Neuroimage. 158, 466–479.

Lapper SR, Bolam JP. 1992. Input from the frontal cortex and the parafascicular nucleus to the cholinergic interneurons in the dorsal striatum of the rat. Neuroscience. 51(3), 553-545

Laroche S, Davis S, Jay TM. (2000). Plasticity at hippocampal to prefrontal cortex synapses: Dual roles in working memory and consolidation. Hippocampus. 10(4):438-446.

Laubauch M, Amaranthe LM, Swanson K, White SR. (2018). What, if anything, is rodent prefrontal cortex? eNeuro. 5(5):1-14.

Layfield DM, Patel M, Hallock H, Griffin AL. 2015. Inactivation of the nucleus reuniens/rhomboid causes a delay-dependent impairment of spatial working memory. Neurobiol. Learn. Mem. 125, 163–167.

Lee L, Sakurai M, Matsuzaki S, Arancio O, Fraser P. 2013. SUMO and Alzheimer's disease. Neuromolecular Med. 15(4), 720–736.

Lehn H, Steffenach HA, Strien NM, Veltman DJ, Witter MP, Haberg AK. 2009. A specific role of the human hippocampus in recall of temporal sequences. J Neurosci 29(11):3475-3484.

Li J, Hu Z, and de Lecea L. 2013. The hypocretins/orexins: integrators of multiple physiological functions. Br J Pharmacol. 171(2), 332-350.

Li S, and Kirouac GJ. 2008. Projections from the paraventricular nucleus of the thalamus to the forebrain, with special emphasis on the extended amygdala. J. Comp. Neurol. 506(2), 263-287.

Li S, and Kirouac GJ. 2012. Sources of inputs to the anterior and posterior aspects of the paraventricular nucleus of the thalamus. Brain Struct. Funct. 217(2), 257–273.

Li W, Antuono PG, Xie C, Chen G, Jones JL, Ward BD, Singh SP, Franczak MB, Goveas JS, Li SJ. 2014. Aberrant functional connectivity in Papez circuit correlates with memory performance in cognitively intact middle-aged APOE4 carriers. Cortex. 57, 167–176.

Linley SB, Athanason AC, Rojas AKP, Vertes RP. 2021. Role of the reuniens and rhomboid thalamic nuclei in anxiety-like avoidance behavior in the rat. Hippocampus. 31(7): 756-769.

Lisman JE, Pi HJ, Zhang Y, Otmakhova NA. 2010. A thalamo-hippocampal-ventral tegmental area loop may produce the positive feedback that underlies the psychotic break in schizophrenia. Biol. Psychiatry. 68(1), 17–24.

Long HMK, Kahana NM. 2019. Hippocampal contributions to serial-order memory. Hippocampus 29(3):252-259.

Loureiro M, Cholvin T, Lopez J, Merienne N, Latreche A, Cosquer B, Geiger K, Kelche C, Cassel JC, Pereira de Vasconcelos A. 2012. The ventral midline thalamus (reuniens and rhomboid nuclei) contributes to the persistence of spatial memory in rats. J. Neurosci. 32(29), 9947–9959.

Luo W, Guo F, McHahon A, Couvertier S, Jin H, Diaz M, Fieldsend A, Weerapana E, Rosbash M. 2018. NonA and CPX link the circadian clockwork to locomotor activity in drosophila. Neuron. 99(4), 768-780.

Mahler SV, Smith RJ, Moornam DE, Sartor GC, Aston-Jones G. 2012. Multiple roles for orexin/hypocretin in addiction. Progress in brain research. 198:79-121.

Mai JK, and Forutan F. 2012. Thalamus. In The Human Nervous System (Academic Press), 618–677.

Mai JK, and Majtanik M. 2018. Toward a Common Terminology for the Thalamus. Front. Neuroanat. 12(114): 1-23.

Malik R, Li Y, Schamiloglu S, Sohal VS. 2021. Top-down control of hippocampal signal-to-noise by prefrontal long-range inhibition. BioRxiv.

Malone E. 1912. Oberservation concerning the comparative anatomy of the diencephalon. Anatomical Record. 6(8): 281-290.

Maloney L, Zhang H. 2010. Decision-theoretic models of visual perception and action. Vis Res 50(23):2363-2374.

Mankin EA, Sparks FT, Slayyeh B, Sutherland RJ, Leutgeb S, Leutgeb JK. 2012. Neuronal code for extended time in the hippocampus. Proc Natl Acad Sci U S A 109(47):19462-19467.

Manns JR, Howard MW, Eichenbaum H. 2007. Gradual changes in hippocampal activity support remembering the order of events. Neuron 56(3):530-540.

Marchant NJ, Furlong TM, McNally GP. 2010. Medial dorsal hypothalamus mediates the inhibition of reward seeking after extinction. J. Neurosci. 30(42), 14102–14115.

Marcus JN, Aschkenasi CJ, Lee CE, Chemelli RM, Saper CB, Yanagisawa M, Elmquist JK. 2001. Differential expression of orexin receptors 1 and 2 in the rat brain. J. Comp. Neurol. 435(1), 6–25.

Matzeu A and Martin-Fardon R. 2018. Drug seeking and relapse: New evidence of a role for orexin and dynorphin co-transmission in the paraventricular nucleus of the thalamus. Front. Neurol. 9(720): 1-13.

Mau W, Sullivan DW, Kinsky NR, Hasselmo ME, Howard MW, Eichenbaum H. 2018. The same hippocampal CA1 population simultaneously codes temporal information over multiple timescales. Curr Biol 28(10):1499-1508.

Mayberg HS, Liotti M, Brannan SK, McGinnis S, Mahurin RK, Jerabek PA, Silva JA, Tekell JL, Martin CC, Lancaster JL, Fox PT. 1999. Reciprocal limbic-cortical function and negative mood: converging PET findings in depression and normal sadness. Am. J. Psychiatry. 156(5), 675–682.

McKenna JT, and Vertes, R.P. 2004. Afferent projections to nucleus reuniens of the thalamus. J. Comp. Neurol. 480(2), 115-142.

Meffre J, Sicre M, Diarra M, Marchessaux F, Paleressompoulle D, Ambroggi F. 2019. Orexin in the posterior paraventricular thalamus mediates hunger-related signals in the nucleus accumbens core. Curr. Biol. 29(19), 3298-3306.

Mehler WR. 1980. Subcortical afferent connections of the amygdala in the monkey. J. Comp. Neurol. 190(4), 733–762.

Middlebrooks EH, Tuna IS, Almeida L, Grewal SS, Wong J, Heckham MG, Lesser ER, Bredel M, Foote KD, Okun MS, Holanda VM. 2018. Structural connectivity-based segmentation of the thalamus and prediction of tremor improvement following thalamic deep brain stimulation of the venral intermediate nucleus. Neuroimage: Clinical. 20: 1266-1273.

Mikula S, Trotts I, Stone J, Jones EG. 2007. Internet-Enabled High-Resolution Brain Mapping and Virtual Microscopy. NeuroImage. 35(1), 9-15

Milner B, Petrides M, Smith ML. 1985. Frontal lobes and temporal organization of memory. Hum Neurobiol 4(3):137-142.

Moga MM, Weis RP, Moore RY. 1995. Efferent projections of the paraventricular thalamic nucleus in the rat. J. Comp. Neurol. 359(2), 221–238.

Morel A, Magnin M, Jeanmonod D. 1997. Multiarchitectonic and stereotactic atlas of the human thalamus. J Comp Neurol. 387(4), 588-630.

Morton NW, Polyn SM. 2016. A predictive framework for evaluating models of semantic organization in free recall. Journal of memory and language 86:119-140.

Neumeister A, Nugent AC, Waldeck T, Geraci M, Schwarz M, Bonne O, Bain EE, Luckenbaugh DA, Herscovitch P, Charney DS, Drevets WC. 2004. Neural and behavioral responses to tryptophan depletion in unmedicated patients with remitted major depressive disorder and dontrols. Arch. Gen. Psychiatry. 61(8), 765.

Nieuwenhuys R, Voogd J,van Huijzen C. 2008. The human central nervous system (Springer).

Olney JW, Newcomer JW, Farber NB. 1999. NMDA receptor hypofunction model of schizophrenia. J. Psychiatr. Res. 33(6), 523–533.

Orlov T, Amit DJ, Yakovlev V, Zohary E, Hochstein S. 2006. Memory of ordinal number categories in macaque monkeys. J Cogn Neurosci 18(3):399-417.

Orlov T, Yakovlev V, Amit D, Hochstein S, Zohary E. 2002. Serial memory strategies in macaque monkeys: Behavioral and theoretical aspects. Cereb Cortex 12(3):306-317.

Orlov T, Yakovlev V, Hochstein S, Zohary E. 2000. Macaque monkeys categorize images by their ordinal number. Nature 404(6773):77-80.

Otake K, Kin K, Nakamura Y. 2002. Fos expression in afferents to the rat midline thalamus following immobilization stress. Neurosci. Res. 43(3), 269–282.

Otis JM, Zhu M, Namboodiri VMK, Cook CA, Kosyk O, Matan AM, Ying R, Hashikawa K, Trujillo-Pisanty I, Guo J, Ung RL, Rodriquez-Romaguera J, Anton ES, Stuber GD. 2019. Paraventricular thalamus projection neurons integrate cortical and hypothalamic signals for cue-reward processing. Neuron. 103(3), 423-431.

Padilla-Coreano N, Do-Monte FH, Quirk GJ. 2012. A time-dependent role of midline thalamic nuclei in the retrieval of fear memory. Neuropharmacology. 62(1):457-463.

Passingham R. 2009. How good is the macaque monkey model of the human brain? Curr Opin Neurobiol. 19(1), 6-11.

Passingham RE, and Wise SP. 2012. The neurobiology of the prefrontal cortex: anatomy, evolution, and the origin of insight (Oxford Univ. Press).

Parsons MP, Li S, Kirouac GJ. 2007. Functional and anatomical connection between the paraventricular nucleus of the thalamus and dopamine fibers of the nucleus accumbens. J Comp Neurol. 500(6): 1050-1063.

Passingham RE, and Wise SP. 2012. The neurobiology of the prefrontal cortex: anatomy, evolution, and the origin of insight (Oxford Univ. Press).

Pautler RG, Silva AC, Koretsky AP. 1998. In vivo neuronal tract tracing using manganese-enhanced magnetic resonance imaging. Magn Reson Med. 40(5):740–748.

Penzo MA, Tucciarone RJ, De Bundel D, Wang M, Van Aelst L, Parada LF, Palmiter RD, He M, Huang ZJ, Li B. 2015. The paraventricular thalamus controls a central amygdala fear circuit. Nature 519(): 455-459.

Pereira de Vasconcelos A, Cassel JC, Vasconcelos AP. de Cassel JC, Pereira de Vasconcelos A, and Cassel JC. 2015. The nonspecific thalamus: A place in a wedding bed for making memories last? Neurosci. Biobehav. Rev. 54(), 175–196.

Peyron C, Tighe DK, Van Den Pol AN, De Lecea L, Craig Heller H, Sutcliffe JG, Kilduff TS. 1998. neurons containing hypocretin (orexin) project to multiple neuronal systems. J Neurosci. 18(23), 9996-10015.

Phillipson OT, and Bohn MC. 1994. C1-3 adrenergic medullary neurons project to the paraventricular thalamic nucleus in the rat. Neurosci. Lett. 176(1), 67-70.

Pizzagalli DA, Oakes TR, Fox AS, Chung MK, Larson CL, Abercrombie HC, Schaefer SM, Benca RM, Davidson RJ. 2003. Functional but not structural subgenual prefrontal cortex abnormalities in melancholia. Mol. Psychiatry. 9(4), 393-405.

Polyn SM, Kahana MJ. 2008. Memory search and the neural representation of context. Trends Cogn Sci 12():24-30.

Quet E, Majchrzak M, Cosquer B, Morvan T, Wolff M, Cassel JC, Pereira de Vasconcelos A, Stephan A. 2020. The reuniens and rhomboid nuclei are necessary for contextual fear memory persistence in rats. Brain Structure and Function, Springer Verlag, 225(), 955 - 968.

Ramanathan KR, Ressler RL, Jin J, Maren S. 2018. Nucleus reuniens is required for encoding and retrieving precise, hippocampal-dependent contextual fear memories in rats. J. Neurosci. 38(), 9925–9933.

Preston AR, Eichenbaum H. 2013. Interplay of hippocampus and prefrontal cortex in memory. Curr Biol 23():764-773.

Ray MA, Graham AJ, Lee M, Perry RH, Court JA, Perry EK. 2005. Neuronal nicotinic acetylcholine receptor subunits in autism: an immonohistochemical investigation in the thalamus. Neurobiol Dis 19(): 366–377.

Reagh ZM, Murray EA, Yassa MA. 2017. Repetition reveals ups and downs of hippocampal, thalamic, and neocortical engagement during mnemonic decisions. Hippocampus. 27(2), 169–183.

Reed SJ, Lafferty CK, Mendoza JA, Yang AK, Davidson TJ, Grosenick L, Deisseroth K, Britt JP. 2018. Coordinated reductions in excitatory input to the nucleus accumbens underlie food consumption. Neuron. 99(6), 1260-1273.

Ren S, Wang Y, Ye F, Cheng X, Dang R, Qiao Q, Sun X, Li X, Jiang Q, Yao J, Qin H, Wang G, Liao X, Gao D, Xia J, Zhang J, Hu B, Yan J, Wang Y, Xu M, Han Y, Tang X, Chen X, He C, Hu Z. 2018. The paraventricular thalamus is a critical thalamic area for wakefulness. Science. 362(6413), 429-434.

Rhodes JS, Ryabinin AE, Crabbe JC. 2005. Patterns of brain activation associated with contextual conditioning to methamphetamine in mice. Behav. Neurosci. 119(3), 759–771.

Ritchie JB, Kaplan DM, Klein C. 2017. Decoding the brain: Neural representation and the limits of multivariate pattern analysis in cognitive neuroscience. Brit J Philos Sci 70(2):581-607.

Roche A. 2011. A four-dimensional registration algorithm with application to joint correction of motion and slice timing in fMRI. IEE Trans Med Imaging 30(8):1546-1554.

Roche M, Harkin A, Kelly JP. 2007. Chronic fluoxetine treatment attenuates stressor-induced changes in temperature, heart rate, and neuronal activation in the olfactory bulbectomized rat. Neuropsychopharmacology. 32, 1312–1320.

Rönnbäck A, Sagelius H, Bergstedt KD, Näslund J, Westermark GT, Winblad B, Graff C. 2012. Amyloid neuropathology in the single Arctic APP transgenic model affects interconnected brain regions. Neurobiol. Aging. 33(4), 831.e11-831.e19.

Ross RS, Brown TI, Stern CE. 2009. The retrieval of learned sequences engages the hippocampus: Evidence from fMRI. Hippocampus 19(9):790-799.

Rubin A, Geva N, Sheintuch L, Ziv Yaniv. 2015. Hippocampal ensemble dynamics timestamp events in long-term memory. eLife 4:e12247.

Ryan NS, Keihaninejad S, Shakespeare TJ, Lehmann M, Crutch SJ, Malone IB., Thornton JS, Mancini L, Hyare H, Yousry T, Ridgway GR, Zhang H, Modat M, Alexander DC, Rossor MN, Ourselin S, Fox NC. 2013. Magnetic resonance imaging evidence for presymptomatic change in thalamus and caudate in familial Alzheimer's disease. Brain. 136, 1399–1414.

Sánchez-González MA, García-Cabezas MA, Rico B, Cavada C. 2005. The primate thalamus is a key target for brain dopamine. J Neurosci. 25(26), 6076-6083.

Saper CB., Scammell, T.E., and Lu, J. 2005. Hypothalamic regulation of sleep and circadian rhythms. Nature. 437(7063), 1257–1263.

Saunders RC, Mishkin M, Aggleton JP. 2005. Projections from the entorhinal cortex, perirhinal cortex, presubiculum, and parasubiculum to the medial thalamus in macaque monkeys: Identifying different pathways using disconnection techniques. Exp. Brain Res. 167(1), 1–16.

Schachter AS., and Davis KL. 2000. Alzheimer's disease. Dialogues Clin. Neurosci. 2(2), 91–100.

Sederberg PB, Miller JF, Howard MW, Kahana MJ. 2010. The temporal contiguity effect predicts episodic memory performance. Mem Cognit 38(6):689-699.

Sheps JG. 1945. The nuclear configuration and cortical connections of the human thalamus. J. Comp. Neurol. 83, 1–56.

Sherman SM. 2017. Functioning of Circuits Connecting Thalamus and Cortex. Compr Physiol. 7(2), 713-739.

Sherman, S.M., Guillery, R.W., and Sherman, S.M. 2006. Exploring the thalamus and its role in cortical function (MIT Press).

Shimamura AP, Janowsky JS, Squire LR. 1990. Memory for the temporal order of events in patients with frontal lobe lesions and amnesic patients. Neuropsychologia 28(8):803-814.

Sigurdsson T, Stark KL, Karayiorgou M, Gogos JA, Gordon JA. 2010. Impaired hippocampal-prefrontal synchrony in a genetic mouse model of schizophrenia. Nature. 464(7286), 763–767.

Smith DF. 1999. Neuroimaging of serotonin uptake sites and antidepressant binding sites in the thalamus of humans and 'higher' animals. Eur. Neuropsychopharmacol. 9, 537–544.

Sokal RR, Rohlf FJ. 1995. Biometry: The Principles and Practices of Statistics in Biological Research. New York (NY): W.H. Freeman and Company.

Spencer SJ, Fox JC, Day TA. 2004. Thalamic paraventricular nucleus lesions facilitate central amygdala neuronal responses to acute psychological stress. Brain Res. 997, 234–237.

Sutcliffe JG, and de Lecea L. 2000. The hypocretins: Excitatory neuromodulatory peptides for multiple homeostatic systems, including sleep and feeding. J. Neurosci. Res. 62(2), 161–168.

Takashima A, Petersson KM, Rutters F, Tendolkar I, Jensen O, Zwarts MJ, Mcnaughton BL, Ferná G. 2006. Declarative memory consolidation in humans: A prospective functional magnetic resonance imaging study. Proc Natl Acad Sci USA. 103(3), 756-761.

Takehara-Nishiuchi K, and McNaughton BL. 2008. Spontaneous changes of neocortical code for associative memory during consolidation. Science. 322(5903), 960–963.

Thielen JW, Takashima A, Rutters F, Tendolkar I, Fernández G. 2015. Transient relay function of midline thalamic nuclei during long-term memory consolidation in humans. Learn. Mem. 22(10), 527–531.

Tiganj Z, Kim J, Jung MW, Howard MW. 2017. Sequential firing codes for time in rodent medial prefrontal cortex. Cereb Cortex 27(12):5663-5671.

Tortora GH., and Derrickson BH. 2008. The Diencephalon. In Principles of Anatomy and Physiology (John Wiley & Sons), 510–513.

Traynor C, Heckemann RA, Hammers A, O'Muircheartaigh J, Crum WR, Barker GJ, Richardson MP. 2010. Reproducibility of thalamic segmentation based on probabilistic tractography. Neuroimage. 52(1): 69-85

Tubridy S, Davachi L. 2011. Medial temporal lobe contributions to episodic sequence encoding. Cerebral Cortex 21(2):272-280.

Tulving E. 1984. Precis of elements of episodic memory. Behav Brain Sci 7(2):223-268.

Tulving E. 2002. Episodic memory: from mind to brain. Annu Rev Psychol 53:1-25.

Uhlhaas PJ., and Singer W. 2010. Abnormal neural oscillations and synchrony in schizophrenia. Nat. Rev. Neurosci. 11, 100–113.

Umbricht D, Javitt DC, Schmid L, Koller R, Vollenweider FX, Hell D. 2000. Ketamine-induced deficits in auditory and visual context-dependent processing in healthy volunteers. Arch. Gen. Psychiatry. 57(12), 1139-1147.

Umeda S, Kurosaki Y, Terasawa Y. Kato M, Miyahara Y. 2011. Deficits in prospective memory following damage to the prefrontal cortex. Neuropsychologia 49(8):2178-2184.

Van Essen DC, Smith SM, Barch DM, Behrens TEJ, Yacoub E, Ugurbil K, WU-Minn Consortium. 2013. The WU-Minn humand connectome project: an overview. Neuroimage. 80:62-79.

Varela C, Kumar S, Yang JY, Wilson MA. 2014. Anatomical substrates for direct interactions between hippocampus, medial prefrontal cortex, and the thalamic nucleus reuniens. Brain Struct. Funct. 219(3), 911–929.

Vasconcelos AP, de Cassel JC. 2015. The nonspecific thalamus: A place in a wedding bed for making memories last? Neurosci. Biobehav. Rev. 54, 175–196.

Vertes RP. 2002. Analysis of projections from the medial prefrontal cortex to the thalamus in the rat, with emphasis on nucleus reuniens. J. Comp. Neurol. 442(2), 163–187.

Vertes RP. 2015. Major diencephalic inputs to the hippocampus: Supramammillary nucleus and nucleus reuniens. Prog Brain Res. 219, 121-144.

Vertes RP, Fortin WJ, Crane AM. 1999. Projections of the median raphe nucleus in the rat. J. Comp. Neurol. 407(4), 555–582.

Vertes RP, Hoover WB. 2008. Projections of the paraventricular and paratenial nuclei of the dorsal midline thalamus in the rat. J. Comp. Neurol. 508(2), 212-237.

Vertes RP, Hoover W.B, Do Valle AC, Sherman A, Rodriguez JJ. 2006. Efferent projections of reuniens and rhomboid nuclei of the thalamus in the rat. J. Comp. Neurol. 499(5), 768–796.

Vertes RP, Hoover WB, Szigeti-Buck K., Leranth C. 2007. Nucleus reuniens of the midline thalamus: Link between the medial prefrontal cortex and the hippocampus. Brain Res. Bull. 71(6), 601–609.

Vertes RP, Linley SB, Hoover WB. 2015. Limbic circuitry of the midline thalamus. Neurosci. Biobehav. Rev. 54, 89–107.

Viena TD, Linley SB, Vertes RP. 2018. Inactivation of nucleus reuniens impairs spatial working memory and behavioral flexibility in the rat. Hippocampus. 28(4), 297–311.

Viena TD, Rash GE, Silva D, Allen TA. 2020. Calretinin and calbindin architechture of the midline thalamus associated with prefrontal-hippocampal circuitry. Hippocampus. 31(7):770-789.

Visser PJ, Krabbendam L, Verhey FR, Hofman PA, Verhoeven WM, Tuinier S, Wester A, Den Berg YW, Goessens LF, Werf YD, Jolles J. 1999. Brain correlates of memory dysfunction in alcoholic Korsakoff's syndrome. J Neurol Neurosurg Psychiatry 67(6): 774–778.

Volle E, Gonen-Yaacovi G, Costello AL, Burgess PW. 2011. The role of rostral prefrontal cortex in prospective memory: a voxel-based lesion study. Neuropsychologia 49(8):2185-2198.

Vogt BA, Hof PR, Friedman DP, Sikes RW, Vogt LJ. 2008. Norepinephrinergic afferents and cytology of the macaque monkey midline, mediodorsal, and intralaminar thalamic nuclei. Brain Struct. Funct. 212(6), 465–479.

Walsh DA, Brown JT, Randall AD. 2020. Neurophysiological alterations in the nucleus reuniens of a mouse model of Alzheimer's disease. Neurobiol Aging. 88: 1-10.

Wang X, Wang J, He Y, Huiying L, Yuan H, Evans A, Yu X, He Y, Wang H. 2015. Apolipoprotein E ε4 modulates cognitive profiles, hippocampal volume, and resting-state functional connectivity in Alzheimer's disease. J Alzheimers Dis. 45(3):781–795

Wellman LL, Yang L, Sanford LD. 2015. Effects of corticotropin releasing factor (CRF) on sleep and temperature following predictable controllable and uncontrollable stress in mice. Front. Neurosci. 9, 258.

Wilcock DM, Lewis MR, Nostrand WE. Van Davis J, Previti M. Lou, Gharkholonarehe N, Vitek MP, Colton CA. 2008. Progression of amyloid pathology to alzheimer's disease pathology in an amyloid precursor protein transgenic mouse model by removal of nitric oxide synthase 2. J. Neurosci. 28, 1537–1545.

Winsky-Sommerer R, Yamanaka A, Diano S, Borok E, Roberts AJ, Sakurai T, Kilduff TS, Horvath TL, de Lecea L. 2004. Interaction between the corticotropin-releasing factor system and hypocretins (orexins): a novel circuit mediating stress response. J. Neurosci. 24(50), 11439–11448.

Wolpert DM, Landy MS. 2012. Motor control is decision-making. Curr Opin Neurobiol. 22(6):996-1003

Wouterlood FG, Saldana E, Witter MP. 1990. Projection from the nucleus reuniens thalami to the hippocampal region: Light and electron microscopic tracing study in the rat with the anterograde tracer Phaseolus vulgaris-leucoagglutinin. J. Comp. Neurol. 296(2), 179–203.

Xu W, and Sudhof TC. 2013. A neural circuit for memory specificity and generalization. Science. 339(6125), 1290–1295.

Yamamoto T, Fujimoto Y, Shimura T, Sakai N. 1995. Conditioned taste aversion in rats with excitotoxic brain lesions. Neurosci. Res. 22(1), 31–49.

Yasoshima Y, Scott TR, Yamamoto T. 2007. Differential activation of anterior and midline thalamic nuclei following retrieval of aversively motivated learning tasks. Neuroscience. 146(3), 922–930.

Young CD, and Deutch AY 1998. The effects of thalamic paraventricular nucleus lesions on cocaine-induced locomotor activity and sensitization. Pharmacol. Biochem. Behav. 60(3), 753–758.

Zhang DX, and Bertram EH 2002. Midline thalamic region: widespread excitatory input to the entorhinal cortex and amygdala. J. Neurosci. 22(8), 3277–3284.

Zhu X, Peng S, Zhang S, Zhang X. 2011. Stress-induced depressive behaviors are correlated with Par-4 and DRD2 expression in rat striatum. Behav. Brain Res. 223(2), 329–335.

Zhu Y, Wienecke C, Nachtrab G, Chen X. 2016. A thalamic input to the nucleus accumbens mediates opiate dependence. Nature. 530(7589), 2019-222.

Zimmerman EC, and Grace AA. 2016. The nucleus reuniens of the midline thalamus gates prefrontal-hippocampal modulation of ventral tegmental area dopamine neuron activity. J. Neurosci. 36(34), 8977–8984.

Ziv Y, Burns LD, Cocker ED, Hamel EO, Ghosh KK, Kitch LJ, El Gamal A, Schnitzer MJ. 2013. Long-term dynamics of CA1 hippocampal place codes. Nat Neurosci 16(3):264-266.

VITA

PUCK CHARLOTTE REEDERS

2011-2015	B.S., Major: Psychology, minor: Chemistry University of Miami Miami, Florida
2015-2018	M.S., Psychology, Cognitive Neuroscience Program Florida International University Miami, Florida
2016	Graduate & Professional Student Committee Travel fund
2016	Edward and Rita Girden Cognitive Neuroscience Scholarship
2017	Psychology Seed Fund award
2018	Graduate & Professional Student Committee Travel fund
2015-2020	Teaching Assistant Florida International University Miami, Florida
2018-2021	Doctoral Candidate Florida International University Miami, Florida
2019	Center for Children and Families (CCF) Seed Grant
2020	3MT Thesis Competition Finalist
2021	Dissertation Year Fellowship
2021	Edward and Rita Girden Cognitive Neuroscience Scholarship
2021	Dr. Sarah Johnson Data Blitz Award Florida Consortium on the Neurobiology of Cognition

PUBLICATIONS AND PRESENTATIONS

Reeders PC. Hamm M, Allen TA, Mattfeld AM. 2021. Medial prefrontal cortex and hippocampal activity differentially contribute to ordinal and temporal context retrieval during sequence memory. Learning & Memory, 28, 134-147

Reeders PC. 2021. Finding the midline thalamus in humans for the investigation of neurological disorders. Florida Consortium on the Neurobiology of Cognition. Miami, FL.

Reeders PC, Mattfeld AM, Allen TA. 2021. Identification of the human midline thalamus using probabilistic tractography. Poster presentation at the Organization of Human Brain Mapping (OHBM) annual meeting. Virtual.

Reeders PC. 2021. Identification of the midline thalamus in humans. Cognitive Neuroscience Colloquium. Florida International University. Miami, FL.

Reeders PC. 2020. What part of the brain helps us remember life events in the correct sequence? Finalist in the Three Minute Thesis (3MT) Competition. Florida International university. Miami, FL.

Reeders PC, Allen TA, Mattfeld AM. 2019. Medial prefrontal cortex codes for ordinal representation, while the hippocampus codes for temporal context in sequence memory in humans. Poster presentation at Neuroscience Research Day. University of Miami Miller School of Medicine. Miami, FL.

Reeders PC, Allen TA, Mattfeld AM. 2019. mPFC activations reflect ordinal representation during sequence memory in humans. Data blitz at the annual Florida Consortium on the Neurobiology of Cognition. Gainesville, FL.

Reeders PC, Allen TA, Mattfeld AM. 2018. mPFC, dlPFC, and HC activation during sequence memory in humans. Oral presentation at the Neuroscience Colloquium. Florida International University, Miami, FL.

Reeders PC, Allen TA, Mattfeld AM. 2017. Functional and anatomical connectivity of the HC-Thalamus-mPFC circuit in humans. Oral presentation at the Neuroscience Colloquium. Florida International University, Miami, FL.

Reeders PC, Allen TA, Mattfeld AM. 2017. Sequence Memory predicts temporal reward discounting, and both activate medial prefrontal cortex and medial temporal lobe regions. Oral presentation at the Neuroscience Colloquium. Florida International University, Miami, FL.

Reeders PC, Allen TA, Mattfeld AM. 2016. Sequence Memory predicts temporal reward discounting, and both activate medial prefrontal cortex and medial temporal lobe regions. Poster presented at the Society for Neuroscience. San Diego, CA.

Reeders PC, Allen TA, Reeders PC, Vertes RP, Reagh ZM, Yassa MA, Mattfeld AM. 2016. Identification of nucleus reuniens in humans using probabilistic tractography. Poster presented at the Society for Neuroscience. San Diego, CA.